To the Graduate Council:

I am submitting herewith a thesis written by Jerald Andrew Jones entitled "From Waste to Energy – Catalytic Steam Gasification of Broiler Litter." I have examined the final copy of this thesis for form and content and recommend that it be accepted in partial fulfillment of the requirements for the degree of Master of Science, with a major in Chemical Engineering.

Atul C. Sheth

Atul Sheth, Major Professor

We have read this thesis
and recommend its acceptance:

Roger Painter

Accepted for the Council:

Associate Vice Chancellor and
Dean of the Graduate School

FROM WASTE TO ENERGY – CATALYTIC STEAM GASIFICATION OF BROILER LITTER

A Thesis
Presented for the
Master of Science
Degree
The University of Tennessee, Knoxville

Jerald Andrew Jones
August 1998

For my family

and friends

ACKNOWLEDGMENTS

The efforts of many people have contributed to the successful completion of this thesis. I would like to extend my sincere gratitude to these individuals. Dr. Atul Sheth, Dr. John Prados, and Dr. Roger Painter served as members of my thesis committee. I appreciate the suggestions and advice they have each given me. I am especially grateful for the opportunity to expand and develop the innovative ideas of Dr. Sheth on broiler litter disposal and utilization. Several other individuals at the University of Tennessee Space Institute offered their assistance. Alec Bridges assisted with the analytical chemistry utilized in my research. He offered his insights on all aspects of instrumental analysis ranging from gas chromatography and thermogravimetric analysis to atomic absorption spectrometry and sulfur determination. Melissa Weatherford always provided assistance with respect to my research and academic affairs. Becky Stines provided the broiler litter utilized in the majority of the experiments. Anuradha Godavarty provided advice and assisted in performing many hours of experiments. Sam Morton and Vineet Lasrado offered advice on the design of the experimental apparatuses and insight on other aspects of my thesis. I appreciate the efforts each of these individuals has made. Finally, I would like to thank my family for the support and encouragement they have always given me in both academics and life.

ABSTRACT

In 1996, the production of broiler chickens in the United States was approximately 7.60 billion head. The Southeastern United States accounted for nearly 75 percent of this production. For the last fifteen years, broiler production has experienced an annual growth rate of approximately 4.5 percent. The quantity of litter generated is enormous. In 1992, the Southeastern region alone produced over five million tons of broiler litter. Economic and agricultural experts predict the rapid expansion of the broiler industry will continue.

The litter removed from the broiler houses is rich in nutrients and often spread as a fertilizer. Without careful management, however, the associated runoff can cause severe environmental damage. With increasing broiler litter production, the implementation of alternative disposal technologies is essential to the sustainable development of the industry. Decreasing available cropland and increasing broiler farm sizes are compounding the difficulties of litter disposal.

A process originally developed for the conversion of coals to clean fuels may provide an answer. Catalytic steam gasification utilizes an alkali salt catalyst and steam to convert a carbonaceous feedstock to a gas mixture composed primarily of carbon monoxide, carbon dioxide, hydrogen, and methane. The low to medium energy gas produced may be

utilized as an energy source or chemical feedstock. Broiler litter is an attractive candidate for catalytic steam gasification for several reasons. The moisture content of the litter provides sufficient steam alleviating the need for supplementary steam generation. The mineral constituents of the litter serve as inherent catalysts for the steam-carbon reaction. The low sulfur content of the litter produces only small quantities of hydrogen sulfide, an unwanted component of many steam gasification product mixtures.

Thermodynamic modeling of the reaction mechanism indicates that the production of carbon monoxide and hydrogen are favored at low pressures and high temperatures. These constituents are the desirable components of the low energy gas. Bench-scale kinetics studies were performed in a high pressure fixed bed reactor. The effects of temperature, pressure, and catalyst loading on the carbon-steam reaction rate were investigated. The gasification kinetics were found to be favored at low pressures and high temperatures.

The specific gasification rate as measured in the differential bed reactor was then used to perform a technical and economic feasibility study of the catalytic steam gasification of broiler litter. To evaluate the economic viability of the process, a transportable broiler litter gasification unit was designed. The unit, designed to process 1.5 tons of fresh litter per hour, has a payback period of approximately two years.

TABLE OF CONTENTS

CHAPTER PAGE

LIST OF TABLES

LIST OF FIGURES

FIGURE PAGE

FIGURE PAGE

LIST OF SYMBOLS

A	Empirical constant in ideal gas heat capacity equation
$A_{cal,i}$	Gas chromatograph peak area for species i in calibration gas mixture
A_i	Gas chromatograph peak area for species i
B	Empirical constant in ideal gas heat capacity equation
C	Empirical constant in ideal gas heat capacity equation
C_p^o	Constant pressure ideal gas heat capacity
D	Empirical constant in ideal gas heat capacity equation
$D_v\, g(\vec{\varepsilon})$	Directional derivative of g at $\vec{\varepsilon}$ in the direction of $\vec{v}$
F_j	Nonlinear function describing equilibrium state of reaction j
$F(\vec{\varepsilon})$	Column vector with values of nonlinear functions F_j as elements
G	Specific gasification rate
I	Integration constant
J	Integration constant
$J(\vec{\varepsilon})^t$	Transpose of the Jacobian matrix of the vector $F(\vec{\varepsilon})$
K_j	Equilibrium constant for reaction j
M_c	Atomic weight of carbon
N	Total number of experimental data points
N_c	Moles of carbon in the differential fixed bed
P	Total system pressure

P_{atm}	Atmospheric pressure
R	Universal gas constant
T	Absolute temperature
T_{cond}	Condenser temperature
V	Volume
V_i	Cumulative volume of gas which has exited the reactor at time t_i
V_{i-1}	Cumulative volume of gas which has exited the reactor at time t_{i-1}
V_t	Cumulative volume of gas which has exited the reactor at time t
W	Mass of carbon in the differential fixed bed
W_{gas}	Mass of carbon gasified
W_o	Initial mass of carbon in the differential fixed bed
X	Carbon conversion based on fixed carbon in char
X_i	Carbon conversion based on fixed carbon in char at time t_i
X_{i+1}	Carbon conversion based on fixed carbon in char at time t_{i+1}
$\hat{a}_i$	Activity of species i
f_i	Fugacity of pure species i
f_i^o	Standard state fugacity of pure species i
$\hat{f}_i$	Fugacity of species i
g	Objective function minimized in gradient descent algorithm

h	Variable in the definition of the directional derivative
$h(\alpha)$	Objective function of restricted domain in gradient descent algorithm
m	Total char mass
m_{ash}	Mass of ash in original char sample
m_{final}	Final mass of sample
$m_{initial}$	Initial mass of sample
m_o	Initial total char mass
n	Reaction order of carbon-steam reaction with respect to carbon
n_{io}	Initial molar quantity of species i
n_o	Initial total molar quantity
r	Coefficient of regression
$-r_c$	Specific rate of disappearance of solid carbon
t	Time
$\vec{v}$	Three-dimensional unit vector
w_{H_2O}	Mass fraction of moisture in fresh broiler litter
w_{vol}	Mass fraction of volatiles in fresh broiler litter
$y_{cal,i}$	Mole fraction of species i in calibration gas mixture
y_i	Mole fraction of species i in the gas phase
ΔG^o	Standard Gibbs energy of reaction
ΔH^o	Standard heat of reaction

ΔH^{o}_{298}	Standard heat of reaction at 298.15 K
ΔV_i	Volume of gas which exits the reactor between time t_i and time t_{i-1}
Δt	Time elapsed between t_i and t_{i+1}
α	Multiplier utilized in gradient descent algorithm
β	Correction factor
ε_j	Reaction coordinate for reaction j
$\vec{\varepsilon}$	Column vector of reaction coordinates
$\hat{\phi}_i$	Fugacity coefficient for species i
κ	Ratio of ash mass to fixed carbon mass in original char sample
$\overline{\rho}$	Total molar density
$\overline{\rho}_c$	Total molar density of gaseous carbonaceous compounds
$\overline{\rho}_{c,i}$	Total molar density of gaseous carbonaceous compounds at time t_i
$\overline{\rho}_{c,i}$	Total molar density of gaseous carbonaceous compounds at time t_{i-1}
$\overline{\rho}_i$	Molar density of species i
$\upsilon_{i,j}$	Stoichiometric coefficient for species i in reaction j
υ_j	Overall stoichiometric coefficient for reaction j
$\frac{\partial g}{\partial \varepsilon_j}$	Partial derivative of g with respect to reaction coordinate ε_j
$\nabla g(\vec{\varepsilon})$	Gradient of the objective function g at $\vec{\varepsilon}$

$\Re$	Space containing all real numbers
$\Re^3$	Three-dimensional real space

LIST OF ABBREVIATIONS

AGA	American Gas Association
Btu	British thermal unit
DOC	United States Department of Commerce
DOE	United States Department of Energy
EPA	Environmental Protection Agency
ft^3	Cubic feet
g	Gas
g	Grams
HEG	High Energy Gas
hr	Hours
ICP	Inductively Coupled Plasma
IGT	Institute of Gas Technology
kg	Kilograms
kJ	Kilojoules
lb	Pounds
LEG	Low Energy Gas
MEG	Medium Energy Gas
mg	Milligrams
min	Minutes
ml	Milliliters

mm Hg	Millimeters of mercury
mol	Gram-moles
NCSU	North Carolina State University
NASS	National Agricultural Statistics Service
NPT	Nominal Pipe Thread
OD	Outer Diameter
PI	Pressure Indicator
ppm	Parts per million
psia	Pounds per square inch absolute
PWQC	Poultry Water Quality Consortium
scf	Standard cubic feet
SERI	Solar Energy Research Institute
SNG	Substitute Natural Gas
TGA	Thermogravimetric Analyzer
TI	Temperature Indicator
USDA	United States Department of Agriculture
wt.	Weight

Chapter I

Introduction

Definition of Problem

The production of broiler chickens is one of the most quickly growing sectors in the United States' agriculture. In 1996, the production of broiler chickens was approximately 7.60 billion head. For the last fifteen years, broiler production has experienced an annual growth rate of approximately 4.5 percent. Broiler production facilities are concentrated in the Southeastern United States. In 1992, the Southeastern region accounted for nearly 75 percent of broiler production. Economic and agricultural experts predict the rapid expansion of the broiler industry will continue.

The increasing production of broiler chickens is creating a severe waste disposal problem, however. A lignocellulosic material is generally utilized as bedding in the broiler houses. This material is usually removed and replaced between one and four times per year. The litter removed from the houses must be either disposed or utilized. The quantity of litter generated is tremendous. In 1992, the Southeastern region alone produced over five million tons of broiler litter. The litter is rich in nutrients and often spread as a fertilizer. Without careful management, however, the associated agricultural runoff can cause severe environmental damage. The recent outbreak of *Pfiesteria piscicida* in the Chesapeake Bay has been linked to improper broiler litter disposal

techniques. Other environmental accidents in Arkansas, Oklahoma, and Alabama have been linked to poor disposal techniques. With increasing broiler litter production, the implementation of alternative disposal technologies is essential to the sustainable development of the industry.

Statement of Hypothetical Solution

A process developed for the conversion of coals to clean fuels may provide an answer. Catalytic steam gasification utilizes an alkali metal salt as a catalyst and steam to convert a carbonaceous feedstock to a gas mixture composed primarily of carbon monoxide, carbon dioxide, hydrogen, and methane. At low pressures and high temperatures, the process produces synthesis gas, a gas rich in carbon monoxide and hydrogen. The gas produced has a low to medium heat content and may be utilized as an energy source or chemical feedstock.

Broiler litter is an attractive candidate for catalytic steam gasification for several reasons. The chars produced from biomass are typically more reactive than those produced from coal. The large amount of potassium and other minerals in the litter may also serve as an inherent catalyst. The sulfur content of broiler litter is very low. This limits the production of hydrogen sulfide, an undesirable constituent of gaseous fuels. The catalytic steam gasification of broiler litter could generate a valuable product. More importantly, however, it could protect the environment by utilizing broiler litter in an environmentally benign manner.

Chapter II

Literature Review

Poultry Production in the Southeastern United States

The quantity of broiler litter produced in a given period of time is obviously related to the number of broiler chickens raised during that period. For large populations of broilers, the litter production is, in fact, directly proportional to the number of broilers raised. To assess both the technical and economic feasibility of catalytic steam gasification of these litters, it is important to first study the number of broilers raised annually. Since the Southeastern region produces nearly three-quarters of the nation's broilers, the scope of this thesis is limited to that region. The Southeastern United States, as defined in this thesis, includes thirteen states: Alabama, Arkansas, Florida, Georgia, Kentucky, Louisiana, Mississippi, Missouri, North Carolina, South Carolina, Tennessee, Virginia, and West Virginia.

Annual Broiler Production

Broiler chicken production is one of the most quickly growing sectors in the United States' agriculture. This production has been driven primarily by two factors. First, the market has experienced increased domestic demand due to the increasing popularity of chicken. Chicken meat is seen by many to be a healthier alternative to beef and other meats. Second, the poultry industry has experienced increased international demand due

to rising exports to emerging global markets. For the past fifteen years, broiler production has grown by approximately 4.5 percent annually. This strong growth is expected to continue well into the next century.

The number of broilers produced in the United States in 1950 was under one billion head. In 1996, U.S. broiler production was estimated to be 7.60 billion head. Figure 2.1 shows the U.S. broiler production from 1950 to 1996. This graph is not only evidence of the increase in broiler production but also evidence of the strong growth the industry is currently experiencing. The Southeastern United States has experienced similar broiler production growth and is now accountable for about 74 percent of the country's production. Figure 2.2 summarizes the broiler production of both the entire United States and the Southeastern region as measured by the last three agricultural censuses. The production by each Southeastern state is detailed in Table 2.1. Other major broiler producing regions of the country include the Chesapeake Bay area, Oklahoma, Texas, and California. It is obvious that the issue of broiler litter disposal will be of utmost importance in the near future to all states participating in the broiler chicken industry.

Average Broiler Farm Size

The broiler chicken industry is experiencing a phenomenon which is common throughout the agricultural sector. While the quantity of broilers produced is increasing steadily, the number of farms raising broilers is steadily decreasing. In fact, the number of broiler

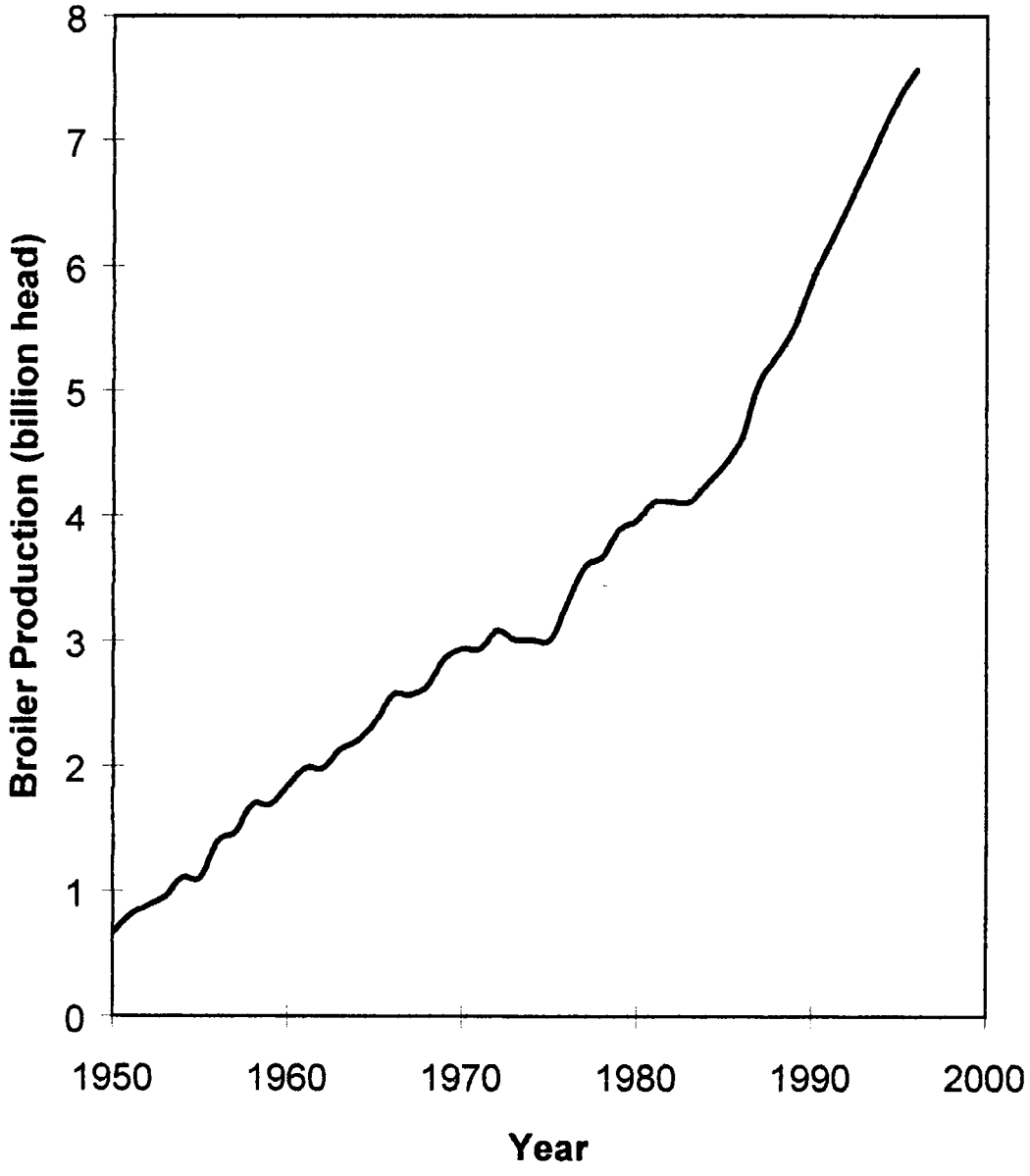

Figure 2.1 United States Broiler Production 1950-1996

Source: USDA National Agricultural Statistics Service

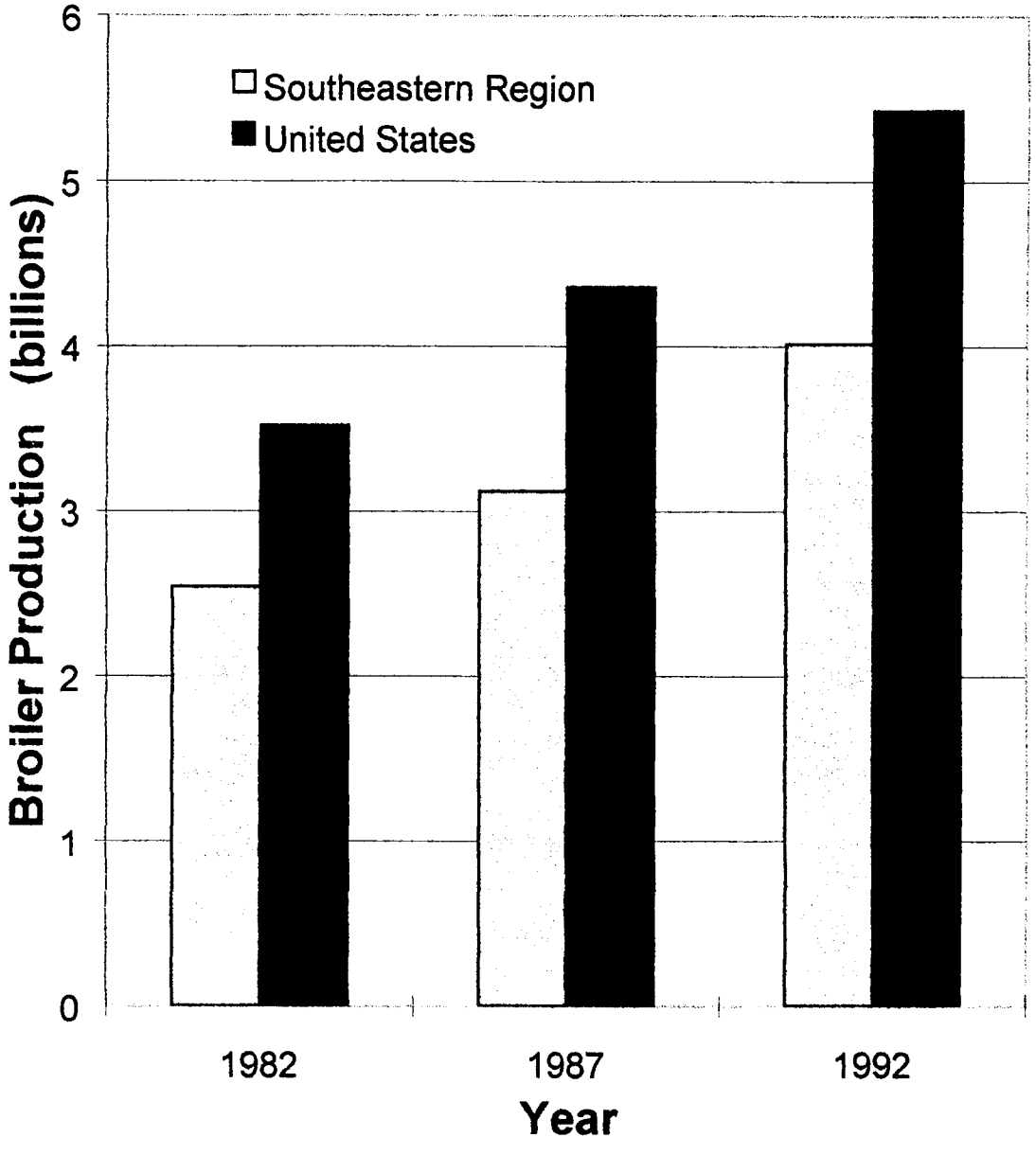

Figure 2.2 Annual Broiler Production

Source: 1992 Census of Agriculture

Table 2.1 Annual Production of Broiler Chickens

(broilers produced)

Region	1992	1987	1982
United States	5,428,589,485	4,361,975,630	3,516,622,889
Southeastern Region	4,017,012,579	3,120,257,341	2,543,855,879
Alabama	737,608,903	564,583,477	426,623,399
Arkansas	862,403,824	719,764,548	569,303,000
Florida	97,854,566	93,224,832	76,456,724
Georgia	749,018,187	609,503,009	521,508,557
Kentucky	27,623,677	2,201,169	2,410,306
Louisiana	115,258,369	96,147,369	91,851,892
Mississippi	388,128,497	276,652,292	247,236,533
Missouri	82,990,149	40,991,224	21,466,182
North Carolina	499,071,743	408,721,082	348,434,068
South Carolina	106,171,059	60,295,197	41,578,104
Tennessee	98,516,358	75,974,462	53,916,803
Virginia	201,697,436	142,971,809	120,078,522
West Virginia	50,669,811	29,226,871	22,991,789

farms in the United States has decreased at an annual rate of nearly three percent over the past five years. The combined effect of the production increase and farm decrease is resulting in alarming growth in average broiler farm size. In the United States, the average annual broiler farm production increased at an annual rate of over 7.5 percent between 1987 and 1992. The corresponding annual increase in the Southeastern region was 6.24 percent over the same period. Figure 2.3 shows the average sizes of broiler farms from the last three agricultural censuses. The average sizes for each state are detailed in Table 2.2.

The increasing average broiler farm size currently is a disadvantage but could become advantageous in the future. The larger farms must transport their broiler litter greater distances to dispose of it in an environmentally sound method. Unfortunately, economics often prevails over ecology and the litter disposal creates negative environmental impacts. As the farm sizes continue to increase, these environmental accidents will become frequent. If an alternative disposal method such as catalytic steam gasification is adopted, however, the growing farm size can become advantageous. The economics of scale will result in lower conversion costs if the litter is located at a few large sources rather than many scattered small sources. The growing farm sizes could, in fact, be the ultimate factor in adopting an alternative disposal technology.

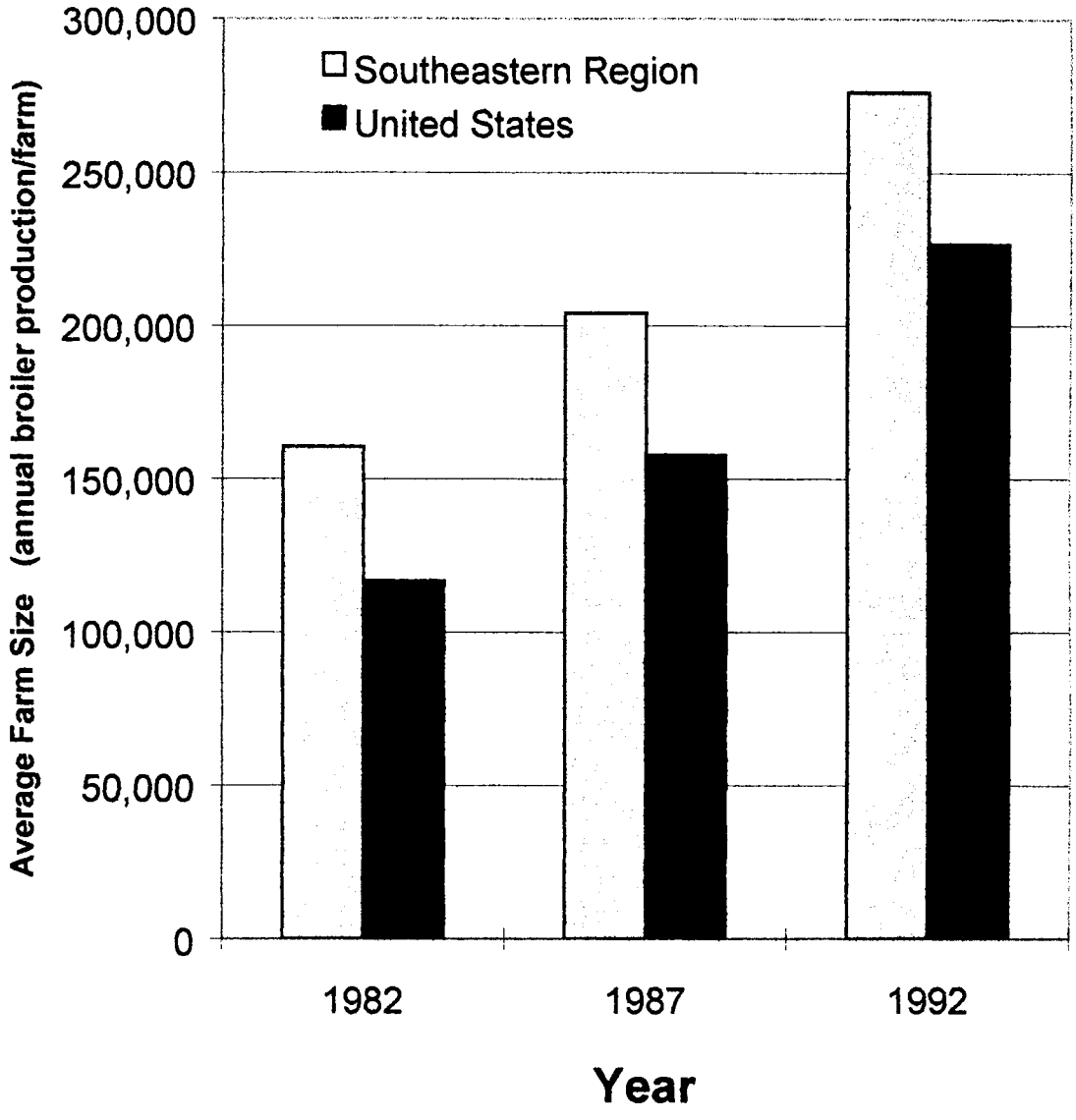

Figure 2.3 Average Annual Broiler Production per Farm

Source: 1992 Census of Agriculture

Table 2.2 Average Annual Broiler Production per Farm

(broilers / farm)

Region	1992	1987	1982
United States	226,673	157,785	116,831
Southeastern Region	276,197	204,058	160,556
Alabama	299,841	220,799	160,445
Arkansas	235,244	174,193	143,655
Florida	269,572	231,903	176,574
Georgia	311,183	216,520	168,446
Kentucky	251,124	30,153	24,347
Louisiana	368,238	308,165	242,353
Mississippi	320,502	245,042	203,991
Missouri	243,373	129,719	60,298
North Carolina	235,856	189,838	158,740
South Carolina	363,600	265,618	197,991
Tennessee	201,465	149,262	108,267
Virginia	315,152	252,155	214,810
West Virginia	372,572	295,221	124,280

Available Cropland Area in Farms

Since the majority of broiler litter is currently disposed of by land spreading, the amount of cropland available is an important variable. If excessive litter is applied to a given area, the environmental impacts can be severe. Although statistics are not available for land owned by the integrated poultry producers, the trend should be similar to that for total available cropland. The United States has experienced a slight decrease in cropland area over the past fifteen years. The Southeastern region has experienced a considerably greater decrease in cropland over the same period. Figure 2.4 illustrates the trends in cropland area as measured in the most recent agricultural censuses. Table 2.3 details the cropland area for each Southeastern state. Although the decrease in cropland is not dramatic, it may contribute to the adoption of alternate broiler litter disposal methods. The Poultry Water Quality Consortium (PWQC) sites the decrease in cropland as an emerging obstacle to land spreading (PWM/2 - 1).

Annual Broiler Litter Production

The annual broiler litter production is directly proportional to the annual broiler production. Jones and Ogden have estimated the economically recoverable energy from animal wastes in the South (1). To calculate the quantity of animal manures generated annually, they utilize manure output ratios. These multipliers can be used to estimate the dry weight of wastes available for energy use. The manure output ratio for broiler chickens is 1.25 tons of manure per 1,000 birds on a dry-weight basis during their 8-week

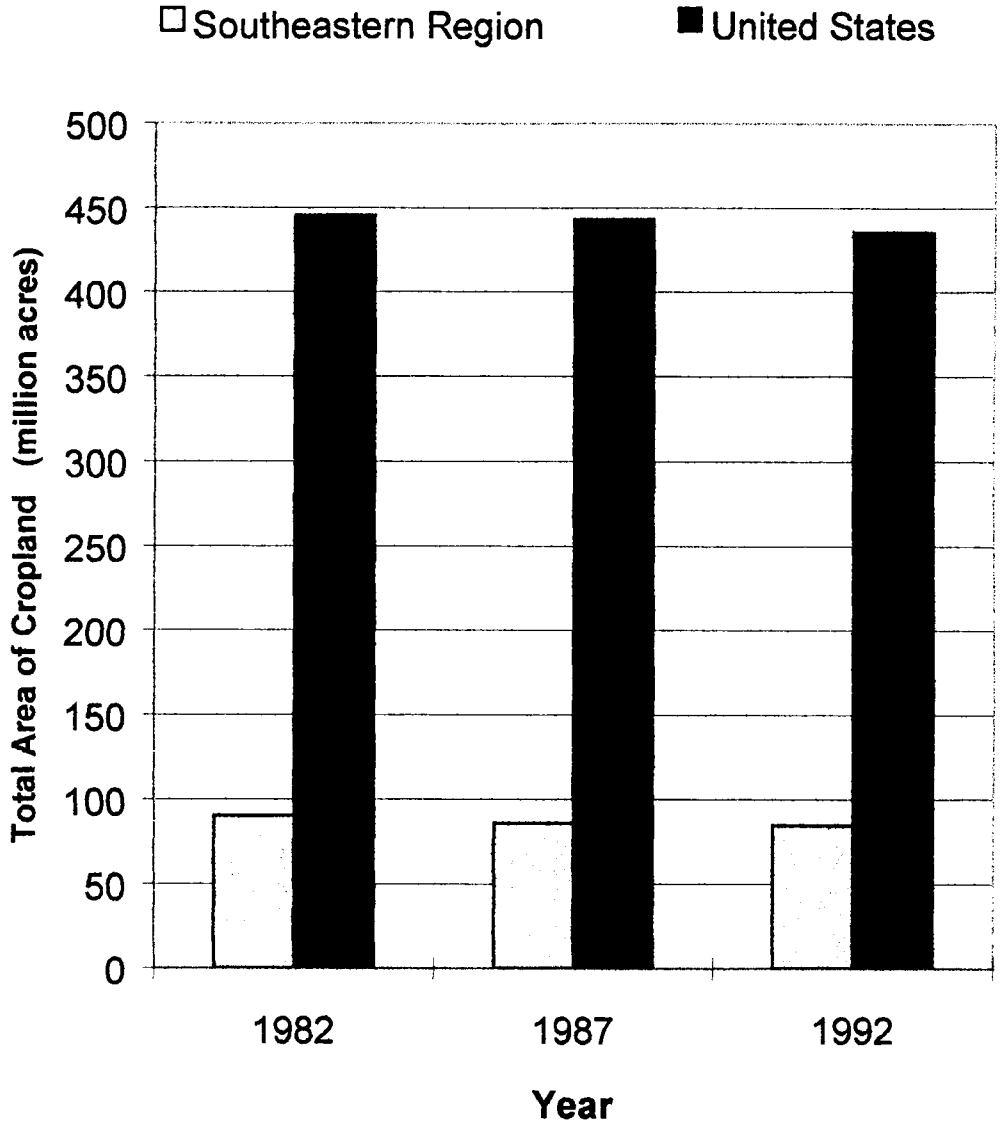

Figure 2.4 Total Available Cropland

Source: 1992 Census of Agriculture

Table 2.3 Available Cropland Area

(acres)

Region	1992	1987	1982
United States	435,365,878	443,318,233	445,362,028
Southeastern Region	84,659,633	85,843,597	90,559,041
Alabama	4,237,057	4,496,607	5,105,734
Arkansas	10,064,948	9,950,401	10,042,942
Florida	3,841,505	3,790,599	4,093,583
Georgia	5,475,712	5,780,330	6,531,234
Kentucky	8,880,989	8,900,086	8,960,250
Louisiana	5,552,733	5,562,736	6,093,474
Mississippi	6,518,288	6,747,639	7,745,113
Missouri	19,228,832	19,378,031	19,376,192
North Carolina	5,578,191	5,716,256	5,950,155
South Carolina	2,588,525	2,686,117	3,179,278
Tennessee	7,086,879	7,185,903	7,602,106
Virginia	4,311,840	4,363,106	4,559,543
West Virginia	1,294,134	1,285,786	1,319,437

production cycle (Jones and Ogden 10). The thermal energy content of the dry litter based on direct combustion is approximately 11 million Btu per ton dry weight (Jones and Ogden 10). The thermal energy content of broiler litter produced in the Southeastern region in 1992 was approximately 55 trillion Btu. As depicted in Figure 2.5, the trend in broiler litter production is similar to that of broiler production. A detailed listing of litter production for each Southeastern state is given in Table 2.4.

Environmental Impact of Poultry Production

The primary impetuses for developing alternative broiler litter disposal technologies are the adverse effects the current disposal techniques have on the environment. Although the current techniques are supposedly environmentally benign when applied properly, the frequency of environmental accidents is increasing. Through utilization of a technology such as catalytic steam gasification, these incidents can be reduced significantly or even eliminated.

Current Disposal Methods for Broiler Litter

Most broilers are grown in enclosures with concrete, wooden, or earthen floors. A 2- to 6-inch layer of bedding material is placed on the flooring to absorb the urine and manure. The bedding material is generally a lignocellulosic material such as wood shavings or peanut hulls. The resulting bedding and manure mixture is termed litter. The litter is

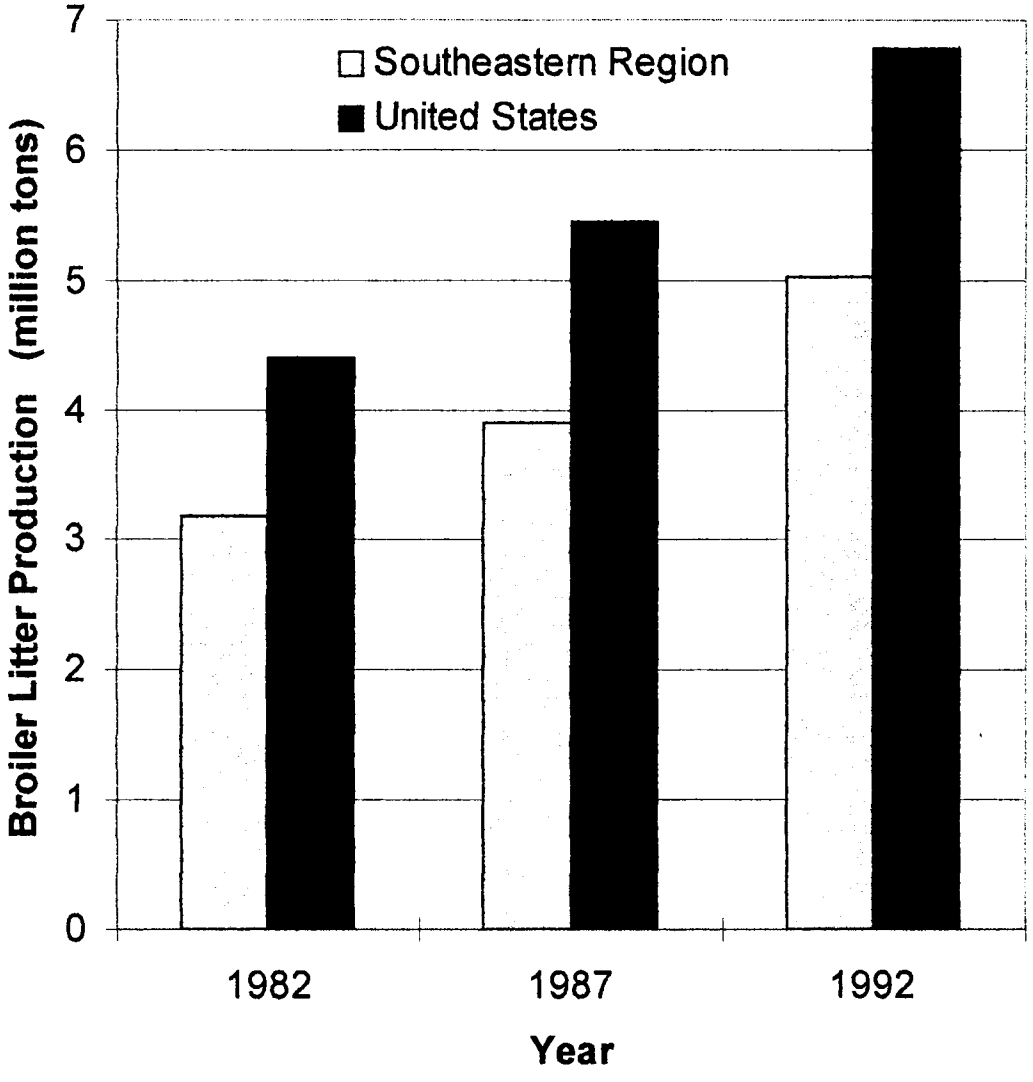

Figure 2.5 Annual Broiler Litter Production

Table 2.4 Annual Broiler Litter Production

(tons)

Region	1992	1987	1982
United States	6,785,737	5,452,470	4,395,779
Southeastern Region	5,021,266	3,900,322	3,179,820
Alabama	922,011	705,729	533,279
Arkansas	1,078,005	899,706	711,629
Florida	122,318	116,531	95,571
Georgia	936,273	761,879	651,886
Kentucky	34,530	2,751	3,013
Louisiana	144,073	120,184	114,815
Mississippi	485,161	345,815	309,046
Missouri	103,738	51,239	26,833
North Carolina	623,840	510,901	435,543
South Carolina	132,714	75,369	51,973
Tennessee	123,145	94,968	67,396
Virginia	252,122	178,715	150,098
West Virginia	63,337	36,534	28,740

removed and replaced at regular intervals. The removed litter must then be utilized or disposed.

Traditionally, broiler litter has been used as a fertilizer for row crops and pastures. The nutrient content of broiler litter is dependent on several factors. For this reason, the nutrient content of litters is highly variable. A representative litter, however, contains approximately 62 lb/ton of nitrogen, 60 lb/ton of phosphate measured as P_2O_5, and 40 lb/ton of potash measured as K_2O (Payne and Donald 20). This nutrient content estimate is used to determine the allowable fertilizer loading. The application rate is generally based on the nitrogen requirements of the fertilized crop. The nitrogen-based application rate is much larger than that based on phosphorus requirements. Typical yearly application rates for broiler litter range from three tons per acre for cotton to eight tons per acre for silage corn (Payne and Donald 23).

In addition to its traditional role as a fertilizer, poultry waste is being used as a feed supplement for cattle, in rooting media for horticultural crops, and as an organic fertilizer and soil amendment for the landscaping industries.

Environmental Impact of Current Disposal Methods

Land spreading methods can affect the environment through numerous routes. The three primary concerns with land spreading are application of excessive macronutrients, accumulation of excessive micronutrients, and introduction of pathogenic organisms to an ecosystem. Poultry waste is considered a nonpoint source of pollution. Nonpoint source pollution originates from a diffuse source such as runoff from agricultural land (Payne and Donald 35). Although the three classes of pollutants can have terrestrial effects, the most commonly impacted areas are aquatic.

The three macronutrients of interest in broiler litter and other fertilizers are nitrogen, phosphorus, and potassium. As indicated previously, poultry litters are rich in these nutrients. Collectively, these compounds can result in eutrophication, or overenrichment of surface waters. Eutrophication is evident from a heavy growth of algae on the water surface. This heavy algae population can lower dissolved oxygen levels. These oxygen-starved conditions can result in the killing of fish or in severe stress on the fish population. This effect is compounded by the presence of excessive organic matter in the runoff. The bacterial decomposition of the organic matter results in a flourishing bacterial population with enormous oxygen requirements.

The nitrogen can have negative impacts as either ammonia or nitrates. Ammonia is toxic to fish at small concentrations (Payne and Donald 35). The Environmental Protection Agency (EPA) has established a limit of 0.02 ppm for ammonia in surface waters. This

level has been exceeded by a factor of 3,000 near some poultry operations (Payne and Donald 35). Nitrates are water-soluble and capable of migration past the root zone in soil. After passing the root zone, the nitrates continue downward to the groundwater. At this point, the nitrates become a threat to humans. The alkaline environment of infant stomachs converts nitrates to nitrites causing blue-baby syndrome (Payne and Donald 37). In extreme cases, this disease may be fatal. The EPA has established a limit of 10 ppm of nitrate in drinking waters. In certain poultry-producing regions of Maryland, Delaware, and Alabama, a high percentage of wells exceed this standard (Payne and Donald 37).

Generally, if the nitrogen-based application rates are employed, the quantity of phosphorus applied will exceed the crop's phosphorus requirements. If not carefully managed, these compounds can degrade water quality. Phosphorus-laden soil is carried with agricultural runoff to surface waters (Poultry Water Quality Consortium [PWQC] PWM/1 - 2). This may contribute to fish kills or premature aging of surface waters. Even small soil losses may result in significant runoff leading to high nutrient depositions in the water (PWQC PWM/1 - 2). J. Thomas Sims, a soil expert at the University of Delaware, describes phosphorus pollution as "one of the real dilemmas with management of poultry wastes." He continues, "When you apply wastes based on the amount of nitrogen crops need, you always apply more phosphorus than the crops need, by a pretty wide margin" (Warrick and Shields A01). The governor of Maryland, Parris N. Glendening, has called for plans to use a phosphorus-based loading calculation (Shields

B10). This would decrease the allowable broiler litter application rate and require additional commercial fertilizers to satisfy the crop's nitrogen requirements. Farmers in the region are now concerned about finding an alternate disposal technique.

The final macronutrient, potassium, and micronutrients are relatively minor environmental threats when compared to nitrogen, phosphorus, and pathogens. Excessive amounts of potassium can retard plant growth at some developmental stages (PWQC PWM/1 - 2). Most micronutrients and heavy metals form stable complexes with clays or organic matter. Broiler litter may contain copper, selenium, nickel, lead, zinc, arsenic, and other potentially toxic elements. If these elements exceed the adsorptive capacity of the soil, leaching of contaminants into the groundwater is possible. Erosion and the associated runoff can also carry these contaminants to surface waters. In addition to water pollution, these elements can cause numerous diseases in grazing livestock (Payne and Donald 37).

Microorganisms contained in broiler litter include bacteria, viruses, protozoa, parasites, and fungi. Approximately 150 disease-causing organisms or pathogens have been identified in animal wastes (PWQC WQI/3 - 2). Exposure routes for humans include ingestion of contaminated water, dermal contact, and consumption of diseased fish and other aquatic animals. Although most pathogens die quickly, they can persist for considerable periods of time in groundwater (PWQC WQI/3 - 2). Some pathogens

commonly found in poultry wastes include Salmonella, Listeria, coliform, New Castle virus, ringworm, coccidiosis, and Ascaris (PWQC WQI/3 - 2).

Examples of Environmental Impact

A United States Senate study, "Animal Waste Pollution in America: An Emerging National Problem," was released in January 1998. The study indicated that 60 percent of rivers and streams are identified by agricultural officials as "impaired" (Feuerbach and Hadish 1). Agricultural runoff was cited as the largest contributor to this impairment. The National Wildlife Federation gave failing grades to nineteen states in their efforts toward identifying these "impaired waters" (Prichard 2). Several of these states are plagued by agricultural runoff. In an October 1997 report, the EPA identified agricultural runoff as one of the largest and least regulated sources of pollution. The agency concluded that more than half of the country's 2,000 watersheds face moderate or serious water quality problems (Warrick and Shields 1). Although this problem is obviously systemic, two of the most prominent regions are the Chesapeake Bay region and Arkansas and Oklahoma.

The Chesapeake Bay region is representative of the degree of environmental damage improperly managed broiler litter can cause. Broiler production is especially concentrated in some portions of Delaware. A study by a Delaware engineering firm suggests that by 2000, Sussex County, Delaware will have to transport 90 percent of its poultry litter outside the region for disposal (Warrick and Shields 1). Major poultry-

producing counties of Virginia, Maryland, and Delaware already appear to have more litter than crops could absorb before any other fertilizers are added (Warrick and Shields 1). In 1997, *Pfiesteria piscicida* killed tens of thousands of fish and closed portions of three rivers on Maryland's Eastern Shore. The *Pfiesteria* outbreak threatened many sectors of the Chesapeake Bay economy. Donald F. Boesch, director of the University of Maryland's Center for Environmental Science, told the investigative committee that there was evidence that *Pfiesteria* thrives in waters with excessive nutrients (Cronan 2). Only sixty-eight percent of farms near the Pocomoke River were in compliance with all recommended practices (Cronan 3). Others had problems with manure management and erosion control. The evidence indicated that the current broiler litter disposal techniques were to blame.

Pfiesteria piscicida is a toxic dinoflagellate known to cause major fish kills and fish disease events (North Carolina State University [NCSU] 1). Experiments show that excessive nutrient enrichment can promote *Pfiesteria*'s toxic effects. *Pfiesteria* has an extremely complex life cycle. The amoeboid and flagellated forms of the cells excrete toxins which cause fish to become lethargic. In addition, the toxins injure the skin of fish causing internal salt imbalances. The skin is then destroyed resulting in bleeding and hemorrhaging (NCSU 3). The effects are not limited to aquatic species. Humans may be affected by water contact or by the inhalation of toxic aerosols. Effects include development of sores, severe headaches, vomiting, difficulty breathing, kidney and liver

dysfunction, acute short-term memory loss, and severe cognitive impairment (NCSU 4-5).

Northwest Arkansas and eastern Oklahoma are also experiencing serious broiler litter disposal problems. The rapidly growing broiler industry in the region is considered a threat to the water supply of Tulsa, Oklahoma (Tiernan 1). Illegal disposal of poultry wastes is now a familiar environmental problem throughout Arkansas. As Arkansas' poultry production capacity is reached, nearby Oklahoma will continue to experience these problems.

To reduce these incidents of environmental damage, federal and state legislators are proposing tighter regulations. In 1997, Senator Tom Harkin of Iowa introduced legislation that would set minimum standards for handling animal wastes (Lynch 1). The bill would require that litter application rates be no greater than both the nitrogen and phosphorus demands of the crops (Lynch 1). In Maryland, Governor Parris Glendening plans to propose legislation in 1998 which will require nutrient management plans and enforcement mechanisms including fines (The Capital Online 1). He also is planning to propose a three-year tax credit of $3,000 to $4,500 for farmers who discontinue the use of broiler litter as a fertilizer (The Capital Online 1). Legislators in Oklahoma have proposed an operating fee and license. The money generated by these fees would be used to administer and enforce waste management recommendations (Ray 1). An alternate

disposal technology could make obsolete the environmentally unsound practices currently utilized.

Catalytic Steam Gasification of Coal

Since both coal and biomass are of carbonaceous composition, many of the processes utilizing coal can be modified to accommodate a biomass feedstock. Coal gasification converts solid coal to a mixture of combustible gases through controlled partial oxidation. The conversion is achieved by introducing a gasification agent and a coal feedstock to a reactor vessel at controlled temperature, pressure, and flow regime conditions. The gases generated by the gasification process may be used for a wide variety of applications. The four energy systems which dominate are:

- production of fuel for electric power generation systems
- manufacturing of substitute natural gas (SNG) for pipeline distribution
- generation of medium energy fuel gas for industrial applications
- production of synthesis gas for use as a chemical feedstock (Lee 96)

There is an extensive body of literature on the thermodynamics, kinetics, and catalysis of coal gasification processes.

Early History of Coal Gasification

As early as the seventeenth century, it was known that coals evolved gases upon application of heat (Lee 98). Around 1750, in England, gases used for lighting were being produced by the pyrolysis of coal (Lee 98). A reliable process for producing water

gas, a mixture of hydrogen and carbon monoxide, was developed in 1872 (Lowry 1721). The gas is produced by alternating blasts of air and steam across hot coke. The air combusts a portion of the coke. The heat of combustion provides the necessary heat for the gasification process. The subsequent introduction of steam results in the generation of carbon monoxide. By the early 1920s, there were at least five Winkler fluidized bed processes yielding producer gas at a rate of 10 million scf per hour (Lee 118). The Winkler gasifier operates at atmospheric pressure and temperatures approaching 1000°C. The gasifier utilizes oxygen and steam to produce a gas rich in carbon monoxide and hydrogen (Lowry 1632). In 1936, the first commercial gasifier operating with the Lurgi process went operational (Lee 98). The Lurgi process uses pressurized steam and oxygen to produce a mixture of carbon monoxide, hydrogen, and methane (Lowry 1811). In 1942, the Koppers-Totzek suspension gasification process was developed in Germany (Lee 98). The process utilizes an entrained flow reactor operating at atmospheric pressure and temperatures of approximately 1500°F. The gas produced is rich in both carbon monoxide and hydrogen.

Development of Catalytic Steam Gasification of Coal

The development of catalytic steam gasification offered a route to produce gases of higher heating value at significantly lower temperatures. The gasification agent utilized is generally oxygen-free. In 1924, Taylor and Neville tested the catalytic effects of numerous alkali salts (Hirsch et al. 122). They found that K_2CO_3 and Na_2CO_3 were particularly active. In the 1970s, Exxon developed a continuous catalytic coal

gasification process (Anderson and Smith 1). The process utilizes steam and recycled synthesis gas as the gasification agent. The catalyst utilized is either KOH or K_2CO_3. The overall reaction yields the product, methane, and a byproduct, carbon dioxide.

Thomson and Sy studied the steam gasification of a Kentucky oil shale char in a semibatch fixed bed reactor (223). They found that gasification rates were increased by a factor of three in the presence of K_2CO_3 at a catalyst loading of 10 weight percent. Researchers in Japan have evaluated the effects of various metals on the gasification rate and evolved gas composition (Miura et al. 407). The metal salts tested for catalytic effect were K_2CO_3, Na_2CO_3, and $CaCO_3$. The researchers also conducted experiments with two metal oxides, Fe_2O_3 and Ni_2O_3. The carbonaceous substrates used in the experiments were coconut shell carbon and carbon black. The catalysts with the most profound impacts on gasification rate were sodium, potassium, and nickel. The ratio of CO to CO_2 in the evolved gas also was affected by the catalyst selection. Takayuki Takarada and fellow researchers tested 34 coals in a thermogravimetric analyzer (TGA). They found the catalytic effect of K_2CO_3 to be extremely large and nearly independent of coal rank (Takarada, Tamai, and Tomita 679). Nickel was found to be a good catalyst for low rank coals but decreased in efficacy with increasing rank. Takarada and other researchers also demonstrated the tremendous effect an ion-exchanged alkali metal has on the gasification rate (Takarada et al. 505). By using aqueous solutions of NaCl and KCl and a pH-adjusting agent, alkali metals were ion-exchanged to brown coal. The chloride ions were removed by simple water washing. The procedure increased the rate

by a factor of 20 to 30 over that of untreated coal. Liu and Zhu investigated the catalytic effect of alkali and alkaline earth metals on the gasification of Chinese Linnancang coal char (1334). Their experiments were conducted at atmospheric pressure with a reactor temperature of 800°C. Potassium sulfate and potassium carbonate were found to have the greatest catalytic activity. These compounds were followed in catalytic activity by Na_2CO_3, KCl, NaCl, $CaCl_2$, and CaO. Research performed at the University of North Dakota Energy Research Center showed that both pure and mineral forms of alkali carbonates exhibit catalytic activity in the steam gasification of low rank coals (Galegher et al. 1). Four low-rank coals and one bituminous coal were evaluated. Catalysts included in the study were K_2CO_3, Na_2CO_3, trona, nahcolite, sunflower hull ash, and lignite ash. The reactivity measured when using trona and nahcolite was determined to be nearly 3.5 times the gasification rate of uncatalyzed chars. They concluded that these inexpensive, naturally-occurring alkalis could eliminate the need for catalyst recovery operations. The trials were conducted at temperatures ranging from 700°C to 800°C in a laboratory-scale TGA.

Effect of Reactor Conditions and Substrate on Gasification Rate

The gasification rate has been shown to be dependent on the reactor temperature and pressure and the catalyst loading. Van Tuyl and Thomson have shown that increased temperatures effect a much larger reaction rate (60). A TGA was used to perform gasification trials with Michigan Antrim oil shale char. The reaction rate was increased considerably with increasing temperature for both carbon dioxide gasification and steam

gasification. Thomson and Sy also investigated the effect of temperature on gasification rate (225). By increasing the temperature from 700°C to 850°C, it was demonstrated that the gasification rate of Kentucky oil shale char could be increased by a factor of nearly ten for uncatalyzed char and a factor of three for potassium catalyzed char. Elevated pressures were found to have only a small positive effect on gasification rate. The mole fraction of methane in the effluent gas was significantly increased, however. The catalyst loading was found to have very little or no effect at loadings over 10 percent. Schumacher and fellow researchers studied the steam gasification of the low ash German bituminous coal Westerholt (1360). Unlike Thomson and Sy, the researchers showed a considerable increase in reaction rate with increasing pressure below 15 bar. At pressures above 15 bar, an increase in pressure resulted in negligible effects on the rate. The temperature was found to have a strong influence on the rate. Galegher and others also investigated the effects of temperature (16). Experimental trials were performed at 700°C, 750°C, and 800°C. The rate of gasification at 800°C was observed to be 2.5 to 4 times that at 700°C depending on the coal rank.

The rank of a coal has also demonstrated a significant influence on the steam gasification rate. Guo and Zhang determined that the steam gasification activity of coal chars at elevated pressures decreases with increasing coal rank (1366). The highest reactivity was observed for Shenbei lignite char. The least reactive coal was Jingxi anthracite. Hashimoto and fellow researchers observed higher gasification rates for lower rank coals (1521). Coals with a carbon content above 80 percent on a dry ash-free basis were

considerably less reactive. Takarada, Tamai, and Tomita reached similar conclusions with respect to rank (1441). They concluded that coals with a carbon content below 78 percent on a dry ash-free basis were much more reactive than those with higher carbon contents. Researchers at the University of North Dakota Energy Research Center demonstrated the effect of coal rank by a series of TGA experiments performed at 750°C (Galegher et al. 14). Lignite coals were shown to have reactivities nearly ten times greater than that of bituminous coals. Most researchers have concluded that this enhanced reactivity is due to higher mineral content, higher concentrations of active sites, and increased porosity of low-rank coals (Galegher et al. 11).

Gasification of Biomass

The similar carbonaceous character of biomass and coal has allowed processes originally developed for coals to be applied to biomass. Antal notes that, historically, fuel scientists have treated biopolymer materials as low-grade coals (1483). The transferred processes have not been optimized to exploit the unique thermochemical properties of biomass, however (Antal 1483).

Previous Methods of Biomass Gasification

Although there are many parameters which can be used to classify a biomass gasification process, there are three of particular importance. These three process characteristics are the gasification medium, the reactor flow regime, and the energy content of the gaseous

products. The energy content is dependent on both the gasification medium and the reactor flow regime.

Low energy gas (LEG) is a mixture of carbon monoxide, hydrogen, and other gases. The heating values of low energy gases range from 150 to 300 Btu/scf. This low heating value is due to the presence of undesirable components such as nitrogen, carbon dioxide, and water vapor. It may also contain hydrogen sulfide which must be removed before the product gas can be utilized (Lee 97). Medium energy gas (MEG) is a mixture of methane, carbon monoxide, hydrogen, and other gases with a heating value ranging from 300 to 700 Btu/scf. The product gas is used primarily in the synthesis of methanol and higher hydrocarbons via Fischer-Tropsch synthesis (Lee 98). These gases can also be used to produce steam or to drive a gas turbine. High energy gas (HEG) is composed predominately of methane. The heating value of high energy gases is typically between 900 Btu/scf and 1000 Btu/scf. High energy gas is compatible with natural gas and can be utilized as substitute natural gas (Lee 98).

There are four gasification mediums commonly used in gasification. These gases are air, oxygen, steam, and hydrogen. A separate category of gasifiers termed pyrolytic gasifiers utilize no gasification agent. Air-blown gasification produces a low energy gas because it is diluted by large quantities of nitrogen. Although the process requires an independent pyrolytic step, it is relatively simple. About a million air gasifiers were built in the United States during World War II (Solar Energy Research Institute [SERI] I-1).

Oxygen-blown gasifiers are equivalently simple but produce a medium energy gas. The higher heating value is due to the absence of nitrogen. Gasifiers operating with oxygen can achieve a greater fuel throughput as well (Ferguson 4). Steam gasification also produces a medium energy gas. Since no combustion can occur in the reactor, heat must be supplied indirectly from an external source. The superheated steam introduced to the reactor provides a portion of the heat and participates in the gasification mechanism. Hydrogasification utilizes a hydrogen-rich atmosphere and fine particulate feedstocks to produce a high energy gas rich in methane (Ferguson 5). The process requires high pressures and a suitable gasification catalyst. Pyrolytic gasifiers use heat to effect gasification without a gasification agent. The process proceeds by thermal decomposition of the feedstock. The process requires high heating rates and rapid quenching of the product gases to inhibit secondary reactions (Ferguson 5). The product is a medium energy gas composed of carbon monoxide, hydrogen, methane, and other hydrocarbons (SERI I-1).

There are three reactor flow regimes which dominate the area of biomass gasification. They are the updraft fixed bed gasifier, the downdraft fixed bed gasifier, and the fluidized bed gasifier. In fixed bed gasifiers, plugs of the raw biomass fuel are usually gravity-fed through the gasifier (Ferguson 3). Since the reactor operates in this manner, it can contain separate reaction zones for drying, pyrolysis, reduction, and combustion. In updraft gasifiers, the gasification agent flows countercurrent to the fuel flow. These gasifiers can accommodate fuels with moisture contents as high as 30 to 50 percent, high

ash contents, and relatively large fines contents (Ferguson 3). The product gas exits the reactor with a high tar and condensable aqueous content, but is usually low in particulates (Ferguson 3). Problems associated with updraft fixed bed gasifiers include channeling and tar condensation in the upper reactor. In downdraft gasifiers, all gases must pass co-current to the fuel flow. A throat or constriction is generally designed into the gasifier. In a combustion zone near the throat, tar and oil components from the upper reactor gasification zone are thermally cracked (Ferguson 4). The primary contaminants in the product gas generated by downdraft gasifiers are ash and char particulate. Unlike the updraft gasifier, downdraft gasifiers require a relatively low moisture content and fuel of relatively large particle size. The principal problems in downdraft gasifiers are primarily related to fuel quality. They include bridging in the upper reactor, slagging from high ash content, bed plugging from high fines content, and poor gas quality due to excessive fuel moisture (Ferguson 4). Unlike fixed beds, the flow pattern in a fluidized bed reactor is much less predictable. Most fluidized beds utilize an inert granular bed such as hot silica sand. Upon fluidization, the bed expands and experiences intense bubbling and mixing. Rapid heating provided by the hot silica particles dries, pyrolyzes, and gasifies biomass particles as they circulate. In addition to high heat transfer rates, the fluidization provides a relatively uniform bed temperature. The primary advantage conferred by a fluidized bed gasifier is its compatibility with low quality fuels. A fluidized bed reactor can accommodate a wide range of particle sizes, high ash contents, and high moisture feedstocks (Ferguson 4). Unfortunately, the automated control

systems required to operate a fluidized bed reactor make small units uneconomical (Ferguson 4).

Research has been performed on gasifiers with a wide variety of gasification mediums and reactor flow regimes. Battelle-Columbus Laboratories in Columbus, Ohio has conducted research on a medium energy gas process using an indirectly heated fluidized bed with steam as the gasification medium (Schiefelbein 351). The gasifier has been tested with biomass feedstocks including hard and soft wood chips, hogged fuel, and bark strips at feed rates as high as 960 kg/hr. With operating temperatures of 715°C to 1010°C, their process produces gases with heating values ranging from 429 Btu/scf to 513 Btu/scf. The University of Missouri-Rolla has investigated the technical feasibility of using a metal, fired-tube, heat exchanger to provide heat to a fluidized bed gasifier (Schiefelbein 351). Their process utilizes steam as the gasification medium. With wood feed rates of 45 to 180 kg/hr, the gasifier can produce a gas with heating values of 392 to 580 Btu/scf. The Institute of Gas Technology (IGT) in Chicago, Illinois has conducted research with an oxygen-blown, fluidized bed gasifier (Evans et al. 573). Their gasifier has been tested with wood feed rates as high as 465 kg/hr with operating pressures of 83.4 to 345 psia and operating temperatures of 755°C to 900°C. The gas produced had heating values ranging from 309 Btu/scf to 464 Btu/scf. The Solar Energy Research Institute in Golden, Colorado has studied the performance of an oxygen-blown, downdraft fixed bed gasifier (Schiefelbein 353). Their gasifier accommodates wood feed

rates as high as 900 kg/hr. The gaseous product has heating values ranging from 322 Btu/scf to 349 Btu/scf.

Catalytic Steam Gasification of Biomass

The application of the catalytic steam gasification concept to biomass is a relatively new area of research. W.B. Hauserman demonstrated gasification rates comparable to that of lignites when gasifying hybrid poplar (415). The poplar was catalyzed with wood ash at a loading of ten weight percent. Timpe and Hauserman concluded that both hybrid poplar and *Typha augustifolia* possess reactivities similar to low-rank coals in both catalyzed and uncatalyzed conditions (903). Addition of a potassium-rich catalyst increased the reactivity by factors as large as 28. Their experiments were conducted on a laboratory-scale TGA.

Chapter III

Catalytic Steam Gasification Theory

Reaction Mechanisms of Catalytic Steam Gasification

The conversion of coal or biomass to a gaseous product is achieved via a two step process. Primary gasification or devolatilization involves the thermal decomposition of the feedstock to char and volatiles.

$$Biomass \longrightarrow Char + Volatiles \qquad (3 - 1)$$

In general, devolatilization and pyrolysis reactions are endothermic. Volatiles typically generated by primary gasification include tars, phenols, methane, oils, naphtha, H_2S, and some CO and H_2 (Lee 135). The char produced by the primary gasification is the reactant for the secondary gasification reaction. Steam gasification involves the reaction of the char and steam to form a gaseous mixture composed primarily of carbon monoxide, carbon dioxide, hydrogen, and methane. For most situations, it is sufficient to represent the char as pure carbon. There are two steam-carbon reactions participating in the secondary gasification.

$$C + H_2O\,(g) \longrightarrow CO + H_2 \qquad (3 - 2)$$

$$C + 2H_2O\,(g) \longrightarrow CO_2 + 2H_2 \qquad (3 - 3)$$

Both steam-carbon reactions are endothermic with standard heats of reaction of 131.3 kJ/mol and 90.1 kJ/mol, respectively.

The char may also be gasified by reaction with carbon dioxide and hydrogen produced by the steam-carbon reactions. In the Boudouard reaction, carbon dioxide reacts with carbon to form carbon monoxide.

$$C + CO_2 \longrightarrow 2CO \qquad (3-4)$$

This carbon dioxide gasification is endothermic (ΔH^{o}_{298} = 172.5 kJ/mol) and is favored at high temperatures. In hydrogasification, the char reacts with hydrogen to form methane.

$$C + 2H_2 \longrightarrow CH_4 \qquad (3-5)$$

Unlike the reactions discussed to this point, hydrogasification is exothermic with a standard heat of reaction of -74.8 kJ/mol.

The final two reactions of importance in catalytic steam gasification are gas-phase reactions. The water gas shift reaction involves the reaction of steam and carbon monoxide to form carbon dioxide and hydrogen.

$$CO + H_2O\,(g) \longrightarrow CO_2 + H_2 \qquad (3-6)$$

Unlike most gasification reactions, the reaction is slightly exothermic with a standard heat of reaction of -41.2 kJ/mol. The methanation reaction forms methane and steam from carbon monoxide and hydrogen.

$$CO + 3H_2 \longrightarrow CH_4 + H_2O\,(g) \qquad (3-7)$$

The reaction is highly exothermic (ΔH^{o}_{298} = -206.1 kJ/mol) and favored at lower temperatures.

Thermodynamic Effects on Catalytic Steam Gasification

The two areas of concern when assessing the technical feasibility of the catalytic steam gasification of broiler litters are thermodynamics and kinetics. Thermodynamics can be used to evaluate the equilibrium composition of the steam gasification products. Kinetics can be used to evaluate reaction rates and the variables affecting them. By studying both, a more thorough understanding of the catalytic steam gasification process can be achieved.

Computational Algorithm for Equilibrium Compositions

Calculations of equilibrium compositions for the steam gasification reactions are relatively straightforward. The difficulty lies in the solution of a system of nonlinear equations. The solution method developed in this thesis utilizes a gradient descent algorithm to arrive at the appropriate mole fractions.

It is important to note that the equilibrium state of a given set of reactions is not path dependent. In other words, the actual reactions occurring in the reaction system are not important with respect to thermodynamics. This allows the reduction of the six reaction system to one containing only three reactions. The three reactions which are omitted are actually linear combinations of the forward and reverse reactions encompassed in the remaining equations. The three equations selected to represent the system are the

bimolecular steam-carbon reaction, the water gas shift reaction, and the methanation reaction.

$$C + H_2O\,(g) \longrightarrow CO + H_2 \qquad (3\text{-}8)$$

$$CO + H_2O\,(g) \longrightarrow CO_2 + H_2 \qquad (3\text{-}9)$$

$$CO + 3H_2 \longrightarrow CH_4 + H_2O\,(g) \qquad (3\text{-}10)$$

The equilibrium mole fractions for this three reaction system will be identical to that for the six reaction system introduced earlier.

The equilibrium constant K for each reaction is a function of temperature only. The standard Gibbs energy of each reaction ΔG^o is related to the respective equilibrium constant.

$$\Delta G^o = -RT \ln K \qquad (3\text{-}11)$$

The effect of temperature on each equilibrium constant is related to the standard heat of reaction ΔH^o. The differential and integrated forms of the relationship are shown below. The symbol I in Equation *(3-13)* is an integration constant.

$$\frac{d \ln K}{dT} = \frac{\Delta H^o}{RT^2} \qquad (3\text{-}12)$$

$$\ln K = \int \frac{\Delta H^o}{RT^2} dT + I \qquad (3\text{-}13)$$

A general expression for the heat of reaction and the ideal gas heat capacity C_p^o are then substituted into the integral. The symbol J in Equation *(3-14)* is an integration constant.

$$\Delta H^o = J + \int \Delta C_p^o \, dT \qquad (3 - 14)$$

$$\frac{C_p^o}{R} = A + BT + CT^2 + DT^{-2} \qquad (3 - 15)$$

Upon substitution and integration, a generalized expression for the equilibrium constant is obtained.

$$\ln K = -\frac{J}{RT} + \Delta A \ln T + \frac{\Delta B}{2} T + \frac{\Delta C}{6} T^2 + \frac{\Delta D}{2T^2} + I \qquad (3 - 16)$$

The first step in the calculation of equilibrium compositions is to obtain an expression for the three reactions of interest.

Next, expressions for the equilibrium constant in terms of pressure and the mole fraction of each species are developed. The definition of the equilibrium constant K_j for reaction j is given below. The activity for each species i is represented by $\hat{a}_i$. The stoichiometric coefficient for species i in reaction j is represented by $\upsilon_{i,j}$.

$$K_j = \prod (\hat{a}_i)^{\upsilon_{i,j}} \qquad (3 - 17)$$

The activity of a pure solid is equal to $\frac{f_i}{f_i^o}$ where f_i and f_i^o represent the fugacity and the standard state fugacity, respectively. Since the effect of pressure on the fugacity of a solid is very small, negligible error is introduced by assuming that this ratio is unity (Smith and Van Ness 533). The activity of each gaseous species is equal to $\frac{\hat{f}_i}{f_i^o}$. The

standard state fugacity of each species is equal to 1 bar. The fugacity of a gaseous species is given by Equation *(3-18)*. The fugacity coefficient is represented by $\hat{\phi}_i$.

$$\hat{f}_i = \hat{\phi}_i y_i P \qquad (3 - 18)$$

At low to moderate pressures, the mixture is nearly ideal and the fugacity coefficients can be approximated as unity with no significant error. The equilibrium constant expression for each reaction in terms of activities is shown below.

$$K_1 = \frac{a_{CO}\, a_{H_2}}{a_C\, a_{H_2O}} \qquad (3 - 19)$$

$$K_2 = \frac{a_{CO_2} a_{H_2}}{a_{CO}\, a_{H_2O}} \qquad (3 - 20)$$

$$K_3 = \frac{a_{CH_4}\, a_{H_2O}}{a_{CO}\, a_{H_2}^3} \qquad (3 - 21)$$

By applying the assumptions of ideality of the gas and solid phases, the equilibrium constants can be expressed as functions of pressure and component mole fractions.

$$K_1 = \frac{y_{CO}\, y_{H_2}}{y_{H_2O}} P \qquad (3 - 22)$$

$$K_2 = \frac{y_{CO_2}\, y_{H_2}}{y_{CO}\, y_{H_2O}} \qquad (3 - 23)$$

$$K_3 = \frac{y_{CH_4}\, y_{H_2O}}{y_{CO}\, y_{H_2}^3} P^{-2} \qquad (3 - 24)$$

The mole fractions can now be expressed in terms of the reaction coordinates ε_j. The symbols n_{io} and n_o represent the initial molar quantities of each species i and the initial total molar quantity, respectively.

$$y_i = \frac{n_{io} + \sum_j \upsilon_{i,j}\,\varepsilon_j}{n_o + \sum_j \upsilon_j \varepsilon_j} \qquad (3 - 25)$$

The equilibrium constants in terms of reaction coordinates can be incorporated into three nonlinear functions F_j. The values of the reaction coordinates satisfying the equations represent the equilibrium state.

$$F_1(\varepsilon_1,\varepsilon_2,\varepsilon_3) = \frac{y_{CO}\,y_{H_2}}{y_{H_2O}} P - K_1 = 0 \qquad (3 - 26)$$

$$F_2(\varepsilon_1,\varepsilon_2,\varepsilon_3) = \frac{y_{CO_2}\,y_{H_2}}{y_{CO}\,y_{H_2O}} - K_2 = 0 \qquad (3 - 27)$$

$$F_3(\varepsilon_1,\varepsilon_2,\varepsilon_3) = \frac{y_{CH_4}\,y_{H_2O}}{y_{CO}\,y_{H_2}^{\,3}} P^{-2} - K_3 = 0 \qquad (3 - 28)$$

The nonlinear system of functions F_1, F_2, and F_3 has a solution at $\vec{\varepsilon} = (\varepsilon_1,\varepsilon_2,\varepsilon_3)^t$ precisely when the function g defined by

$$g(\varepsilon_1,\varepsilon_2,\varepsilon_3) = \sum_{j=1}^{3} \left[F_j(\varepsilon_1,\varepsilon_2,\varepsilon_3)\right]^2 \qquad (3 - 29)$$

has the minimal value zero. The multivariable function g maps the three-dimensional space $\Re^3$ into the real space $\Re$. The directional derivative of g at $\vec{\varepsilon}$ in the direction of the three-dimensional unit vector $\vec{v}$ is defined by

$$D_v\, g(\vec{\varepsilon}) = \lim_{h \to 0} \frac{1}{h} \left[g(\vec{\varepsilon} + h\vec{v}) - g(\vec{\varepsilon}) \right] \qquad (3 - 30)$$

It is easily shown that the maximum value for the directional derivative occurs when $\vec{v}$ is chosen to be parallel to $\nabla g(\vec{\varepsilon})$, provided that $\nabla g(\vec{\varepsilon}) \neq 0$. The direction of steepest descent is therefore given by $-\nabla g(\vec{\varepsilon})$.

$$\nabla g(\vec{\varepsilon}) = \left(\frac{\partial g}{\partial \varepsilon_1}(\vec{\varepsilon}), \frac{\partial g}{\partial \varepsilon_2}(\vec{\varepsilon}), \frac{\partial g}{\partial \varepsilon_3}(\vec{\varepsilon}) \right)^t \qquad (3 - 31)$$

Since the object is to minimize $g(\vec{\varepsilon})$, an appropriate choice for $\vec{\varepsilon}^{(n+1)}$ is

$$\vec{\varepsilon}^{(n+1)} = \vec{\varepsilon}^{(n)} - \alpha \nabla g\left(\vec{\varepsilon}^{(n)}\right) \qquad (3 - 32)$$

where α is greater than zero. The value of α is determined by minimizing the function g along the line containing the vector $-\nabla g(\vec{\varepsilon})$. This function of limited domain is represented by the function $h(\alpha)$.

$$h(\alpha) = g\left(\vec{\varepsilon}^{(n)} - \alpha \nabla g\left(\vec{\varepsilon}^{(n)}\right)\right) \qquad (3 - 33)$$

The value of α that minimizes h is determined by fitting a quadratic polynomial through three points in the restricted domain. After the improved value of $\vec{\varepsilon}$ is calculated, the process is iterated until the value converges to within an allowable tolerance.

The gradient ∇g is a column vector containing three elements. This column vector is obtained from the following equation where $J(\vec{\varepsilon})^t$ is the transpose of the Jacobian matrix and $F(\vec{\varepsilon})$ is the column vector with the values of F_1, F_2, and F_3 as elements.

$$\nabla g(\varepsilon_1, \varepsilon_2, \varepsilon_3) = 2\, J(\vec{\varepsilon})^t\, F(\vec{\varepsilon}) \qquad (3 - 34)$$

This algorithm has been incorporated into a FORTRAN program. The program is included in Appendix I. The program was utilized in the calculation of equilibrium compositions for various temperatures, pressures, and hydrogen-to-oxygen ratios. The influence of these process variables is discussed in the following section.

Effect of Reactor Conditions on Equilibrium Composition

The FORTRAN algorithm outputs the equilibrium mole fraction of carbon monoxide, carbon dioxide, methane, hydrogen, and steam. The three variables used to specify the equilibrium system are the temperature, pressure, and hydrogen-to-oxygen atomic ratio. A typical output from the equilibrium program is included in Appendix II.

The effect of temperature on the equilibrium composition of a reaction system is dependent on the heats of reaction. Endothermic reactions are shifted toward their products as temperature increases. On the other hand, exothermic reactions are shifted toward their reactants as temperature increases. In the three reaction system, the bimolecular steam-carbon reaction is endothermic. The water gas shift and methanation reactions are exothermic. The effect of temperature on each equilibrium mole fraction is readily apparent. The production of methane and carbon dioxide is favored at lower temperatures. Carbon monoxide and hydrogen production are favored at higher temperatures. The equilibrium mole fraction of steam decreases with increasing temperature. Since the rate of a reaction is dependent on the displacement from

equilibrium, higher steam-carbon reaction rates are expected when the equilibrium mole fraction of steam is small. In other words, the lower equilibrium mole fractions of steam at high temperatures may contribute to higher gasification rates at those temperatures. The effect of temperature on equilibrium composition is shown graphically for two system pressures. The effects of temperature at 150 psia and 500 psia are shown in Figures 3.1 and 3.2, respectively.

The pressure of a reaction system also affects the equilibrium composition. An increase in system pressure shifts the equilibrium of a reaction toward the side containing the lower number of gas-phase molecules. A decrease in system pressure shifts the equilibrium of a reaction toward the side containing the higher number of gas-phase molecules. Since the water gas shift reaction contains an equal number of gas-phase molecules in the reactants and products, the equilibrium of the reaction is unaffected by pressure. The production of carbon monoxide and hydrogen in the steam-carbon reaction is favored at low pressures. The production of carbon dioxide and methane is favored at higher pressures. It is important to note that steam is capable of reacting to a much further extent at low pressures. Figure 3.3 exhibits the effect of pressure on equilibrium composition at 1300°F in a reaction system with a hydrogen-to-oxygen atomic ratio of 1.00.

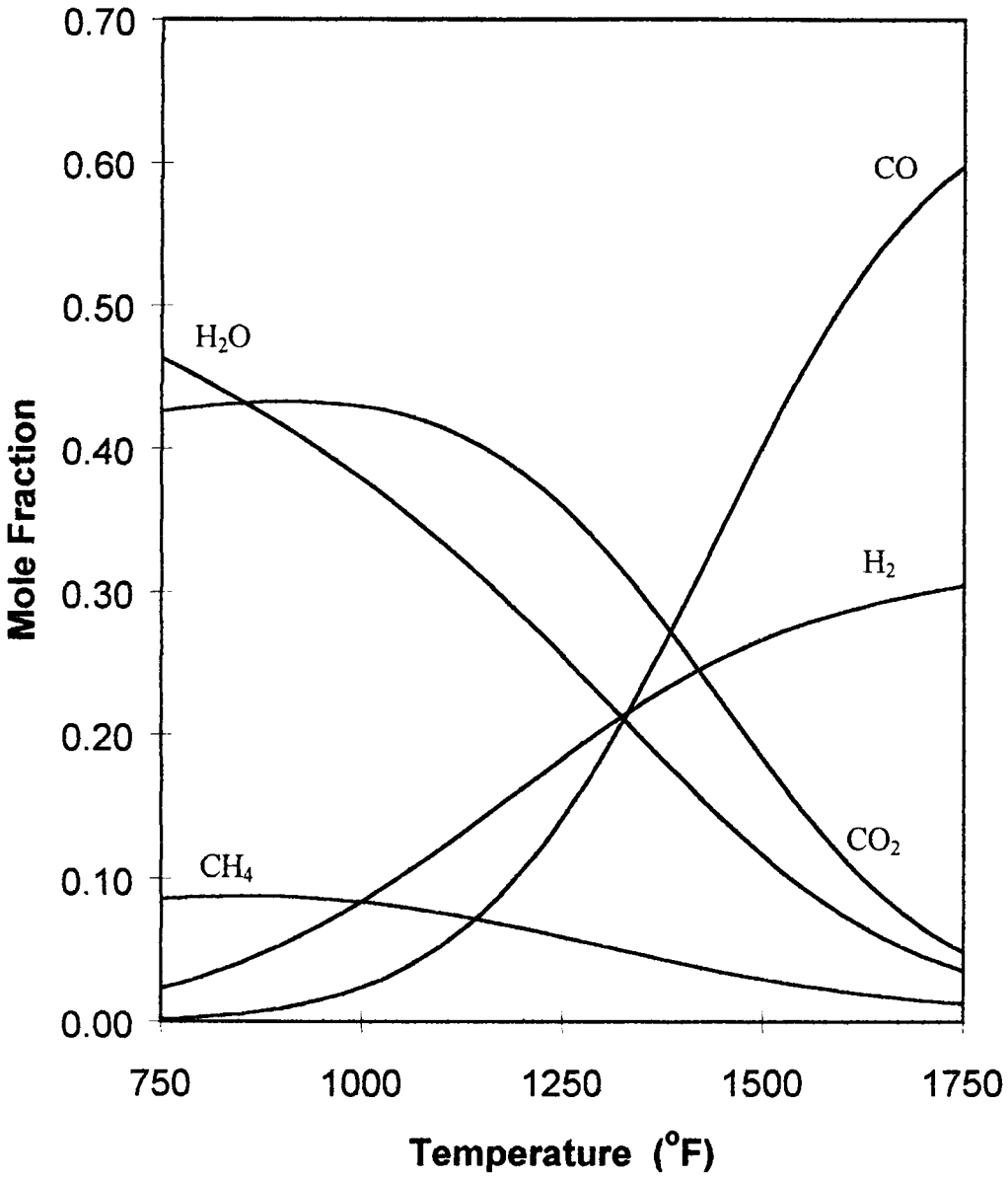

Figure 3.1 Effect of Temperature on Equilibrium Composition – 150 psia, H/O = 1.00

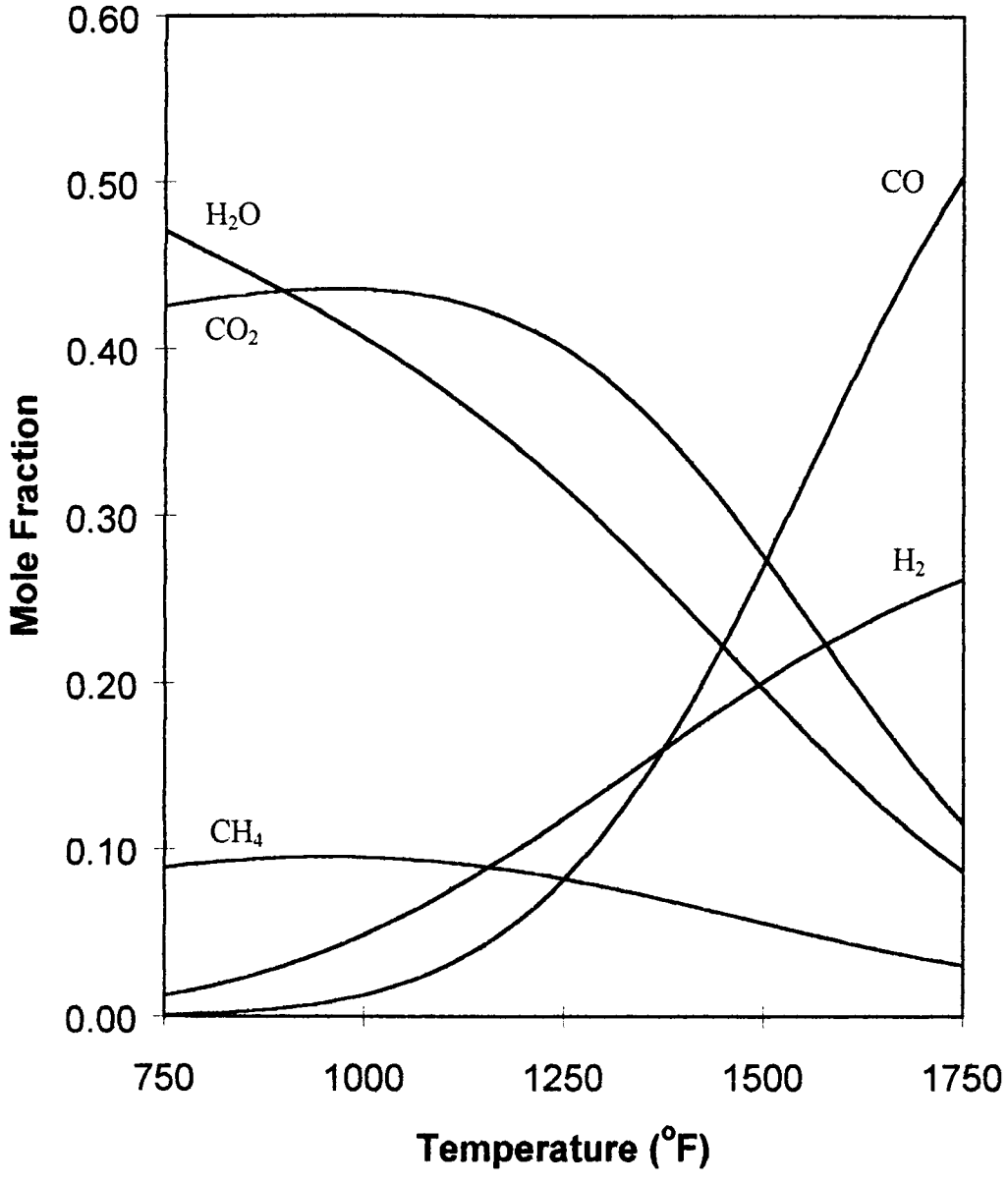

Figure 3.2 Effect of Temperature on Equilibrium Composition – 500 psia, H/O = 1.00

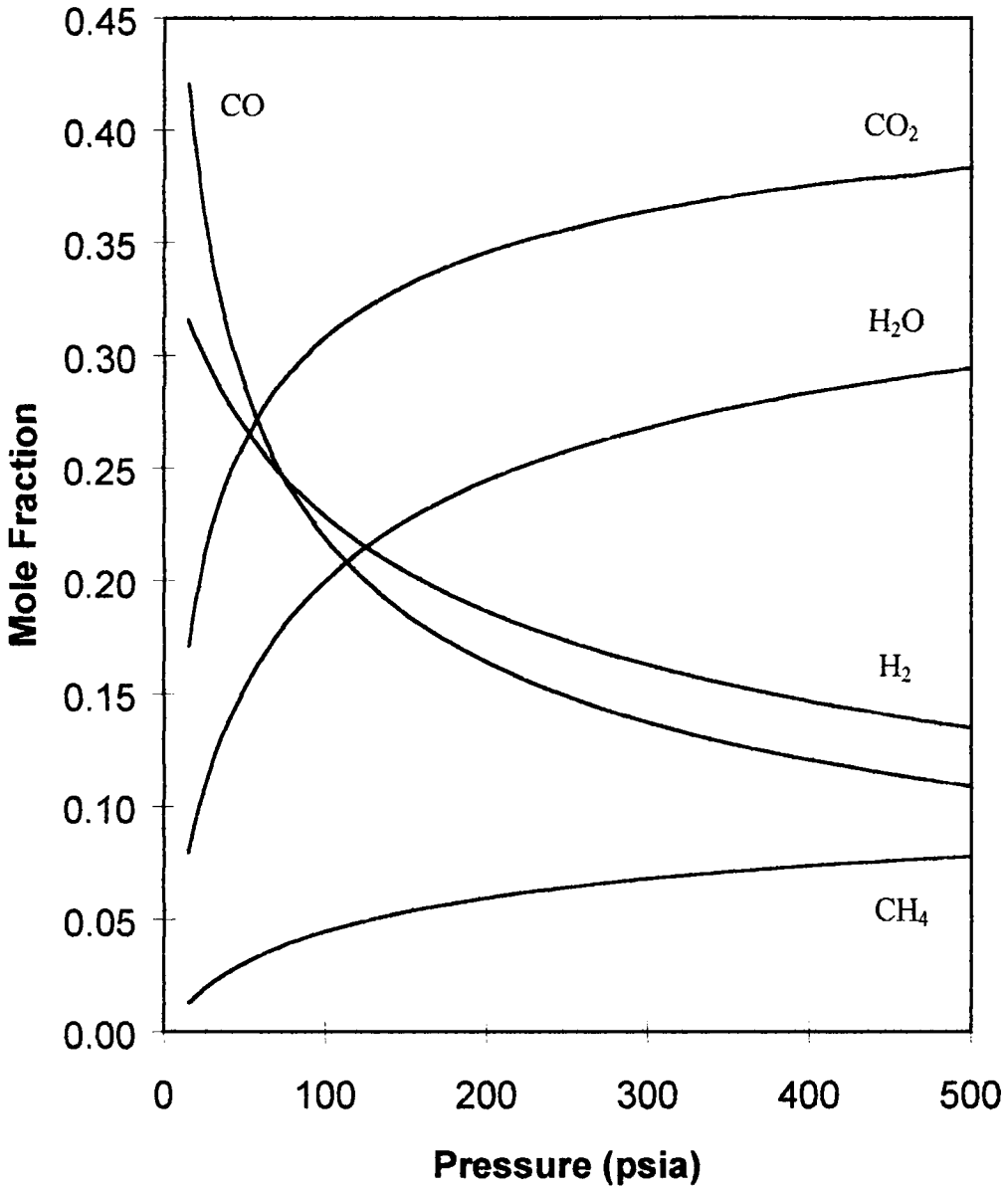

Figure 3.3 Effect of Pressure on Equilibrium Composition – 1300°F, H/O = 1.00

The hydrogen-to-oxygen atomic ratio of a reaction system also affects the equilibrium composition. In a reactor with pure steam feed, the ratio will be very close to two. At low hydrogen-to-oxygen ratios, the equilibrium favors carbon monoxide and carbon dioxide. At high hydrogen-to-oxygen ratios, the formation of methane and hydrogen are favored. Figure 3.4 illustrates the effect of the hydrogen-to-oxygen atomic ratio at a temperature of 1300°F and a pressure of 150 psia.

Kinetics of Catalytic Steam Gasification

Previous research has determined that the rate-controlling reaction in catalytic steam gasification is the steam-carbon reaction.

$$C + H_2O\,(g) \longrightarrow CO + H_2 \qquad (3\text{-}35)$$

The reaction rate is dependent on the mass of carbon present and the concentration of steam in the gas phase. With excess steam, however, the reaction rate is effectively dependent on the mass of carbon only. Hauserman has determined that in the presence of excess steam the reaction order n is generally near one (413). Since this classification requires the condition of excess steam, it is termed pseudo first-order.

To evaluate the steam-carbon reaction dynamics, a material balance is necessary. The material best describing the system is the solid carbon in the fixed bed. A generic material balance equation on carbon is shown below.

$$input + generation = output + consumption + accumulation \qquad (3\text{-}36)$$

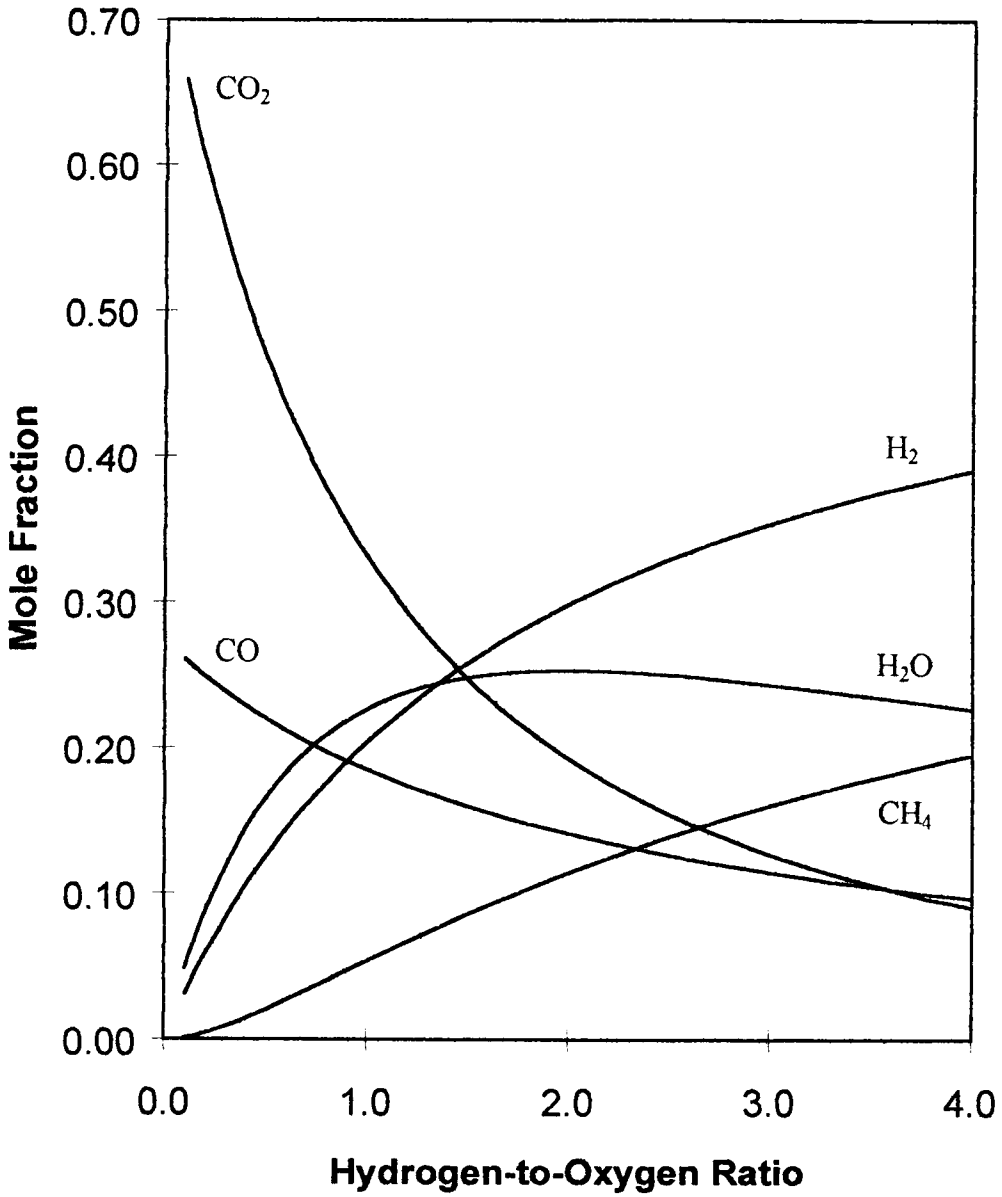

Figure 3.4 Effect of Hydrogen-to-Oxygen Atomic Ratio on Equilibrium Composition – 1300°F, 150 psia

The input and output terms are obviously zero since no solid carbon is carried to or from the bed in a fixed bed system. The generation term is also zero since there are no reactions in the system with solid carbon as a product. After elimination of these terms, the material balance is simplified.

$$consumption + accumulation = 0 \qquad (3 - 37)$$

The consumption term represents the disappearance of solid carbon by reaction. Using the convention of Levenspiel, the reaction rate of solid carbon is based on the unit mass of solid in the fluid-solid system (5). Since the rate is defined per unit mass, it is referred to as a specific reaction rate. The decomposition rate of carbon is symbolized by $-r_c$ and has units of $\frac{mol\ C}{(hr)(g\ C)}$. The mass of carbon remaining in the bed at any time is symbolized by W. Since $-r_c$ is a specific rate, it must be multiplied by the mass of solid carbon W to obtain the absolute rate of consumption.

$$consumption = (-r_c)(W) \qquad (3 - 38)$$

The accumulation term represents the rate of change of the moles of solid carbon in the bed to gaseous products with respect to time. The moles of carbon in the bed at any time is symbolized as N_c.

$$accumulation = \frac{dN_c}{dt} \qquad (3 - 39)$$

These representations of the consumption and accumulation terms can be substituted into the simplified material balance.

$$(-r_c)W + \frac{dN_c}{dt} = 0 \qquad (3-40)$$

$$(-r_c)W = -\frac{dN_c}{dt} \qquad (3-41)$$

Upon rearrangement, the specific reaction rate is expressed in terms of W and N_c.

$$-r_c = -\frac{1}{W}\frac{dN_c}{dt} \qquad (3-42)$$

The mass of carbon in the bed can be related to the initial mass of carbon W_o and the carbon conversion X.

$$W = W_o(1-X) \qquad (3-43)$$

$$\frac{dW}{dt} = -W_o\frac{dX}{dt} \qquad (3-44)$$

The mass of carbon in the bed can also be related to the moles of carbon present and the atomic weight of carbon M_c.

$$W = M_c N_c \qquad (3-45)$$

$$\frac{dW}{dt} = M_c\frac{dN_c}{dt} \qquad (3-46)$$

$$\frac{dN_c}{dt} = \frac{1}{M_c}\frac{dW}{dt} \qquad (3-47)$$

The specific reaction rate in terms of the mass of carbon present is shown below.

$$-r_c = -\frac{1}{WM_c}\frac{dW}{dt} \qquad (3-48)$$

$$-r_c = -\frac{1}{M_c}\frac{\frac{dW}{dt}}{W} \qquad (3-49)$$

By substituting appropriate expressions for $\frac{dW}{dt}$ and W, the specific reaction rate $-r_c$ can be expressed in terms of carbon conversion.

$$-r_c = \frac{1}{M_c}\frac{W_o\frac{dX}{dt}}{W_o(1-X)} \qquad (3-50)$$

$$-r_c = \frac{1}{M_c}\frac{\frac{dX}{dt}}{1-X} \qquad (3-51)$$

Since the gasification rate or specific reaction rate is based on the unit mass of solid, the rate is expected to remain constant with increasing conversion. There are some exceptions to this hypothesis, however. Lee notes that the specific gasification rate in coal gasification generally remains constant through 80 percent conversion (145). At further conversions, specific reaction rates decrease to some extent. If any catalysts are utilized, the assumption of constant specific reaction rates is not valid (Lee 145). The catalytic activity varies considerably even under constant environmental conditions. Finally, if agglomeration occurs during the primary gasification, there may be inhibition of gaseous diffusion during secondary gasification (Lee 145). Very low initial specific reaction rates are observed. They typically increase with increasing conversion since these restrictions are removed and more internal char surface becomes available to the reacting atmosphere (Lee 145).

The carbon conversion can be predicted at any time t if the assumption of constant specific reaction rate is applied. This constant gasification rate is denoted by the symbol G. The differential equation relating this constant rate to the carbon conversion X is given below.

$$G = \frac{1}{M_c} \frac{\frac{dX}{dt}}{1 - X} \qquad (3 - 52)$$

The equation is easily solved by separation of variables to yield an expression for the carbon conversion as a function of time.

$$G M_c \, dt = \frac{dX}{1 - X} \qquad (3 - 53)$$

$$G M_c t = -\ln (1 - X) \qquad (3 - 54)$$

$$1 - X = e^{-G M_c t} \qquad (3 - 55)$$

$$X = 1 - e^{-G M_c t} \qquad (3 - 56)$$

For a constant gasification rate G, it is apparent that the carbon conversion X will approach one as the time t approaches infinity.

The specific gasification rate in catalyzed systems is generally constant at low to moderate conversions. At higher conversions, however, the gasification rate may change considerably. In some situations, the catalyst will become more active with increasing conversion. This catalyst activation will result in an increasing specific rate. In other cases, the catalyst will become less active with increasing conversion. This catalyst

deactivation will result in a decreasing specific rate. Although most catalytic steam gasification processes exhibit catalyst activation or deactivation, it is possible for a catalyst to maintain constant activity at all conversions. The effect of catalysis on the specific rate is shown in Figure 3.5. At high carbon conversions, the gasification rate increases in the case of catalyst activation and decreases in the case of catalyst deactivation. The conversion is determined by numerical approximation of the differential equation relating G and X using the method of Euler. The values of the specific rates utilized in the determination of the hypothetical conversion curves are taken from Figure 3.5. The method of Euler calculates the value of $\frac{dX}{dt}$ at a given conversion X_i. The value of this derivative with respect to time is then used to approximate the subsequent value of the conversion X_{i+1}.

$$X_{i+1} = X_i + \frac{dX}{dt}\Delta t \qquad (3 - 57)$$

The effect of catalytic activity on carbon conversion is demonstrated in Figure 3.6. When the specific reaction rate is not known, carbon conversion data can be used to obtain the rate. The linear relationship between $-\ln(1-X)$ and time is shown in the equation below.

$$-\ln(1-X) = G\,M_c\,t \qquad (3 - 58)$$

When a plot of $-\ln(1-X)$ versus t is constructed, the specific reaction rate can be determined from the slope of the linear portion of the curve. Figure 3.7 demonstrates the

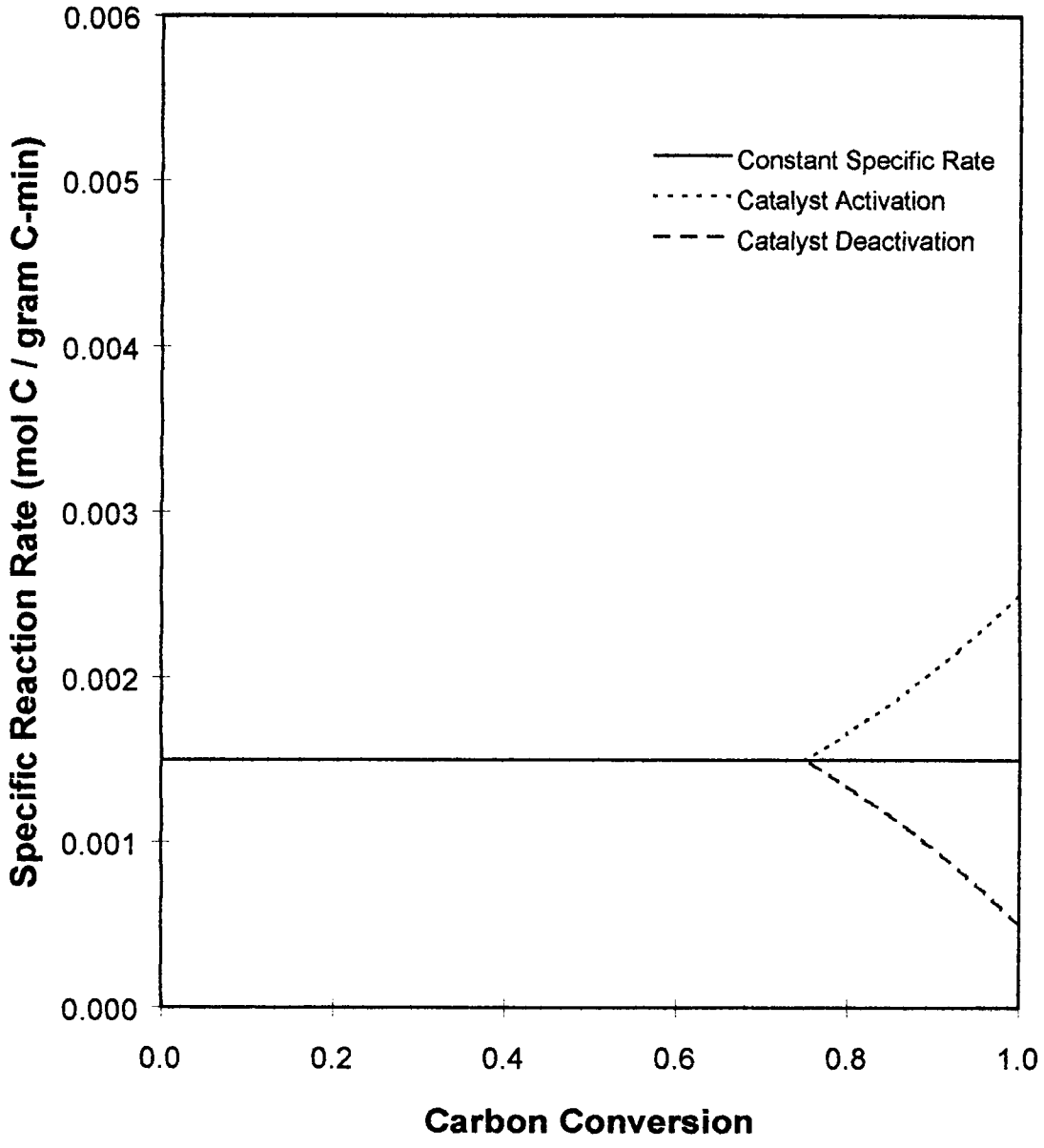

Figure 3.5 Effect of Catalytic Activity on Specific Reaction Rate

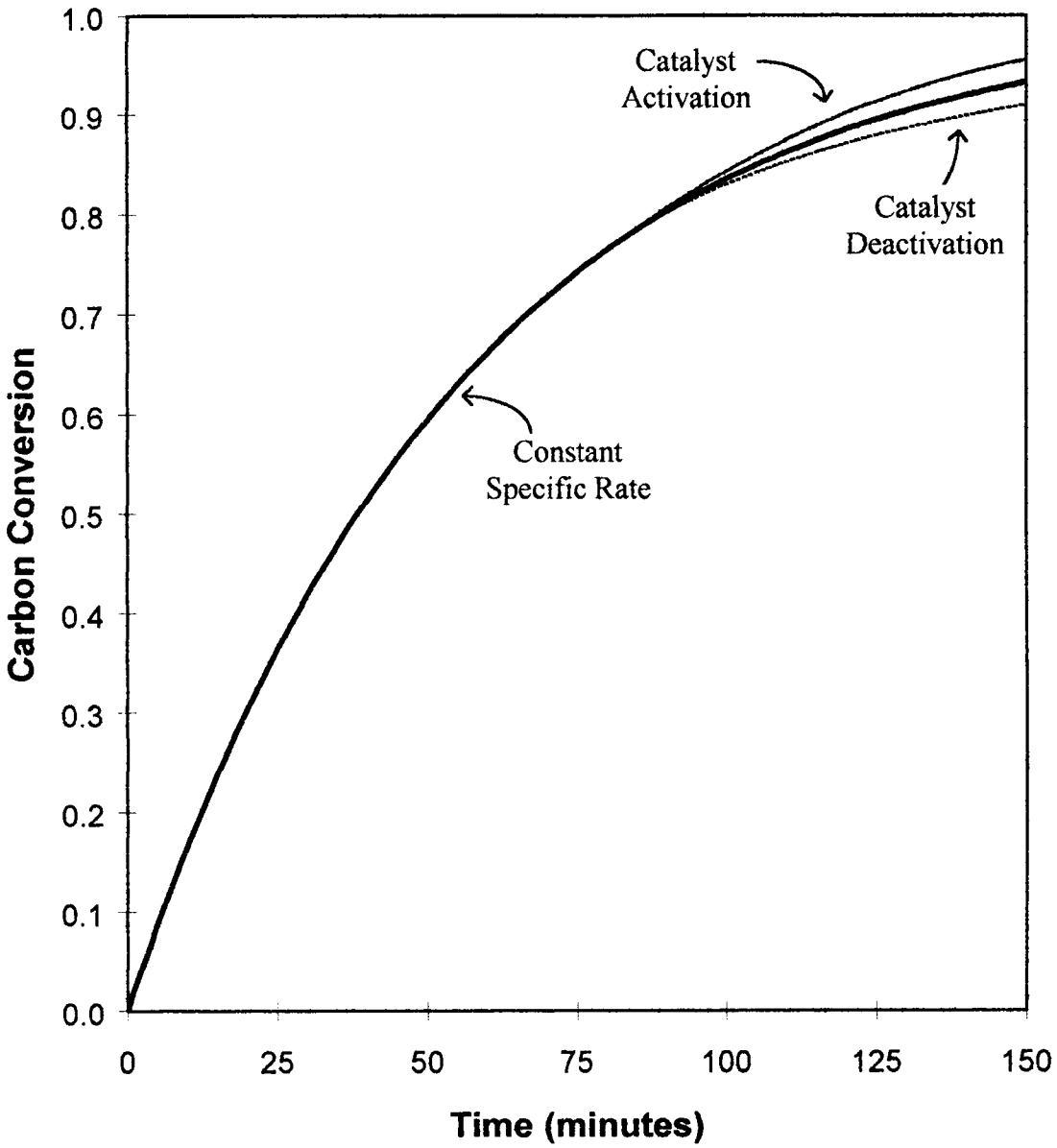

Figure 3.6 Effect of Catalytic Activity on Carbon Conversion

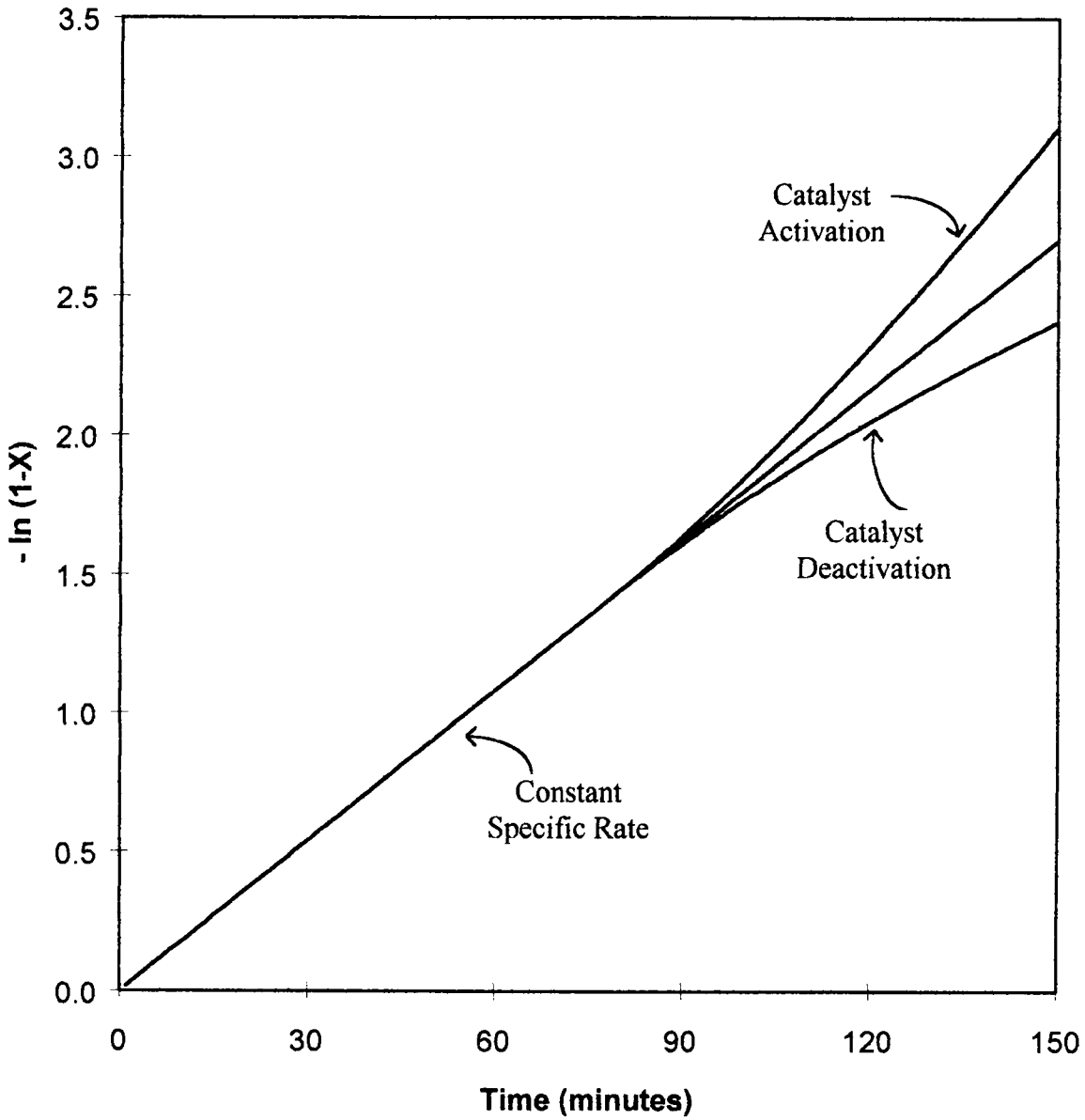

Figure 3.7 Determination of Specific Gasification Rate for Catalytic Reactions

effect of catalytic activation or deactivation on the curve. In the case of catalytic activation, the slope of the curve increases at high conversions. In the case of catalytic deactivation, however, the slope of the curve decreases with increasing carbon conversion.

Chapter IV

Experimental Methods

Analysis of Broiler Litter, Broiler Litter Char, and Ash

The first stage in the analysis of a broiler litter sample is the determination of the moisture, volatiles, and ash contents. Fresh broiler litter has a relatively large moisture content. To determine this moisture content, a 50-gram sample was heated in a Precision Gravity Convection Oven for 72 hours at 105°C. The sample mass before and after drying was measured with a Mettler PM2000 analytical balance. The percent moisture content was calculated from the initial and final masses.

$$Percent\ Moisture = \frac{m_{initial} - m_{final}}{m_{initial}} \times 100\% \qquad (4\text{-}1)$$

The value represents the percentage of the original sample mass attributable to moisture.

The determination of volatile content and ash content was performed with a Perkin-Elmer TGA 7 Thermogravimetric Analyzer. The TGA is essentially a temperature-controlled furnace equipped with an internal microbalance. The composition of the TGA furnace atmosphere can be controlled by the addition of both inert and reactive gases. The volatiles content was measured by heating the furnace and a fresh broiler litter sample to 1000°C at a rate of 7.5 degrees Celsius per minute. The pyrolysis reaction was achieved by maintaining an inert atmosphere of argon gas. The overall weight loss is

attributable to the loss of both moisture and volatiles. To calculate the percent volatiles content in the fresh sample, the moisture contribution must be removed from the weight loss. In the equation below, w_{H_2O} represents the moisture mass fraction in the fresh broiler litter.

$$Percent\ Volatiles = \frac{\left(1 - w_{H_2O}\right) m_{initial} - m_{final}}{m_{initial}} \times 100\% \qquad (4 - 2)$$

The percentage of volatiles present in the dry litter was calculated by dividing the fresh litter percentage by $1 - w_{H_2O}$. The TGA output clearly exhibits a region evident of moisture loss and a separate region evident of the loss of volatiles.

The ash fraction was also determined with the thermogravimetric analyzer. A sample of pyrolyzed broiler litter or char was heated to 800°C at a rate of 5.0 degrees Celsius per minute. Unlike the pyrolysis reaction conducted in the TGA, this reaction utilized an oxygen atmosphere. At approximately 300°C, the fixed carbon in the sample will combust. The remaining residue composed primarily of mineral matter is termed ash. The equation below expresses the percentage ash in the fresh broiler litter in terms of the initial and final masses, the moisture fraction w_{H_2O}, and the volatile fraction w_{vol}.

$$Percent\ Ash = \left(1 - w_{H_2O} - w_{vol}\right)\left(\frac{m_{initial} - m_{final}}{m_{initial}}\right) \times 100\% \qquad (4 - 3)$$

The percentage of ash present in the dry litter was calculated by dividing the fresh litter percentage by $1 - w_{H_2O}$. In the ash fraction experiments, the TGA exhibits a sharp weight loss corresponding to the fixed carbon combustion.

Since certain minerals may either enhance or inhibit catalytic steam gasification, it is important to evaluate the contents of the ash. Approximately five grams of char was heated to 1300°F in a Lindberg Sola Basic Type 51441 furnace. The original char mass and the ash mass were measured with a Mettler PM2000 analytical balance. The metal constituents of the ash were then dissolved in hot aqua regia for two hours. The aqua regia contained a 2:1 ratio of hydrochloric and nitric acids. The supernatant was then filtered of remaining solids. The solid content represented silica and other insoluble minerals. The supernatant volume was subsequently increased to 250 ml in a volumetric flask. The composition of the supernatant solution was then analyzed with a Perkin-Elmer Plasma 40 Emission Spectrometer. This analytical instrument operates on the principle of atomic absorption. The excitation of the atoms is effected by inductively coupled plasma (ICP). The metals are quantified based on the characteristic wavelength and the relative intensity of emissions at that wavelength. Appropriate calculations were then performed to convert the supernatant concentration to an acceptable basis.

The broiler litter and broiler litter char also contain a small quantity of sulfur. Since large hydrogen sulfide concentrations are deleterious to low energy gases, it is important to measure these sulfur levels. A LECO SC132 Sulfur Determinator was used to measure the sulfur content of the char. The LECO Sulfur Determinator heats the sample in an oxidizing environment and measures the sulfur dioxide concentration in the effluent gas with an infrared (IR) detector.

Pyrolysis of Broiler Litter

As mentioned earlier, the primary gasification of carbonaceous compounds generates both char and volatiles. In a bench-scale apparatus, products from this pyrolysis process may interfere with the subsequent secondary gasification. For example, tars and oils, which are volatile at pyrolysis temperatures, may condense at lower temperatures. These compounds may then foul the apparatus or even interfere with operating procedures. For this reason, the production of char was performed in an apparatus devoted to the task.

The pyrolysis apparatus is depicted in Figure 4.1. The unit was operated as a horizontal, fixed bed reactor. The feedstock, fresh broiler litter, was fixed between two 200-mesh stainless steel screens within a 1.25-inch outer diameter (OD), Schedule 40 stainless steel pipe. This reactor was mounted inside a Mellen Model TS-2200-231-3 split-tube furnace. A gas cylinder and regulator provided continuous nitrogen flow through the apparatus. The nitrogen provided the inert conditions necessary for primary gasification. A type K thermocouple and Omega Model 650 thermocouple meter monitored the pyrolysis temperature continuously. The volatile products of pyrolysis were carried by the nitrogen carrier gas to a condenser where condensable products were removed before the gas stream was vented. This apparatus can pyrolyze several hundred grams of broiler litter in a typical pyrolysis run. The reactor was first loaded with fresh broiler litter. The nitrogen flow was then established. After the reactor was purged of oxygen, the furnace temperature was ramped to 1300°F. The furnace was held at this temperature for six

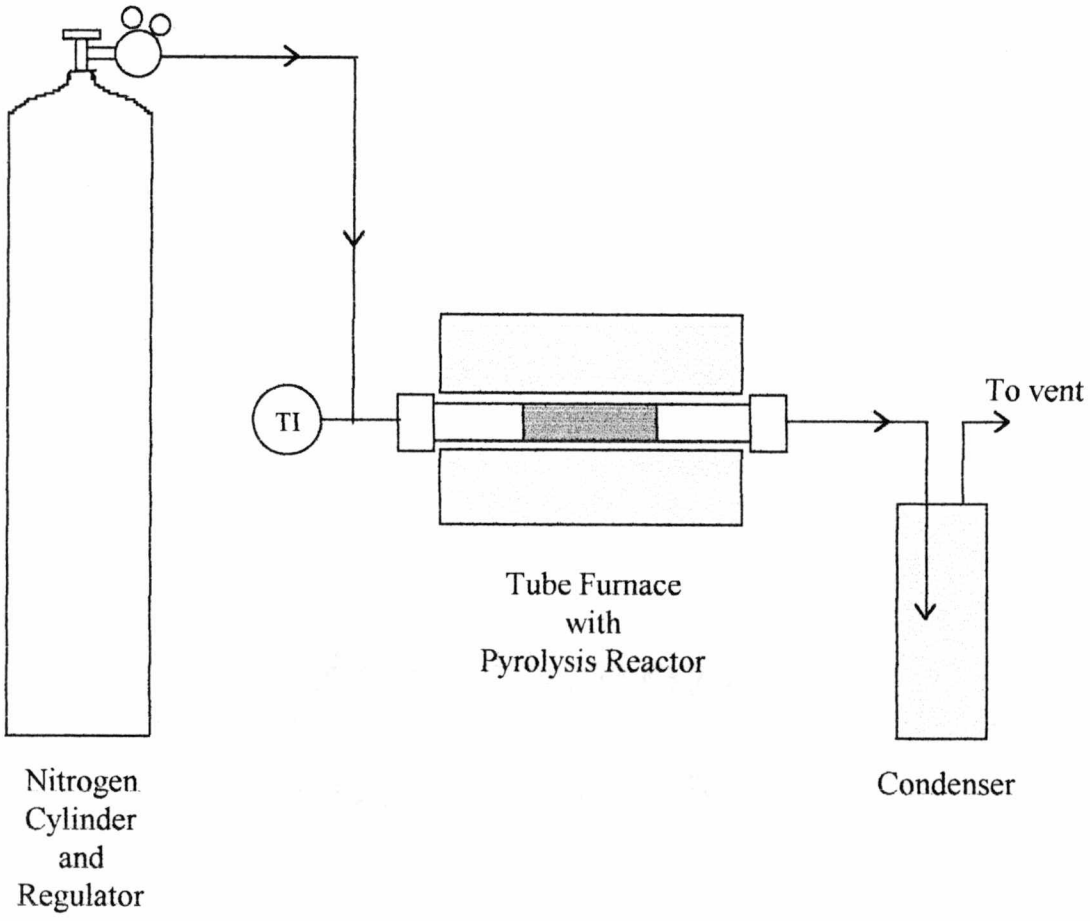

Figure 4.1. Apparatus for Pyrolysis of Broiler Litter

hours. The resulting char was kept under nitrogen flow until the furnace cooled to room temperature. Small samples of the broiler litter char were then used for experimental trials in the gasification apparatus. The complete operating procedures for the pyrolysis apparatus are detailed in Appendix III.

Catalytic Steam Gasification Experiments

Catalytic steam gasification experiments were conducted in a high-pressure fixed bed gasifier apparatus. The apparatus was typically operated with a downdraft flow regime and a differential fixed bed. The apparatus was designed to operate in both a startup and gasification mode.

The most important portion of the apparatus was obviously the reactor. The reactor body is constructed of ¾-inch Type 304 stainless steel tubing. The wall thickness of 0.065 inches allowed a working pressure in excess of 800 psia at a temperature of 1300°F. The char sample to be analyzed was supported by two 200-mesh stainless steel screens in the center of the reactor. Ceramic beads below the reactor provided support for the fixed bed. Ceramic beads above the char provided adequate mixing and distribution of the inlet gases. The reactor had stainless steel caps on each end of the tubing. Each cap had a ⅛-inch NPT port. A Type K thermocouple was mounted so that continuous monitoring of the reactor temperature was possible. A schematic of the differential fixed bed reactor is shown in Figure 4.2.

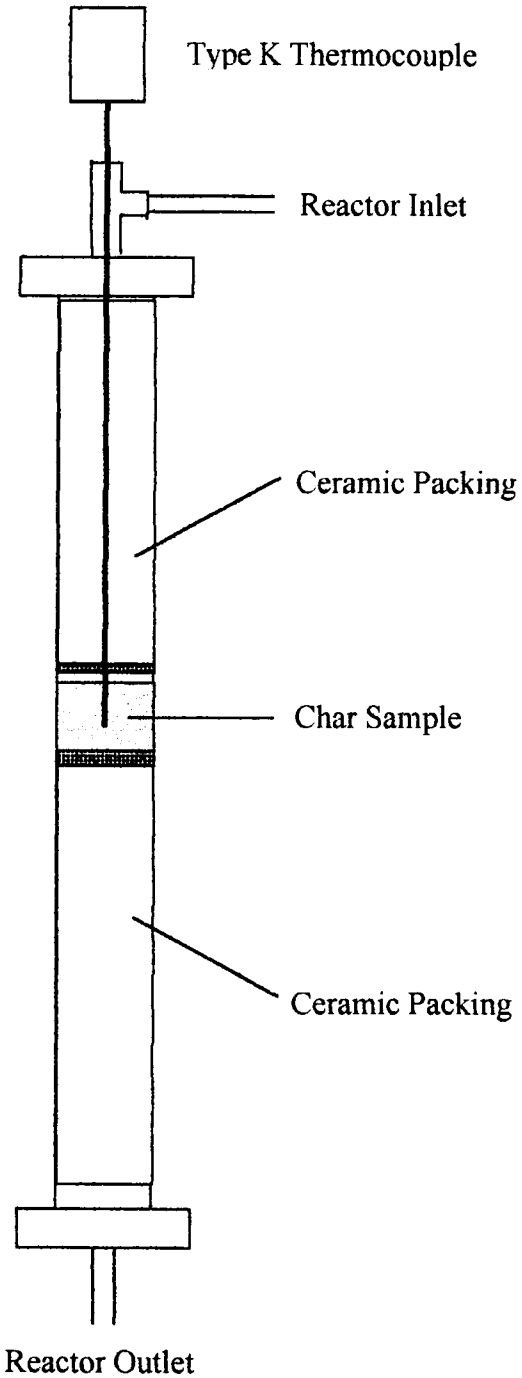

Figure 4.2. Schematic of Differential Fixed Bed Reactor

The high-pressure fixed bed gasifier apparatus was operated in the startup mode until steady state operating conditions were established. During startup, two independent flow paths were present in the apparatus. The first flow path generated steam and preheated any other reactive gases to be introduced to the reactor. The second flow path passed nitrogen through the reactor during startup. This inert gas prevented oxidation of the char sample during reactor heating. Since the apparatus required these accommodations during startup, the apparatus was considerably more complex than the pyrolysis apparatus. The flow paths during startup are depicted in Figure 4.3.

Distilled water was introduced to the system by a Dionex Model DQP-1 metering pump. A burette measured the total quantity of water fed to the apparatus. A four-pass heat exchanger constructed of ¼-inch stainless steel tubing served as a gas preheater and steam generator. The tube bundle was heated in a Lindberg Sola Basic Model 123 split-tube furnace. The pressure in the steam bypass flow path was regulated by a Tescom Industrial Controls Model 26-1726-24 backpressure regulator. The temperature of the preheater and steam mixture were monitored by Type K thermocouples and an Omega Model 650 thermocouple meter. The steam bypass flow was considered to be at steady state when these temperatures stabilized.

The fixed bed reactor was heated in a vertically mounted Lindberg Sola Basic Model 123 split-tube furnace. The differential bed accomodated up to five grams of char and

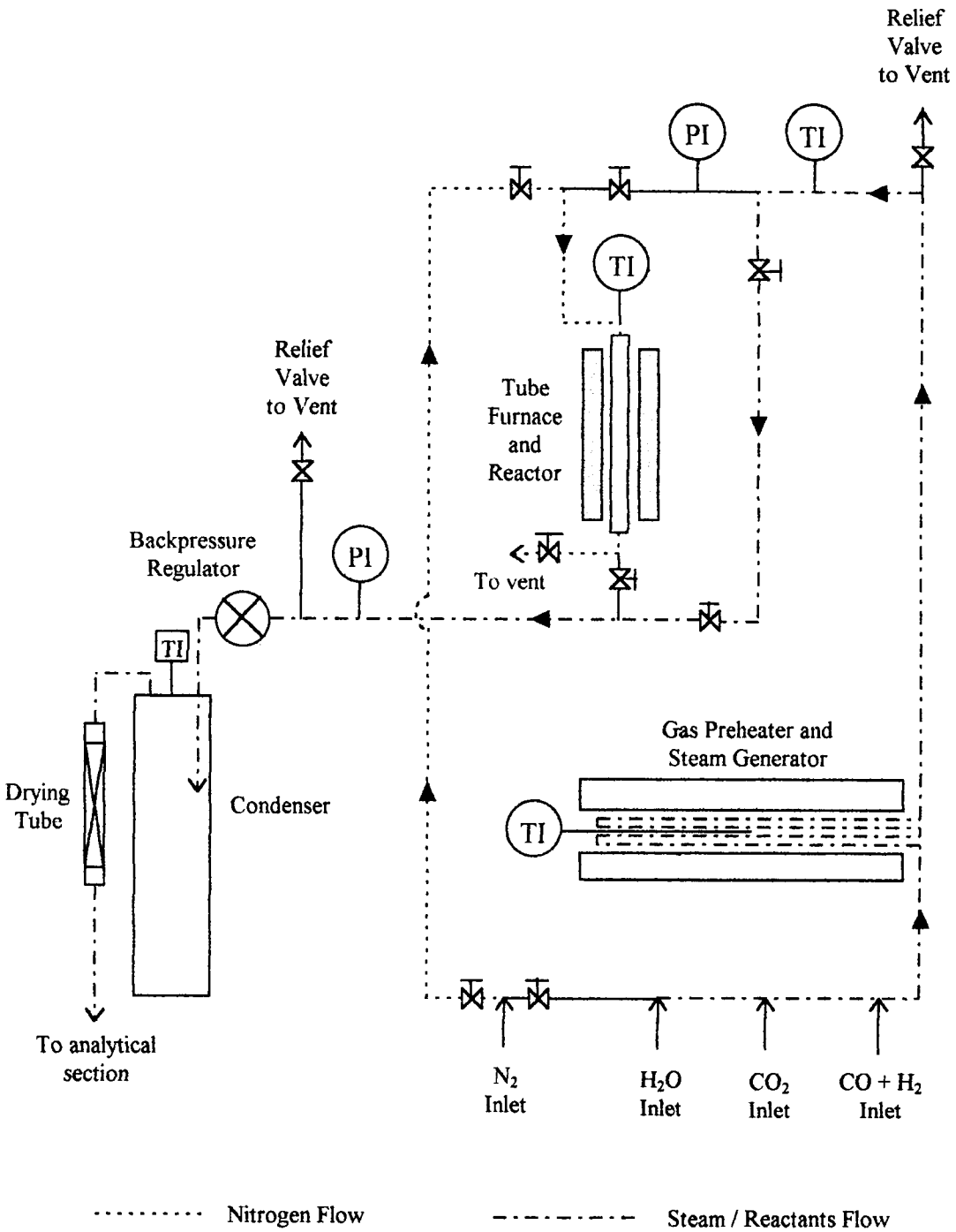

Figure 4.3. High Pressure Fixed Bed Gasifier – Startup Mode

catalyst. The reactor was purged with nitrogen for several minutes before heating. The inert flow was maintained until the apparatus was changed to the gasification mode. The reactor was considered to be at steady state when the fixed bed temperature was stabilized at the desired operating temperature.

When both the steam bypass flow and the reactor reached steady state, the apparatus was changed from the startup mode to the gasification mode. Figure 4.4 depicts the apparatus in the gasification mode. The system pressure was controlled with a Tescom Industrial Controls Model 26-1726-24 backpressure regulator. The nitrogen, excess steam, and catalytic steam gasification products entered a condenser after passing through the backpressure regulator. A drying tube packed with silica gel removed any trace quantities of moisture from the condenser outlet gas. The dry gas stream then entered the analytical section of the apparatus.

The volumetric flow rate of nitrogen during startup and gasification was maintained at approximately 1.5 cubic feet per hour. To simplify the analysis of the gasification kinetics, it was important to provide excess steam to the reactor. The water flow rate to the steam generator was typically between 0.15 and 0.40 grams per minute. The gasification portion of an experiment required four or five hours to complete. The trial was terminated when the concentration of gaseous carbonaceous species reached an undetectable level or an essentially constant low level.

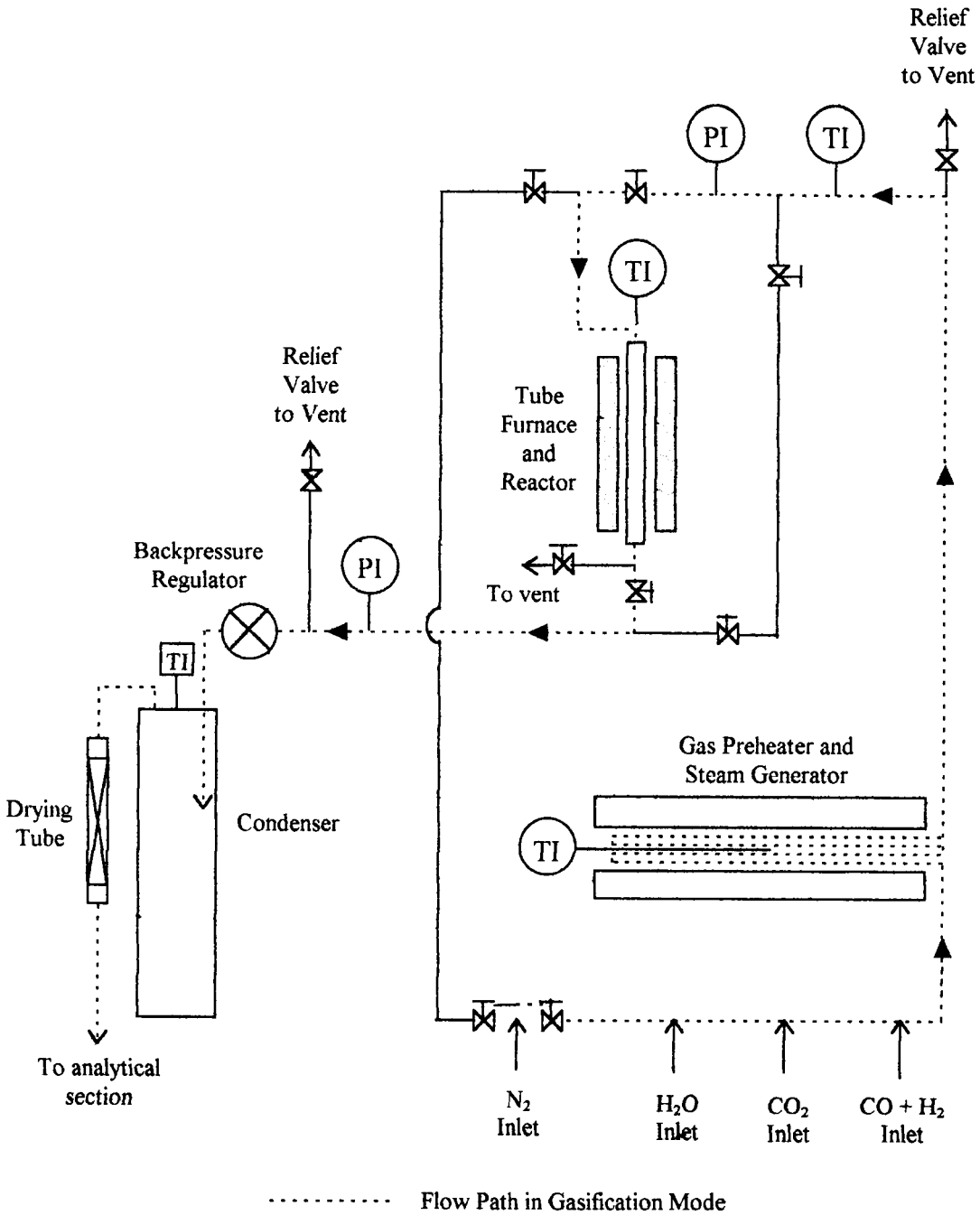

Figure 4.4. High Pressure Fixed Bed Gasifier – Gasification Mode

In the analytical section, the process variables required to calculate the rate of gasification were measured. A Rockwell cumulative gas flowmeter determined the total volume of gas which had exited the reactor. An SRI 8610C gas chromatograph analyzed the effluent gases. The gas chromatograph measured the mole fractions of oxygen, nitrogen, carbon monoxide, methane, and carbon dioxide. A Gateway 2000 computer with PeakSimple 1.44 software controled the instrument. The cumulative gas volume and water burette readings were recorded periodically throughout the experiment. The mole fractions and cumulative gas volume were used to calculate the carbon-steam reaction rate.

When the extent of carbon conversion was satisfactory, the apparatus was returned to the startup configuration. The reactor furnace was allowed to cool to room temperature. The nitrogen flow through the reactor prevented further reaction of the char. After cooling, the remainder of the char sample was weighed. The carbon and ash contents were measured as well. The complete operating procedures for the high pressure fixed bed gasifier apparatus are detailed in Appendix IV.

Chapter V

Experimental Results and Discussion

Analysis of Broiler Litter, Broiler Litter Char, and Ash

The broiler litter was first analyzed to determine the moisture and volatiles content. The moisture content as measured in the Precision Gravity Convection Oven was 28.5 percent on a fresh litter basis. The Perkin-Elmer Thermogravimetric Analyzer (TGA) was used to determine the volatiles content in the fresh litter. The volatiles content was found to be 39.5 percent on a fresh litter basis. A typical weight profile generated by the TGA and used in the determination of the volatiles content is shown in Figure 5.1. There are two distinct regions of weight loss when fresh broiler litter is heated under an inert atmosphere. The first region corresponds to the loss of moisture from the sample. The second region results from the loss of volatiles in the pyrolysis process. The ash content was also determined with the TGA. The ash content of the fresh litter was determined to be 14.5 percent on a fresh litter basis. A typical weight profile generated by the TGA and used in the determination of the ash content is shown in Figure 5.2. The sharp weight loss is due to the oxidation of the fixed carbon in the char sample. The remaining component of the proximate analysis is the fixed carbon. The fixed carbon content was determined by difference and found to be 17.5 percent on a fresh litter basis. Table 5.1

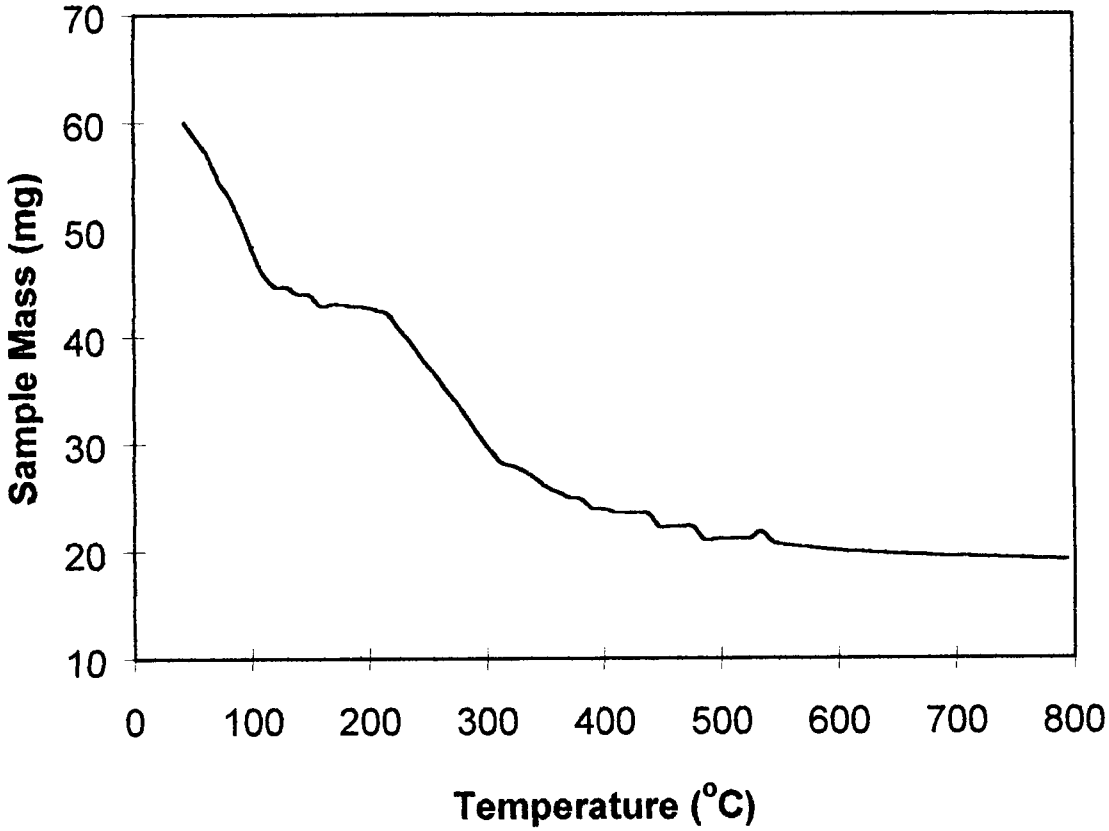

Figure 5.1 Determination of Volatiles Content of Fresh Broiler Litter

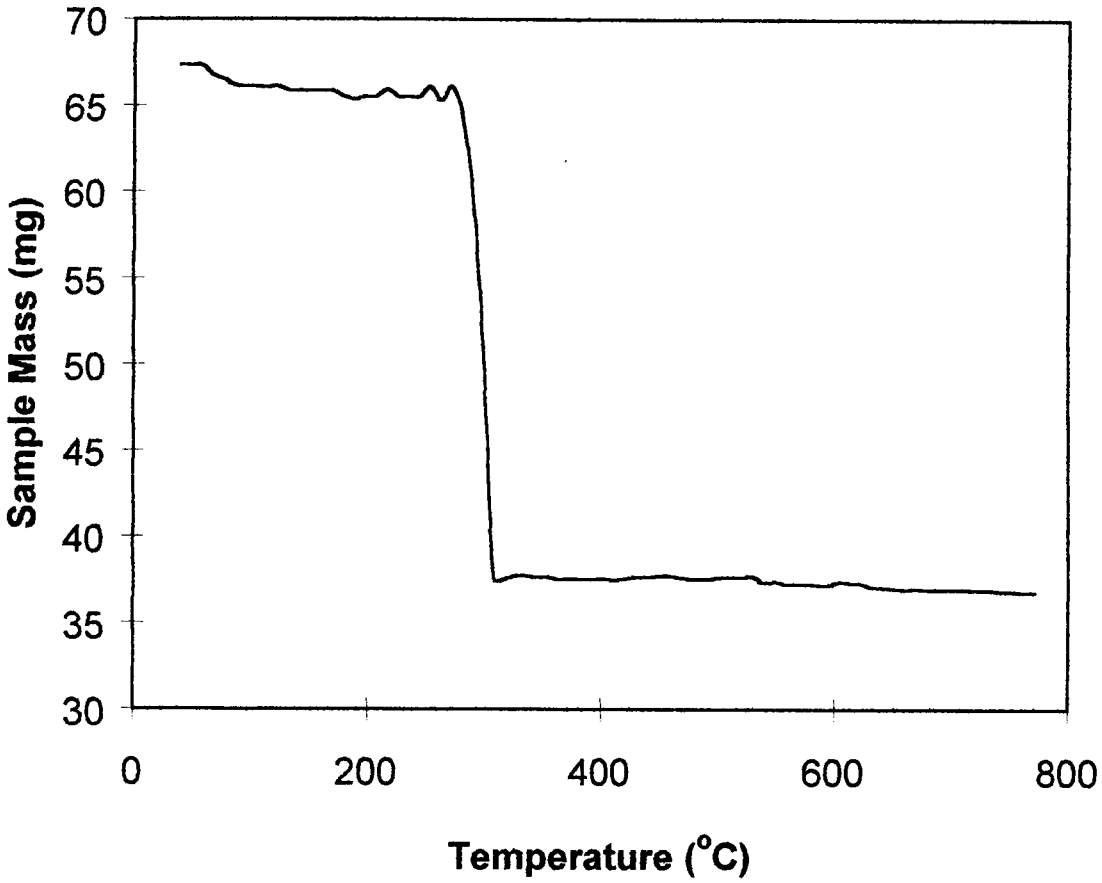

Figure 5.2 Determination of Ash Content of Pyrolyzed Broiler Litter

Table 5.1 Compositions of Broiler Litter and Char

Fraction	Fresh Litter	Dry Litter	Char
Moisture	28.5 %	-----	-----
Volatiles	39.5 %	55.2 %	-----
Fixed Carbon	17.5 %	24.5 %	54.7 %
Ash	14.5 %	20.3 %	45.3 %

summarizes the moisture, volatiles, fixed carbon, and ash contents of the fresh litter, dry litter, and char. The ash percentage is given on an ignited basis.

The mineral and sulfur contents of the broiler litter were also evaluated. The metals content of the litter was determined by analyzing the dissolved metals concentration in a solution of hot aqua regia. The concentrations of six metals were determined with the Perkin-Elmer Emission Spectrometer. The undissolved content of the ash was assumed to be insoluble constituents. The quantity of insoluble material present in the ash was calculated by difference. The sulfur content of the broiler litter was evaluated with the LECO SC132 Sulfur Determinator. The metal, insoluble, and sulfur contents are reported for fresh litter, dry litter, and char in Table 5.2. When reported as oxides, the minerals listed in Table 5.2 account for approximately 6.62 percent of the fresh broiler litter. The remaining 7.88 percent of the ash on the ignited basis is composed of alumina, phosphorus, copper, manganese, zinc, and other minerals which are soluble in hot aqua regia but were not specifically analyzed (Payne and Donald 26).

Catalytic Steam Gasification Experimental Results

The catalytic steam gasification of broiler litter was analyzed for five scenarios. The first experimental trial examined the gasification of uncatalyzed char at 1300°F and a pressure of 150 psia. This experimental trial was used as a basis of comparison for the four remaining runs. The second trial examined the effect of pressure on the gasification rate. Although the reactor temperature was unchanged at 1300°F, the system pressure

Table 5.2 Analysis of Mineral and Sulfur Contents in Broiler Litter

Component	Fresh Litter	Dry Litter	Char
Insolubles	2.46 %	3.45 %	7.70 %
Potassium	1.86 %	2.61 %	5.82 %
Calcium	0.63 %	0.88 %	1.96 %
Sodium	0.53 %	0.74 %	1.65 %
Magnesium	0.21 %	0.30 %	0.67 %
Sulfur	0.10 %	0.14 %	0.31 %
Nickel	102 ppm	143 ppm	319 ppm
Iron	93 ppm	131 ppm	292 ppm

was reduced to 50 psia. The third trial studied the effect of reduced temperature on gasification rate. The reactor temperature was reduced to 1000°F with an operating pressure of 150 psia. The fourth and fifth trials evaluated the effect of additional catalysts on steam gasification. The catalysts tested were langbeinite and potassium carbonate. Each of these trials utilized a catalyst loading of ten weight percent, reactor temperature of 1300°F, and system pressure of 150 psia. The catalyst loading is the weight percentage of the mineral or salt on an uncatalyzed char basis.

The reactor conditions and gas chromatograph peak areas were used to evaluate the gasification performance. The mole fraction of oxygen, nitrogen, carbon monoxide, methane, and carbon dioxide in the reactor effluent were calculated from the corresponding peak area and the peak area of a calibration standard. The calibration standard was produced by Scott Specialty Gases. On a molar basis, the standard contained 5.01 percent oxygen, 5.00 percent nitrogen, 4.99 percent carbon monoxide, 4.01 percent methane, and 5.00 percent carbon dioxide. The balance of the calibration standard was helium. The mole fraction y_i of species i in a mixture of gases is given by the following equation. The mole fraction of species i in the calibration standard and the calibration peak area of species i are symbolized by $y_{cal,i}$ and $A_{cal,i}$, respectively. The area of the corresponding gas chromatograph peak is A_i.

$$y_i = \left(\frac{y_{cal,i}}{A_{cal,i}} \right) A_i \qquad (5 - 1)$$

This formula was used to calculate the mole fraction of each component in the sampled gas at each time. Since a small amount of air was unintentionally introduced to the gas during sampling, the contribution of oxygen and nitrogen from air were removed. The adjusted mole fractions were then normalized.

Another variable important in the evaluation of gasification performance is the total molar density of gases passing through the cumulative flowmeter. Since the volumetric flow is measured near the condenser, the condenser temperature T_{cond} is a sufficient approximation to the temperature at the flowmeter. The flowmeter operates at approximately atmospheric pressure P_{atm}. The total molar density $\overline{\rho}$ can be calculated using the condenser temperature and atmospheric pressure.

$$\overline{\rho} = \frac{P_{atm}}{R\,T_{cond}} \qquad (5 - 2)$$

The molar density of each carbonaceous gaseous component is the product of the component mole fraction and the total molar density.

$$\overline{\rho}_{CO} = y_{CO}\,\overline{\rho} \qquad (5 - 3)$$

$$\overline{\rho}_{CH_4} = y_{CH_4}\,\overline{\rho} \qquad (5 - 4)$$

$$\overline{\rho}_{CO_2} = y_{CO_2}\,\overline{\rho} \qquad (5 - 5)$$

Each carbonaceous species produced by the catalytic steam gasification reactions contains only one carbon atom. Since each mole of carbon monoxide, carbon dioxide, and methane contains one mole of carbon, the total molar density of carbon in the reactor

of the component molar densities. In the following equation, $\overline{\rho}_C$ olar density of carbonaceous compounds in the reactor effluent.

$$\overline{\rho}_C = \overline{\rho}_{CO} + \overline{\rho}_{CH_4} + \overline{\rho}_{CO_2} \qquad (5 - 6)$$

gasified before any time t is given by the integral of carbon molar to volume where V_t represents the volume of gas which has exited

$$Moles\ of\ Carbon\ Gasified = \int_0^{V_t} \overline{\rho}_C\ dV \qquad (5 - 7)$$

lefinite integral by the atomic weight of carbon M_c, the mass of e any time t can be calculated.

$$Mass\ of\ Carbon\ Gasified = M_c \int_0^{V_t} \overline{\rho}_C\ dV \qquad (5 - 8)$$

l is precise only for carbon molar densities which are not discrete oximation to the integral can be obtained through numerical ical integration allows the integral to be represented by a discrete ints. The numerical integration can be expressed as a summation the number of data points measured.

$$Mass\ of\ Carbon\ Gasified = M_c \sum_{i=1}^{N} \overline{\rho}_C\ \Delta V_i \qquad (5 - 9)$$

finity, the value of the summation approaches the value of the definite n only a finite quantity of data is available, the summation can be cceptable results. Since the data is collected at predetermined times

not effluent volumes, the value of ΔV_i is not constant. This is easily accommodated, however.

$$\Delta V_i = V_i - V_{i-1} \qquad (5 - 10)$$

The symbols V_i and V_{i-1} in Equation *(5-10)* represent the cumulative volumes of gas which has exited the reactor at times t_i and t_{i-1}, respectively. Since the mole fraction of each constituent may change considerably between data points, it is not acceptable to represent the effluent concentration as the second data point, or terminal, concentration. Therefore, the molar density is represented as the arithmetic mean of the molar densities at times t_i and t_{i-1}.

$$\overline{\rho}_C = \frac{\overline{\rho}_{C,i} + \overline{\rho}_{C,i-1}}{2} \qquad (5 - 11)$$

These two approximations are equivalent to the trapezoidal rule for numerical integration. The complete expression for the summation is given below.

$$Mass\,of\,Carbon\,Gasified = M_c \sum_{i=1}^{N} \left(\frac{\overline{\rho}_{C,i} + \overline{\rho}_{C,i-1}}{2} \right) (V_i - V_{i-1}) \qquad (5 - 12)$$

The mass of carbon gasified as calculated by the numerical integration of gas composition data may differ slightly from the value calculated from the carbon content of the initial and final chars. Since the instrumental analysis performed on the chars is much more precise, the value calculated by numerical integration should be adjusted to agree with the mass of carbon gasified as calculated from the carbon content analysis. A

correction factor β is incorporated into the numerical integration formula to represent this adjustment.

$$Mass\ of\ Carbon\ Gasified = \beta\ M_C \sum_{i=1}^{N} \left(\frac{\overline{\rho}_{C,i} + \overline{\rho}_{C,i-1}}{2} \right) (V_i - V_{i-1}) \qquad (5 - 13)$$

The correction factor β typically has values ranging from 1.15 to 1.45.

The amount of carbon remaining in the fixed bed at any time can be expressed in terms of the mass of carbon gasified W_{gas} and the mass of carbon initially in the fixed bed W_o.

$$W = W_o - W_{gas} \qquad (5 - 14)$$

The fraction of the original carbon weight remaining at any time can be obtained from this relationship.

$$\frac{W}{W_o} = \frac{W_o - W_{gas}}{W_o} \qquad (5 - 15)$$

A similar expression can be developed for the total char weight m if the gasifiable fraction of the char is assumed to be fixed carbon only. The symbol κ represents the ratio of the ash mass to the fixed carbon mass in the original char sample and m_{ash} represents the weight of ash in the original char sample

$$\frac{m}{m_o} = \frac{W + m_{ash}}{W_o + m_{ash}} \qquad (5 - 16)$$

$$\frac{m}{m_o} = \frac{\frac{W}{W_o} + \frac{m_{ash}}{W_o}}{1 + \frac{m_{ash}}{W_o}} \qquad (5 - 17)$$

$$\frac{m}{m_o} = \frac{1 - X + \kappa}{1 + \kappa} \qquad (5 - 18)$$

The final expression describes the remaining char weight fraction in terms of the carbon conversion X and the ash-to-carbon ratio in the initial char κ. The carbon conversion X is related to the remaining carbon weight fraction.

$$X = 1 - \frac{W}{W_o} \qquad (5 - 19)$$

The carbon conversion X only represents the fraction of fixed carbon gasified. Carbonaceous volatile species are not included in the calculation of the carbon conversion. Figure 5.3 shows the remaining carbon weight fraction as a function of time for the gasification trial performed at 1300°F and 50 psia. Figure 5.4 is a similar graph illustrating the remaining char weight fraction. Figure 5.5 exhibits a typical carbon conversion curve for catalytic steam gasification. Complete experimental data and graphs for each experimental trial are included in Appendix V.

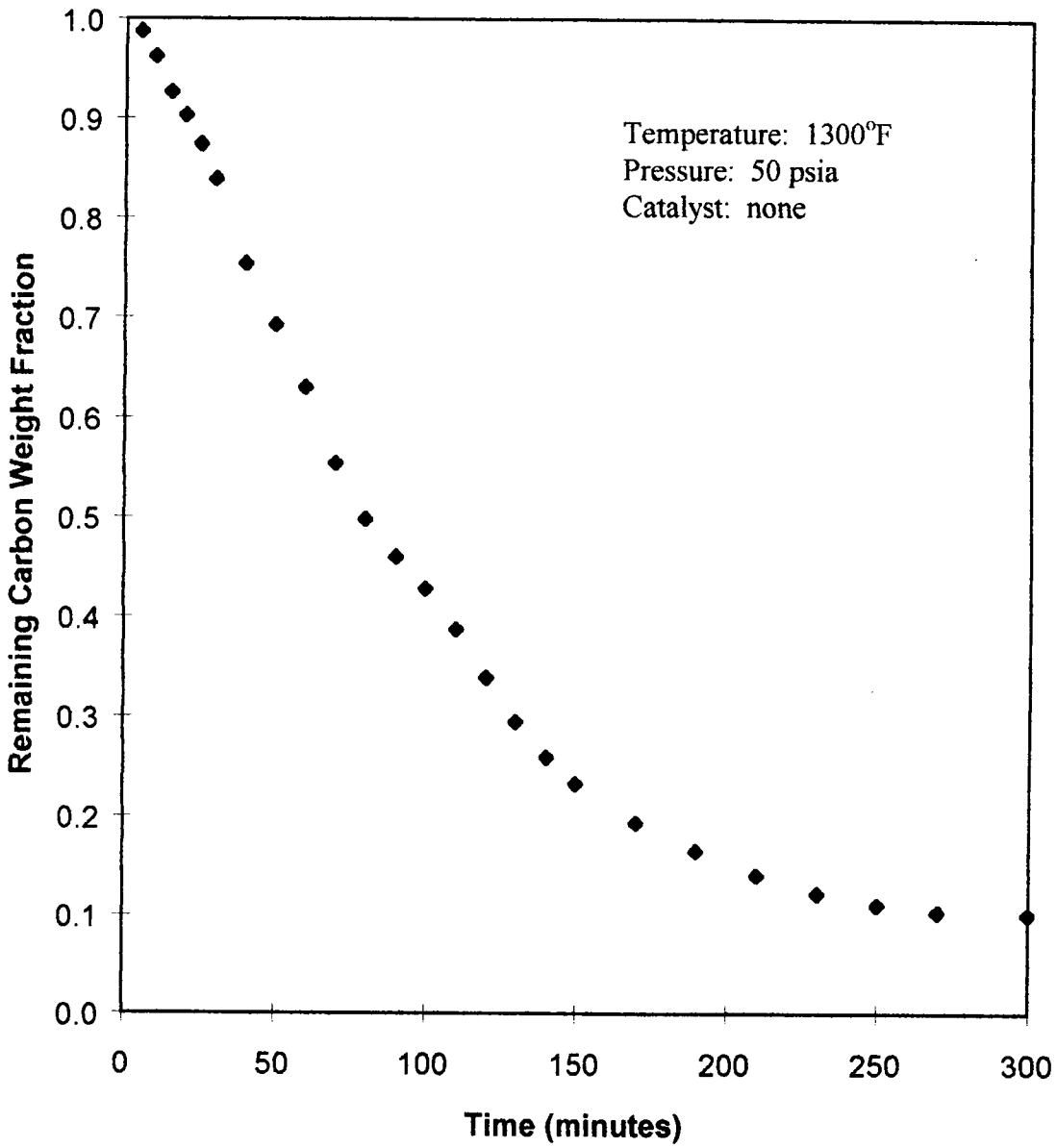

Figure 5.3 Remaining Carbon Weight Fraction

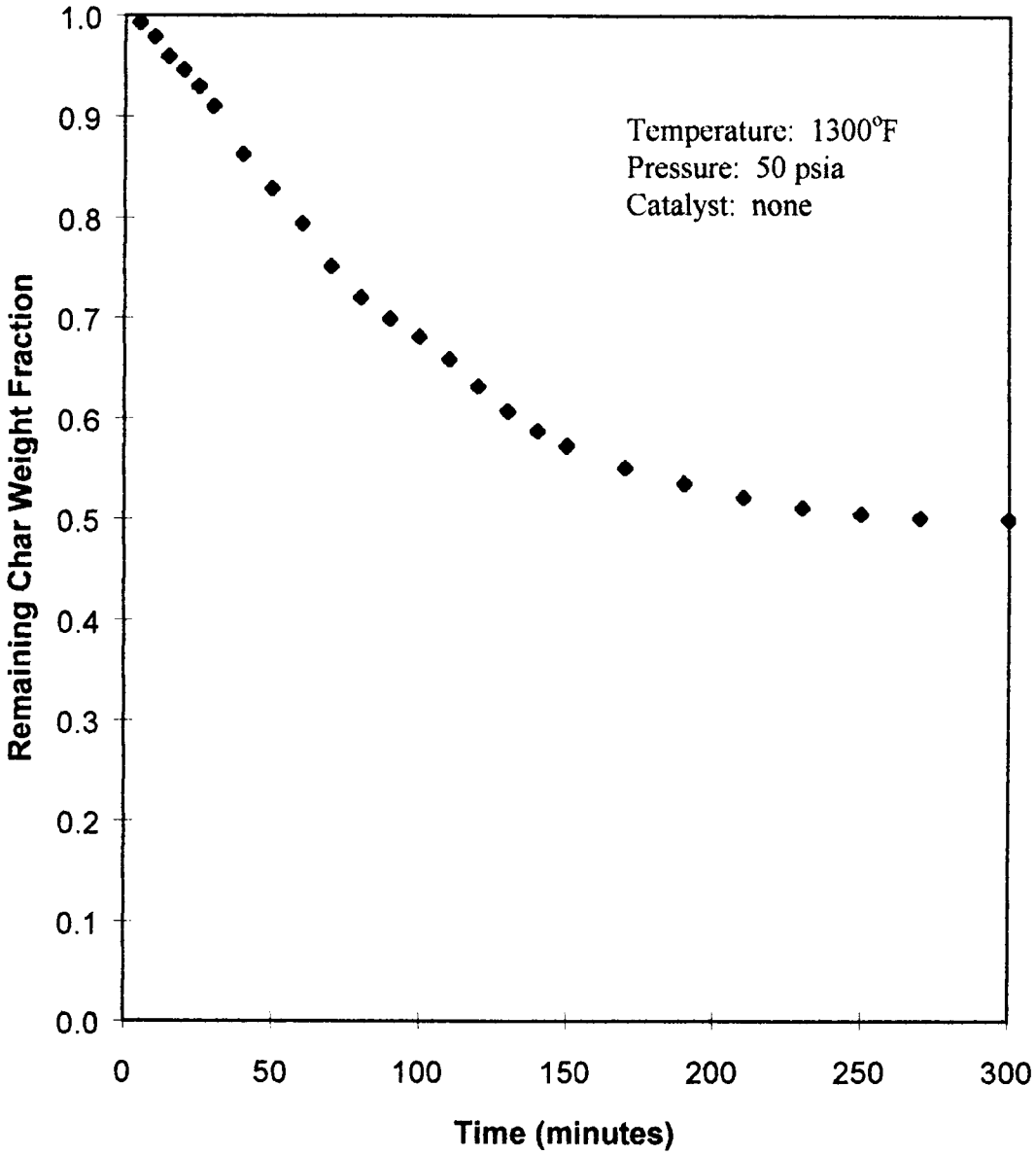

Figure 5.4 Remaining Char Weight Fraction

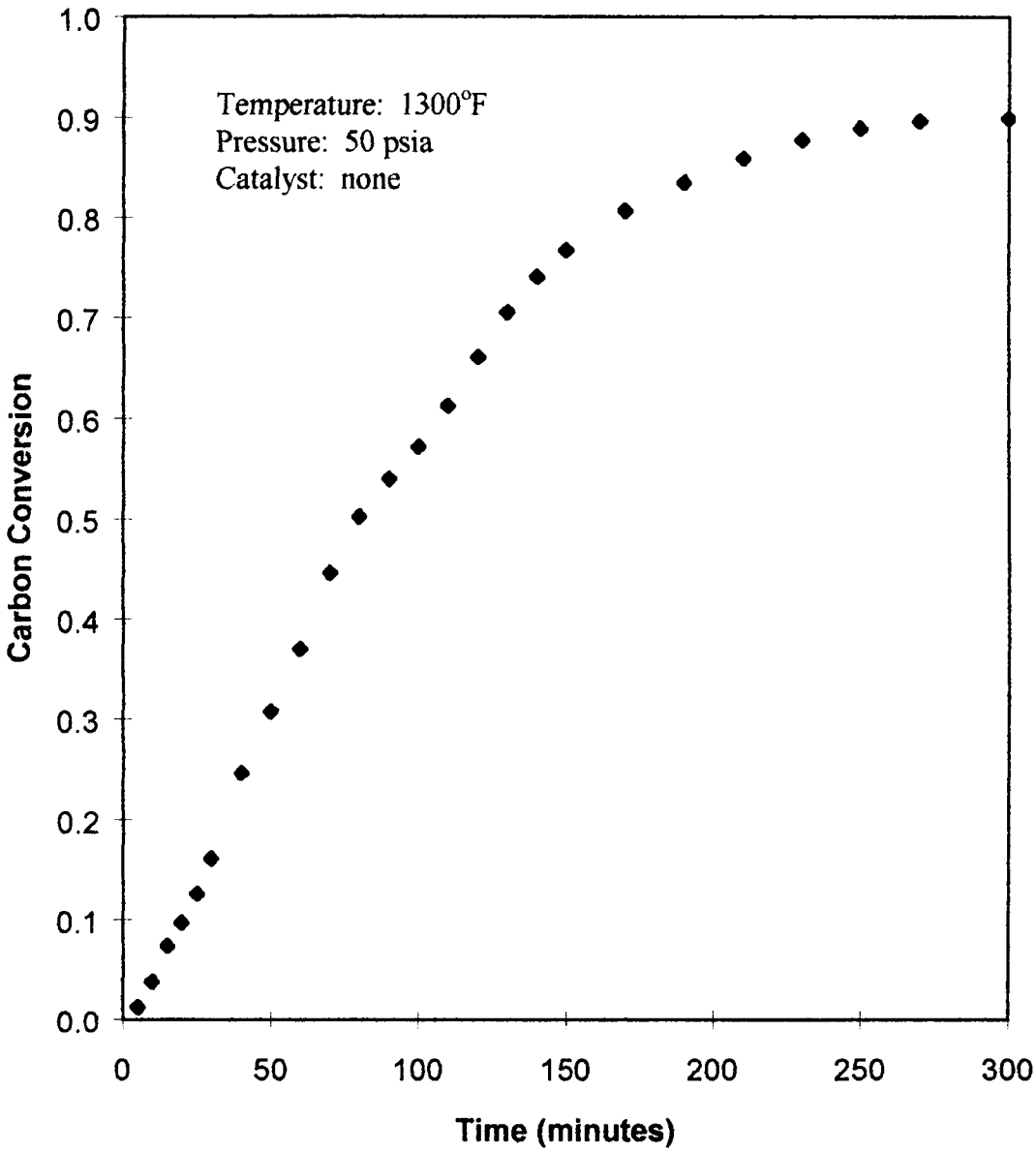

Figure 5.5 Carbon Conversion in Char

For first-order kinetics, the relationship between carbon conversion and time is given by the theoretical expression derived earlier.

$$X = 1 - e^{-GM_c t} \qquad (5 - 20)$$

The expression is easily linearized to yield an expression between $\ln(1-X)$ and the specific gasification rate G.

$$-\ln(1-X) = GM_c t \qquad (5 - 21)$$

It is evident from the linearized expression that a graph of $-\ln(1-X)$ versus t will produce a line of slope GM_c if the specific gasification rate remains constant. If the inherent mineral catalyst or additional catalyst is activated, the slope of the curve will increase at higher carbon conversions. If the catalytic activity is decreased due to deactivation, the slope of the curve will decrease at higher carbon conversions. Figure 5.6 shows the graph of $-\ln(1-X)$ versus t for the experimental trial performed at 1300°F and 50 psia. The graph demonstrates a region of constant specific gasification rate at fixed carbon conversions below 0.85. At a fixed carbon conversion of approximately 0.85, however, the slope of the curve decreases. This decreasing slope at high carbon conversions is indicative of catalyst deactivation. Although the experimental trial associated with the graph utilized no additional catalyst, it is probable that minerals serving as inherent catalysts were deactivated at high carbon conversions. Graphs of $-\ln(1-X)$ versus t are given for each experimental trial in Appendix V. The slope of the linear region corresponding to constant specific gasification rate was determined by

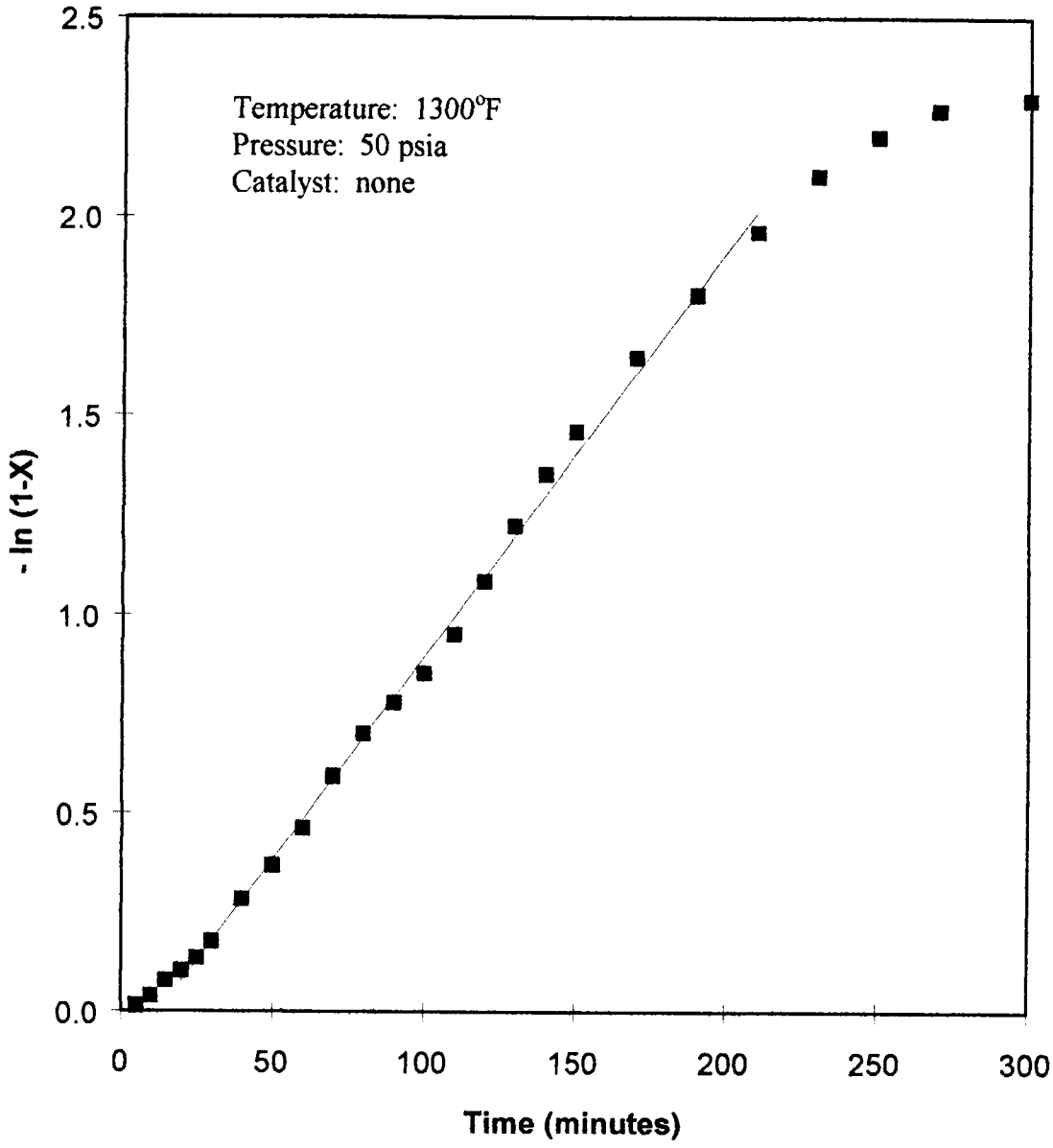

Figure 5.6 Determination of Specific Reaction Rate

linear regression using the method of least squares. Table 5.3 compares the gasification rates for each of the experimental trials. The square of the regression coefficient r^2 is a measure of the linearity in the region of constant specific gasification rate. The region of catalyst deactivation typically begins at fixed carbon conversions between 0.75 and 0.90.

The effect of system pressure on gasification rate is demonstrated in Figure 5.7. The decrease in system pressure from 150 psia in Trial 1 to 50 psia in Trial 2 resulted in an approximately 37 percent increase in the specific gasification rate. This rate increase may be attributed to the equilibrium compositions of steam. With decreasing system pressure, the equilibrium mole fraction of steam decreases. Therefore, a gasifier operating with excess steam at low pressure is further displaced from equilibrium than a gasifier operating at high pressures. Reaction rates can be expressed with the displacement from equilibrium as the driving force. As discussed in the literature review, the research concerning the effects of pressure on catalytic steam gasification rates is inconclusive.

The effect of temperature on the gasification rate was also studied. In Trial 3, the decrease in reactor temperature from 1300°F to 1000°F resulted in a decrease of over 86 percent in the specific gasification rate. The effect of reactor temperature on gasification rate is shown in Figure 5.8. The reasons for the observed effects are twofold. The activation energy barrier for the steam-carbon reaction is decreased significantly with

Table 5.3 Comparison of Specific Gasification Rates

Trial	Temperature	Pressure	Catalyst	G mol C / (g C-min)	r^2
1	1300°F	150 psia	none	6.218×10^{-4}	0.992
2	1300°F	50 psia	none	8.494×10^{-4}	0.997
3	1000°F	150 psia	none	8.484×10^{-5}	0.999
4	1300°F	150 psia	10 wt. % langbeinite	8.354×10^{-4}	0.997
5	1300°F	150 psia	10 wt. % K_2CO_3	1.408×10^{-3}	0.997

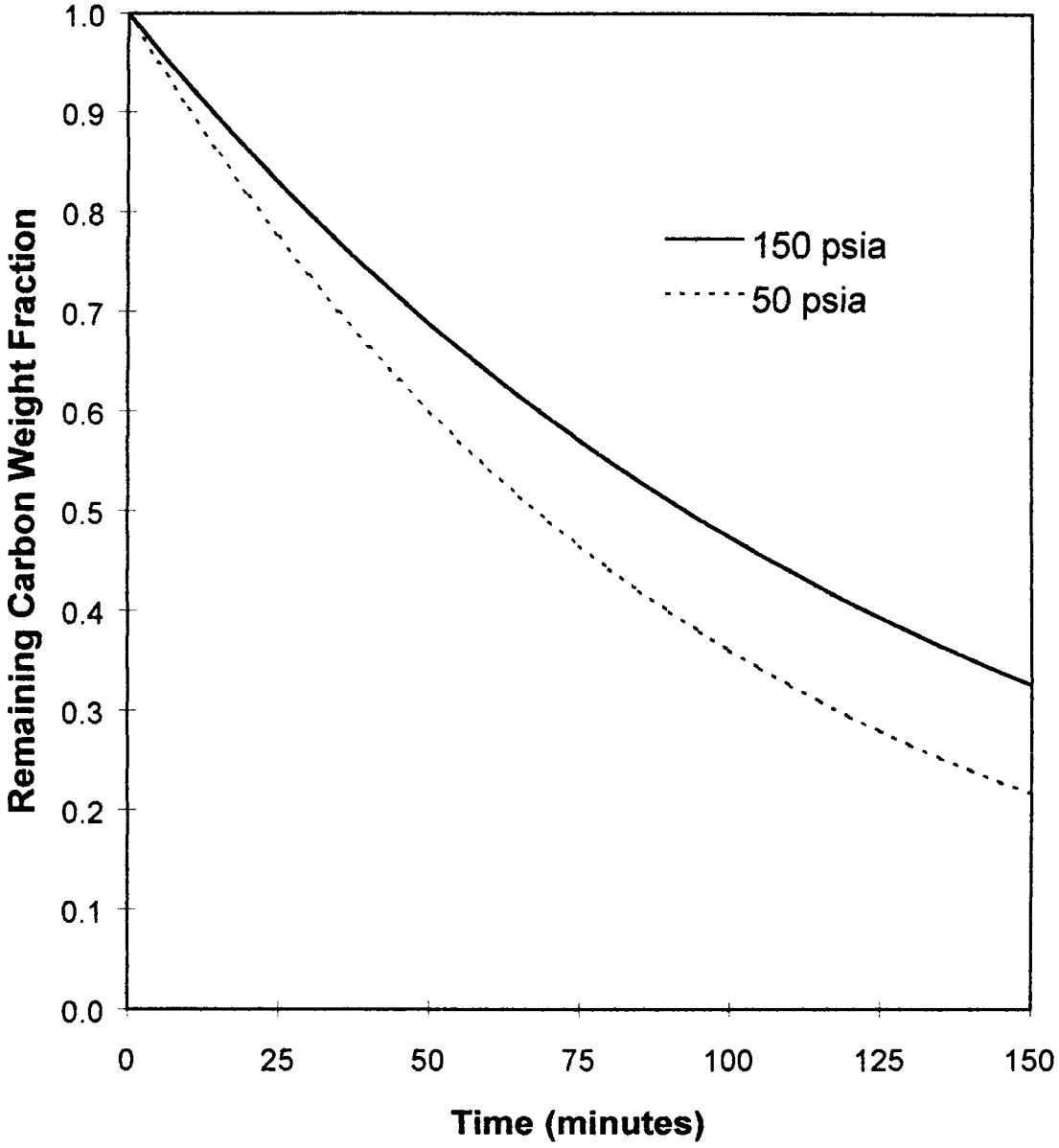

Figure 5.7 Effect of Pressure on Specific Gasification Rate

1300°F

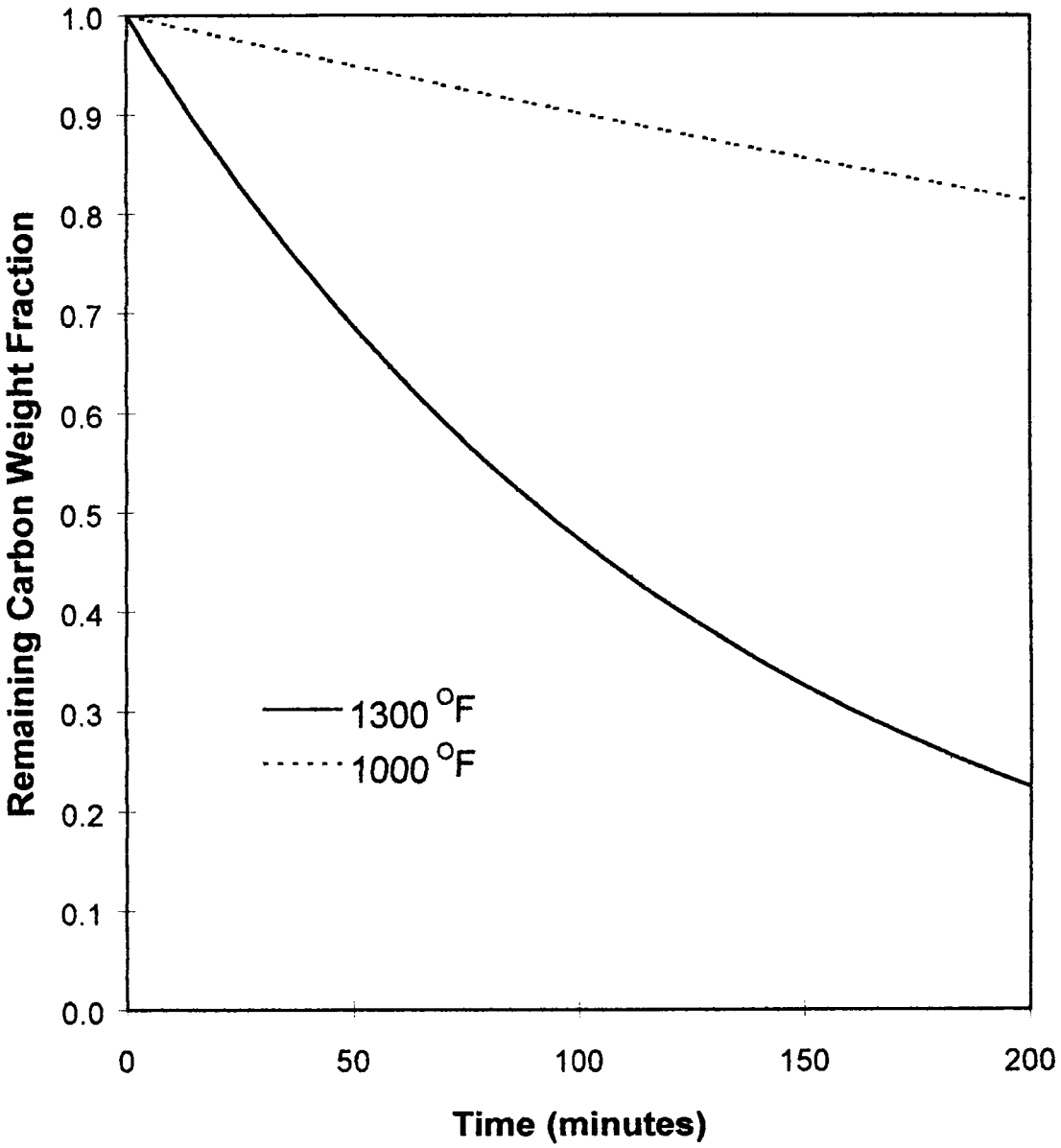

Figure 5.8 Effect of Temperature on Specific Gasification Rate

150 psia

increasing temperature. With decreasing temperatures, this barrier is significantly increased. Activation energies are the most important factor when investigating the effect of temperature on reaction rate. The second factor responsible for the observed temperature effects is the heat of reaction of the steam-carbon reaction. Since the reaction is endothermic, product formation is favored with increasing temperature. This increase in the equilibrium composition of the products may promote higher reaction rates since the displacement from equilibrium is larger at high temperatures. The effect of increasing temperature on the reaction rate is consistent with previous research.

The final comparative studies examined the effect of catalysts on the gasification rate. The catalysts were added to the pyrolyzed broiler litter by physical mixing. Since catalysts in steam gasification are most active when bound to oxygen-containing groups, the effect of additional catalysts may be more pronounced if the catalyst is physically mixed with the fresh broiler litter prior to pyrolysis. When added to pyrolyzed litter, both langbeinite and potassium carbonate increased the specific gasification rate. Langbeinite, $K_2Mg_2(SO_4)_3$, is an inexpensive mineral used in the fertilizer industry. Addition of langbeinite to the char increased the reaction rate by over 34 percent. Addition of potassium carbonate increased the specific gasification rate by nearly 127 percent. The effect of langbeinite and K_2CO_3 are illustrated in Figure 5.9. One possible explanation for the greater catalytic activity exhibited by potassium carbonate is the larger potassium-to-carbon atomic ratio for K_2CO_3 at a weight loading of ten percent.

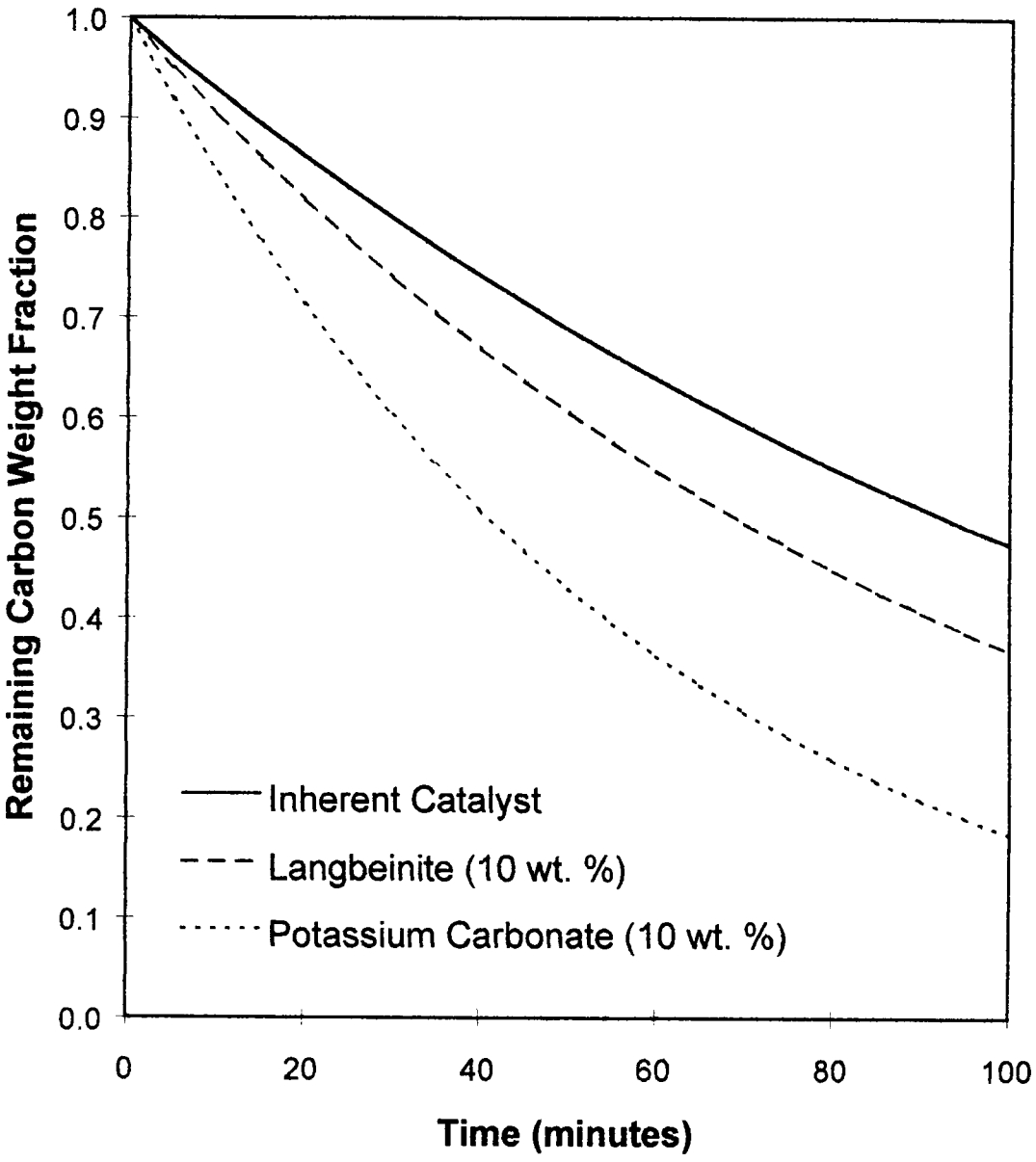

Figure 5.9 Effects of Catalysts on Specific Gasification Rate

1300°F, 150 psia

The potassium-to-carbon atomic ratios for the chars catalyzed with langbeinite and potassium carbonate are 4.328×10^{-2} and 6.447×10^{-2}, respectively. The potassium-to-carbon atomic ratios are based on the potassium inherent in the pyrolyzed litter and present in the supplemental catalyst. The char with no supplemental catalysts has a potassium-to-carbon atomic ratio of 3.270×10^{-2}. The atomic ratio of alkali metals to carbon is also important since sodium can act as a steam gasification catalyst. The atomic ratio of alkali metals to carbon in the char with no supplemental catalysts is 4.846×10^{-2}. The addition of langbeinite at a loading of 10 weight percent increased the potassium and alkali contents of the sample by 32.35 percent and 21.83 percent, respectively. The addition of potassium carbonate at a loading of 10 weight percent increased the potassium and alkali contents of the sample by 97.16 percent and 65.56 percent, respectively. It is obvious that the char contains a significant degree of inherent catalysts. The increase in the gasification rate for the langbeinite and potassium carbonate catalyzed chars would have been more pronounced if the inherent catalyst content was lower. Based on the inherent alkali content in the litter, utilization of a supplemental catalyst is not required to obtain significant gasification rates.

Chapter VI

Feasibility Analysis

Technical Feasibility of Catalytic Steam Gasification of Broiler Litter

The thermodynamics and kinetics of the steam gasification reactions and the physical and chemical properties of the broiler litter are the primary factors affecting the technical feasibility of the catalytic steam gasification of broiler litters. The equilibrium of the six reactions favors carbon monoxide and hydrogen at low pressures and high temperatures. Since gaseous mixtures of carbon monoxide and hydrogen are valuable as either low to medium energy gases or synthesis gas, a gasifier operating at low pressures and high temperatures can yield a valuable product. Favorable gasification kinetics are also attainable at similar conditions. The gasification rate of pyrolyzed broiler litter increases with decreasing pressure and increasing temperature. Since both the thermodynamics and kinetics of catalytic steam gasification are favored at low pressures and high temperatures, the process is technically feasible at these conditions.

Although the reactor conditions can be selected to yield technically feasible equilibrium product compositions and reaction rates, it is important to consider the properties of the broiler litter. The high mineral content of the litter appears to possess some degree of catalytic activity. The potassium and sodium contents by weight percent in the char are

5.82 percent and 1.65 percent, respectively. This high alkali metal content probably provides a considerable amount of catalytic activity.

The broiler litter also contains sufficient quantities of moisture to provide excess steam for the gasification reactions. In a downdraft reactor, the steam and volatiles generated by drying and pyrolysis pass downward through the gasification zone. Any steam generated by the drying process will act as the gasification medium in the steam gasification region of the reactor. The broiler litter analysis indicated a moisture content of approximately 571 pounds per ton of fresh litter. The required steam rate for complete carbon conversion in the pyrolyzed broiler litter is 523 pounds of steam per ton of fresh litter. To obtain a char carbon conversion of 0.75, the stoichiometric steam rate is 392 pounds of steam per ton of fresh litter. Based on the carbon conversion of 0.75 in the pyrolyzed broiler litter and the steam provided by drying, the steam-to-carbon ratio is 1.46 pounds of steam per pound of carbon gasified. The moisture content of the fresh litter alleviates the need to provide additional steam to the reactor.

The low sulfur content in the broiler litter also contributes to the technical feasibility of the steam gasification process. The fresh broiler litter contains 0.10 percent sulfur. Since high sulfur contents promote the formation of hydrogen sulfide, a carbonaceous feedstock with low sulfur content is ideal for gasification. The sulfur content in the broiler litter is considerably less than that of typical low rank coals often utilized in coal gasification.

Although most factors indicate that the catalytic steam gasification of broiler litter is technically feasible, it is important to consider some factors which could result in technical challenges. Broiler litters have highly variable compositions in terms of moisture, volatiles, fixed carbon, and ash contents. Therefore, it is important to study a variety of litters before constructing a gasification unit or facility. Broiler litters are low quality fuels which may affect downdraft operations. Although operation in the downdraft mode is not required, it integrates removal of steam during drying with the steam gasification process. If further tests with broiler litters suggests an incompatibility with downdraft operations, an updraft flow regime should be considered. Although the updraft gasifier does not affect the technical feasibility of the process, the gasifier unit would be considerably more complex. Since the steam from drying would not be integrated with the steam required for gasification, the gasification unit would require accommodations for generation of steam and removal of large quantities of water vapor from the product gas. This would add considerable capital costs and operating costs to the unit. In addition to these costs, the updraft gasification unit generates a larger quantity of condensed liquids. These condensed liquids may represent a waste stream requiring special disposal.

The theoretical and practical considerations of catalytic steam gasification have been considered with respect to the technical feasibility of the process. By operating at low pressures and high temperatures, a favorable gas product rich in carbon monoxide and

hydrogen can be produced at acceptable rates. The moisture content of the litter should be sufficient for gasification if the reactor flow regime is downdraft. The inherent mineral content of the litter provides significant gasification rates but can be supplemented through the addition of alkali metal salts. There are no reasons to suspect that a fully functional gasification unit or facility cannot be constructed.

Economic Feasibility of Catalytic Steam Gasification of Broiler Litters

To assess the economic feasibility of the catalytic steam gasification process, a preliminary design has been developed for a transportable broiler litter gasification apparatus. The gasification apparatus is to be constructed on a flatbed trailer. In the process, the fresh broiler litter is loaded into a feed hopper with a bucket loader. The broiler litter is then transported by screw conveyors to two downdraft moving bed reactors operating in parallel. The residence time of solids in each reactor is 180 minutes. The reactor combines drying, pyrolysis, and steam gasification operations in a single unit. The unreacted char and ash are removed at the base of each reactor by a screw conveyor. The solid residue is conveyed to the ash receiver which is emptied periodically. The unreacted steam, volatiles, and product gases also exit near the base of each reactor. The gas mixture flows through finned tubes in a forced-draft air-cooled heat exchanger. Any condensable species are separated from product gases and other light hydrocarbons in knockout drums at the outlet of the air-cooled heat exchanger. The condensed liquids are drained from the knockout drums to a condensate storage tank. The gas streams exiting the drums flow to a manifold where they are combined into a

single stream. The combined gas stream is sent to a rotary compressor which is capable of compressing the product gases to a pressure of 150 psia. Electricity is provided by four gasoline powered generators. A profile view of the transportable gasification unit is shown in Figure 6.1. A top view of the transportable gasification unit is shown in Figure 6.2.

The bulk density of each substance was measured in the laboratory and utilized in the gasification unit design. The bulk densities of fresh broiler litter, dry broiler litter, char, and ash are given below. The reactors are designed to operate at a char carbon conversion of 0.75. The bulk density of partially converted char (X = 0.75) was determined by linear interpolation between the bulk densities of unconverted char and ash.

Substance	Bulk Density (lb/ft^3)
Fresh Broiler Litter	30.88
Dry Broiler Litter	23.82
Char ($X = 0.00$)	26.25
Char ($X = 0.75$)	28.99
Ash	29.90

The proximate analysis utilized in the design of the transportable unit is based on the analysis of the broiler litter used in the gasification experiments. The fraction of moisture, volatiles, fixed carbon, and ash for the broiler litter used in the design are given below.

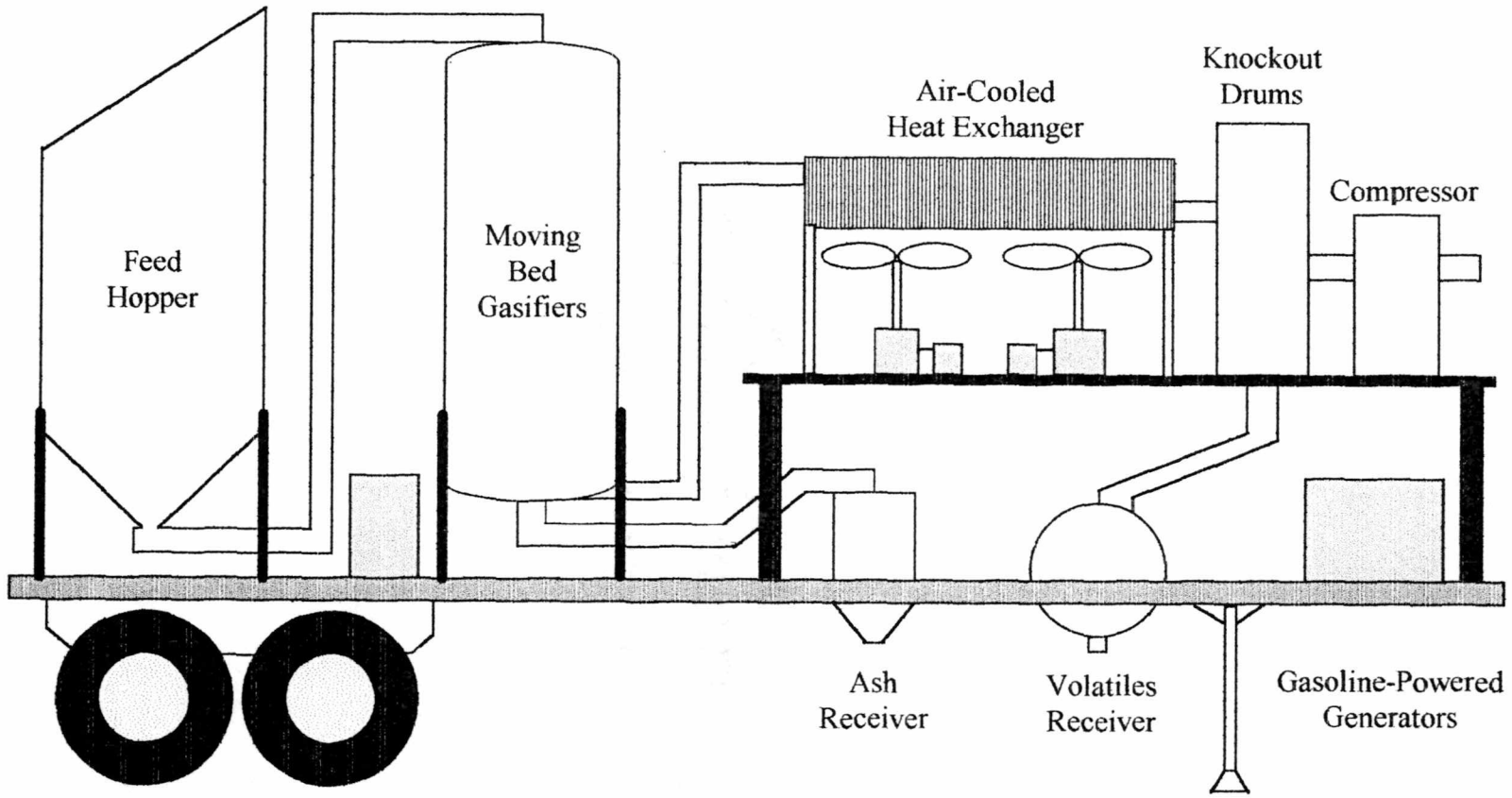

Figure 6.1 Transportable Broiler Litter Gasification Unit – Profile View

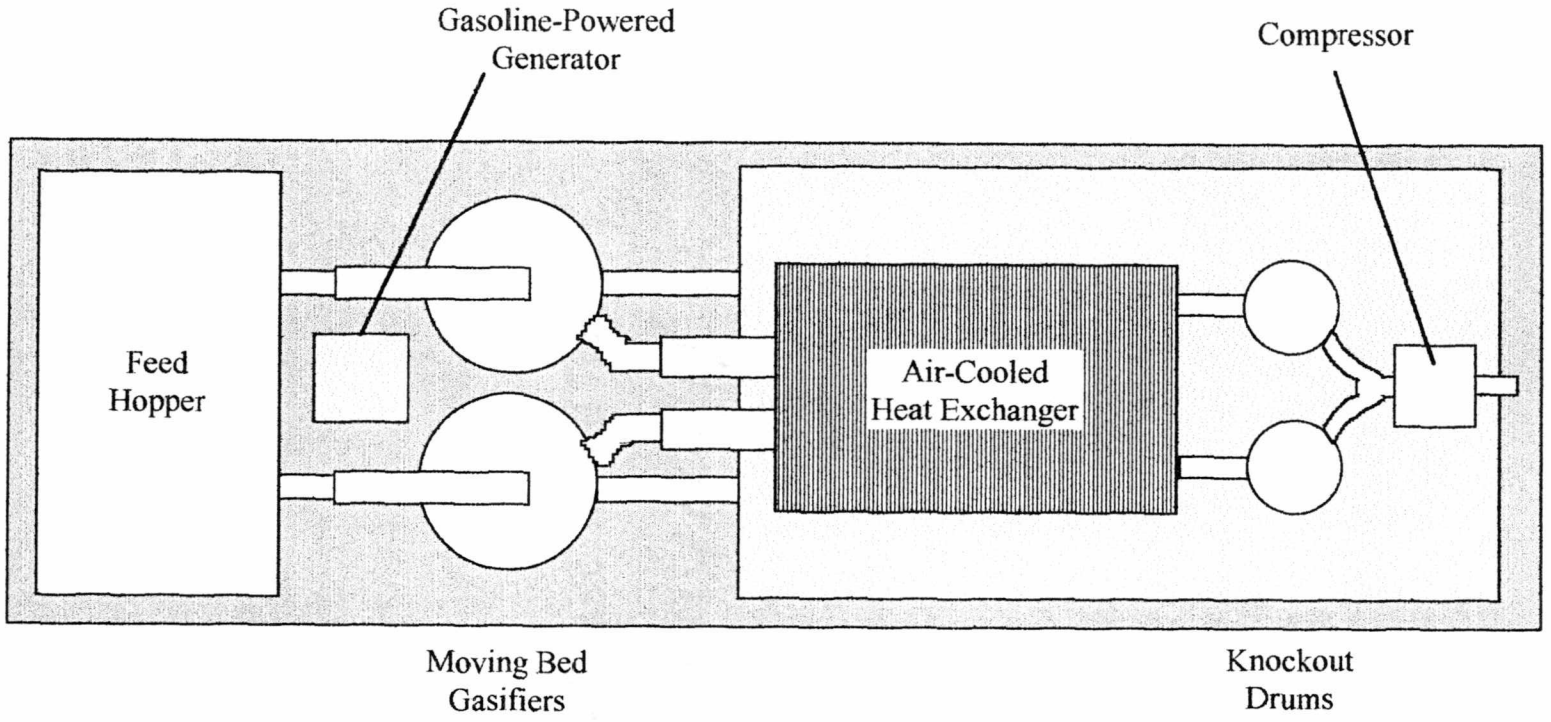

Figure 6.2 Transportable Broiler Litter Gasification Unit – Top View

Broiler Litter Component	Component Fraction (%)
Moisture	28.5
Volatiles	39.5
Fixed Carbon	17.5
Ash	14.5

The total feed rate of broiler litter to the gasification apparatus is 1.50 tons per hour. The feed rate to each reactor is 0.75 tons per hour. Figure 6.3 illustrates the drying, pyrolysis, and steam gasification zones of each reactor. The figure includes the solid mass flow rate and solid volumetric flow rate through each portion of the reactor. The volume of each section of the reactor is based on the residence time τ_i and the average bulk density of the material $\overline{\rho}_{bulk,i}$ in each section.

$$v_i = \tau_i \overline{\rho}_{bulk,i} \qquad (6\text{-}1)$$

The total volume of each reactor is 63.52 ft^3. The height and diameter were selected to maintain an acceptable height and height-to-diameter ratio. The internal diameter of the reactor was specified as 3.28 feet. The height of the reactor was then calculated to be 7.51 feet.

The reactors were designed to utilize the inherent moisture in the fresh broiler litter as the steam gasification medium. In each reactor, steam is removed from the fresh litter at the rate of 428 pounds per hour in the drying zone. The stoichiometric steam requirement for a char carbon conversion of 0.75 is 294 pounds per hour in each reactor.

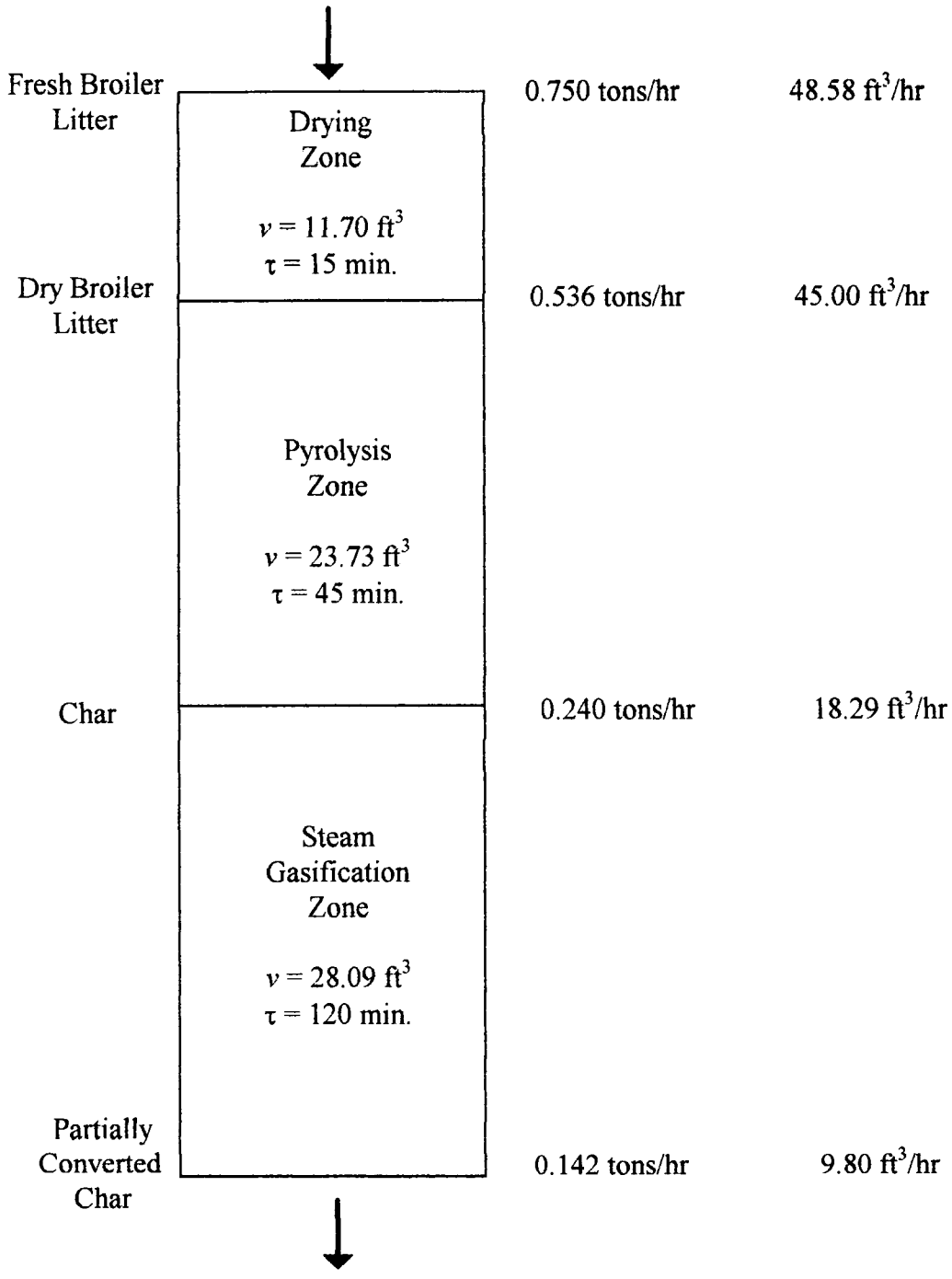

Figure 6.3 Solid Flow Rates and Residence Times in Reactor

The steam-to-carbon ratio for stoichiometric feeds is one. For each reactor in the gasification apparatus, the steam-to-carbon ratio is approximately 1.46.

Previous research has shown that all steam gasification reactions with the exception of the steam-carbon reaction reach equilibrium quickly. This assumption is used to estimate the composition and heating value of the gas produced on a dry basis. The composition given below is based on a reactor operating temperature of 1300°F and a reactor operating pressure of 50 psia.

Component	Mole Fraction
Carbon Monoxide	0.2629
Carbon Dioxide	0.1845
Methane	0.0794
Hydrogen	0.4732

The fraction of carbon converted to valuable gases is also important. The carbon dioxide has no heat of combustion and decreases the heating value of the gas mixture. The fraction of carbon converted to carbon monoxide and methane is 0.650. The heating value of the assumed product gas mixture was calculated to be 279.1 Btu per standard cubic foot. Approximately 196 pounds of carbon per hour is gasified in each reactor. The total volume of low energy product gas produced hourly by both reactors is 22,220 scf. The value of the low energy gas produced is estimated to be $17.06 per hour based on a price of $2.75 per million Btu for natural gas.

The specifications and costs of the equipment required to construct the transportable broiler litter gasification unit are given in Table 6.1. The delivered cost of equipment needed to construct the gasification unit is $64,290. The cost of purchased equipment installation and the cost of instrumentation and controls, piping, and electrical installations are estimated based on the delivered equipment costs and appropriate ratio factors (Peters and Timmerhaus 183). The total initial investment including installation labor and a contingency of 25 percent is $130,100.

The revenues generated from the sale of the low energy gas are $17.06 per hour. The operating costs for the transportable gasification unit are approximately $2.33 per hour. The operating cost is based on the production of electricity from four portable gasoline generators. The payback period for the transportable unit is one of the most important factors in determining the economic feasibility of the catalytic steam gasification process. To estimate the payback period, operations of 300 days per year and 12 hours per day are assumed. The continuous interest rate is estimated to be six percent. The estimated payback period for the transportable unit is approximately 2.27 years or 27 months. With a payback period of just over two years, the process is judged to be economically feasible.

Table 6.1 Equipment Specifications and Delivered Costs for a Transportable Broiler Litter Gasification Unit

Equipment Description	Purchased Equipment Cost (Delivered)
Flatbed Trailer	$ 7,500
Two Moving Bed Reactors 304 Stainless Steel 3.28 feet diameter 7.51 feet height	$ 13,800
Feed Hopper Aluminum	$ 4,190
Ash Receiver Aluminum	$ 2,100
Condensate Receiver Aluminum	$ 1,370
Two Knockout Drums 304 Stainless Steel 50 gallons	$ 2,875
Air-Cooled Heat Exchanger	$ 3,940
Single-Stage Rotary Compressor	$ 13,510
Screw Conveyors and Drives	$ 7,475
Three 19-hp Portable Gasoline Generators	$ 8,210
6.5-hp Portable Gasoline Generator	$ 1,060

Table 6.2 Total Costs for a Transportable Broiler Litter Gasification Unit

Item	Cost
Delivered Equipment	$ 64,290
Purchased Equipment Installation	$ 16,700
Instrumentation and Controls	$ 5,570
Piping	$ 13,280
Electrical	$ 4,280
Total Initial Capital Investment	*$ 104,100*
Contingency	*$ 26,000*
Total Initial Investment	*$ 130,100*

Chapter VII

Conclusions and Recommendations

Conclusions

Disposal of broiler litters in an improper manner will continue indefinitely if an alternate disposal technology is not developed. With the United States' broiler industry experiencing an annual growth rate of approximately 4.5 percent, the problem of litter disposal demands intervention. If broiler litter land application is not terminated, environmental tragedies such as those occurring recently in Delaware and Maryland will become commonplace. Possessing nearly 75 percent of the industry, the Southeastern United States is particularly vulnerable to the impacts of poor poultry waste management. Whether through legislation or education, the threat broiler litter poses to the environment must be eliminated.

Fortunately, one alternate disposal technology appears to be promising. Originally developed for production of clean fuels from coal, catalytic steam gasification can be easily adapted to the gasification of broiler litters. The moisture content of the litter provides sufficient steam alleviating the need for steam generation. The inherent catalytic activity of the litter and its low sulfur content combine to make broiler litter an outstanding candidate for steam gasification. The process produces a low to medium energy gas which can be used as a fuel gas or synthesis gas.

Preliminary gasification experiments with broiler litter indicate that the process is technically feasible. A gasifier operated at low pressures and high temperatures produces a gas rich in carbon monoxide and hydrogen at an appreciable gasification rate. Experiments indicate that the gasification rate can be increased by augmenting the inherent catalyst with alkali metal salts. A preliminary design of a transportable broiler litter gasification unit has revealed that the process is not only technically feasible but also economically attractive. A unit capable of processing 1.5 tons of fresh litter per hour has a payback period of approximately two years.

Recommendations

Although the process appears to be both technically and economically feasible, there are still many questions to be asked and answered. Only through further investigation and study can the process be developed successfully.

The initial gasification experiments described in this thesis were undertaken to demonstrate only the technical and economic feasibility of the process. A complete screening matrix should now be performed. The screening matrix should first determine the optimum temperature and pressure ranges for the catalytic steam gasification process. These experiments should also investigate the effect of various catalysts and catalyst loadings on the specific gasification rate. In addition to the catalyst type and loading, the method of catalyst application should also be investigated for potential effects on the

reaction rate. The screening matrix will determine the actual operating temperature and pressure of a broiler litter gasifier.

Studies should also be undertaken to investigate the effect of various broiler litter properties on both the gasification rate and reactor design. Particularly important are the proximate analysis of the litter and the analysis of the mineral and sulfur contents. Since broiler litter composition is highly variable, an effort should be made to investigate the variance in broiler litter throughout the Southeast region. This investigation would provide data to design a flexible reactor capable of accommodating a wide variety of litter feedstocks. This phase of investigation should also explore the compatibility of broiler litters with both downdraft and updraft flow regimes. Since downdraft operation has several unique advantages over updraft operation, methods of increasing the tolerance of downdraft reactors to low quality fuels should be examined.

Finally, additional economic analyses should be performed. Although the process is economically viable as a transportable gasification unit, other applications may prove more profitable. A stationary gasification plant is the first option which should be explored. The economics of scale may result in a reduction in unit operating costs. Other possible applications include the construction of a broiler litter gasifier at industries in the vicinity of broiler farms. The gasifier could serve as a source of fuel gas or synthesis gas.

REFERENCES

REFERENCES

1. Anderson, George H., and Garrett P. Smith. "The Exxon Process for Catalytic Coal Gasification." 1982 American Gas Association (AGA) Transmission Conference. Chicago, 17-19 May 1982.

2. Antal, Michael Jerry, Jr. "Mathematical Modelling of Biomass Pyrolysis Phenomena." Fuel 64 (1985): 1483-1486.

3. Cronan, Robert. "Panel Weighs Curbing Farm Waste Runoff." 18 Oct. 1997. SunSpot. http://www.sunspot.net (28 Jan. 1998).

4. Evans, R.J., et al. "Gasification of Wood Wastes in the RENUGAS Process." 1986 American Gas Association (AGA) Distribution/Transmission Conference. Chicago, 28-30 Apr. 1986.

5. "Farmers Upset with Governor's Anti-Pfiesteria Plan." 22 Jan. 1998. The Capital Online. http://www.capitalonline.com (28 Jan. 1998).

6. Ferguson, Jim. "Gasification: Thermochemical Conversion of Biomass." Bio-Joule. May 1987: 3-5.

7. Feuerbach, Lynn, and Cindy Hadish. "Study: U.S. Deep in Manure." The Gazette [Cedar Rapids, IA] 29 Dec. 1997.

8. Galegher, S.J., et al. Kinetics of Catalyzed Steam Gasification of Low-Rank Coals to Produce Hydrogen. (DOE/FE/60181-2034). Washington, D.C.: United States Department of Energy (DOE), June 1986.

9. Guo, Chuang-tao, and Li-ming Zhang. "Kinetics of Coal Char Gasification at Elevated Pressures." Fuel 65 (1986): 1364-1367.

10. Hashimoto, Kenji, Kouichi Miura, and Torataro Ueda. "Correlation of Gasification Rates of Various Coals Measured by a Rapid Heating Method in a Steam Atmosphere at Relatively Low Temperatures." Fuel 65 (1986): 1516-1523.

11. Hauserman, W.B. "High-Yield Hydrogen Production by Catalytic Gasification of Coal or Biomass." International Journal of Hydrogen Energy 19 (1994): 413-419.

12. Hirsch, Robert L., et al. "Catalytic Coal Gasification: An Emerging Technology." Science 8 Jan. 1982: 121-127.

13. Jones, Harold B., Jr., and E.A. Ogden. Energy Potential from Livestock and Poultry Wastes in the South. (Agricultural Report Number 522). Washington, D.C.: United States Department of Agriculture (USDA), Nov. 1984.

14. Lee, Sunggyu. Alternative Fuels. Washington, D.C.: Taylor and Francis, 1996.

15. Levenspiel, Octave. Chemical Reaction Engineering. 2nd ed. New York: John Wiley and Sons, 1972.

16. Liu, Zuo-liang, and He-hui Zhu. "Steam Gasification of Coal Char Using Alkali and Alkaline-Earth Metal Catalysts." Fuel 65 (1986): 1334-1338.

17. Lowry, H.H., ed. Chemistry of Coal Utilization: Volume II. New York: John Wiley and Sons, 1945.

18. Lynch, David. "Harkin Bill Calls for Federal Manure Role." The Gazette [Cedar Rapids, IA] 26 Sept. 1997.

19. Miura, Kouichi, et al. "Steam Gasification of Carbon: Effect of Several Metals on the Rate of Gasification and the Rates of CO and CO_2 Formation." Fuel 65 (1986): 407-411.

20. North Carolina State University (NCSU). "Pfiesteria Piscicida Homepage." 1997 NCSU Aquatic Botany Laboratory. http://www2.ncsu.edu/unity/lockers/project/aquatic_botany (5 May 1998).

21. Payne, Victor W.E., and James O. Donald. Poultry: Waste Management and Environmental Protection Manual. (Circular ANR-580). Auburn University, AL: Alabama Cooperative Extension Service, Jan. 1991.

22. Peters, Max S., and Klaus D. Timmerhaus. Plant Design and Economics for Chemical Engineers. 4th ed. New York: McGraw-Hill, 1991.

23. Poultry Water Quality Consortium (PWQC). Poultry Water Quality Handbook. Chattanooga, TN: PWQC, June 1994.

24. Ray, Russell. "Oklahoma Water Proposals Target Poultry Industry." Southwest Times Record [Fort Smith, AR] 4 Dec. 1997.

25. Schiefelbein, G.F. Thermal Gasification of Biomass: An Update on DOE's Research Program. Washington, D.C.: United States Department of Energy (DOE).

26. Schumacher, W., et al. "Kinetics of K-Catalysed Steam and CO_2 Gasification in the Presence of Product Gases." Fuel 65 (1986): 1360-1363.

27. Shields, Todd. "Maryland Farmers Concerned About Focus on Fertilizer Use." Washington Post. 25 Jan. 1998, B10.

28. Smith, J.M., and H.C. Van Ness. Introduction to Chemical Engineering Thermodynamics. 4th ed. New York: McGraw-Hill, 1987.

29. Solar Energy Research Institute (SERI). A Survey of Biomass Gasification. (SERI/TR-33-239). Golden, CO: SERI, July 1979.

30. Takarada, Takayuki, et al. "Steam Gasification of Brown Coal Using Sodium Chloride and Potassium Chloride Catalysts." Industrial and Engineering Chemistry Research 28 (1989): 505-510.

31. Takarada, Takayuki, Yasukatsu Tamai, and Akira Tomita. "Effectiveness of K_2CO_3 and Ni as Catalysts in Steam Gasification." Fuel 65 (1986): 505-510.

32. Thomson, William J., and Ling Yee Sy. "Potassium Catalysed Gasification of Kentucky Oil Shale Char." Fuel 66 (1987): 223-227.

33. Tiernan, Becky. "Chamber Targets Waste." Tulsa World. 23 Jan. 1998.

34. Timpe, Ronald C., and William B. Hauserman. "The Catalytic Gasification of Hybrid Poplar and Common Cattail Plant Chars." Energy from Biomass and Wastes XVI. Orlando, Florida, 1992. Chicago: Institute of Gas Technology (IGT), 1992. 903-19.

35. "U.S. Broiler Production: 1950-1956." 29 Apr. 1997. United States Department of Agriculture (USDA) - National Agricultural Statistics Service (NASS). http://www.usda.gov/nass (13 May 1998).

36. United States Department of Commerce (DOC). 1992 Census of Agriculture. Washington, D.C.: Bureau of Census, 1992.

37. Van Tuyl, David E., and William J. Thomson. "Reaction Kinetics of the Gasification of Michigan Antrim Oil Shale Char." Fuel 65 (1986): 58-62.

38. Warrick, Joby, and Todd Shields. "Maryland Counties Awash in Pollution-Causing Nutrients." Washington Post 3 Oct. 1997, A01.

Appendix I

FORTRAN Program for Equilibrium Analysis

```
*  program name:  equilibrium.for
*
*  creator:  J. Andrew Jones
*
*  original:  February 24, 1998
*  last update:  June 7, 1998
*
*  purpose:  The purpose of this program is to analyze
*  equilibrium compositions for the catalytic steam
*  gasification reaction mechanism.  The program utilizes
*  a gradient descent algorithm to determine the equilibrium
*  mole fraction of each species.
*
*  variable name      description
*  ----------------   ---------------------------------------
*  notot              total moles initially present
*  no                 moles of each species initially
*                     present
*  Ppsi               total pressure in pounds per square
*                     inch absolute
*  Pbar               total pressure in bar
*  TFahr              temperature in degrees Fahrenheit
*  TCels              temperature in degrees Celsius
*  TKelv              temperature in Kelvin
*  K                  equilibrium constant for each reaction
*  HORatio            hydrogen-to-oxygen atomic ratio
*  nuspec             stoichiometric coefficient for each
*                     species in each reaction
*  nureact            overall stoichiometric coefficient for
*                     each reaction
*  Eps                array of reaction coordinates
*  InitEps            array of initial reaction coordinates
*  y                  array of individual species mole
*                     fractions
*  yi                 array of individual species initial
*                     mole fractions
*  nf                 moles of each species present at
*                     equilibrium
*  deltot             change in total number of moles
*  toler              convergence criterion for gradient
*                     descent algorithm
*  J                  Jacobian matrix for column vector F
*  Jt                 transpose of Jacobian matrix for
*                     column vector F
*  F                  column vector of nonlinear functions
*  g                  objective function for gradient
*                     descent algorithm
*  dYdE               partial derivatives of each mole
*                     fraction with respect to each
*                     reaction coordinate
```

```
*  dFdE              partial derivatives of each
*                    nonlinear function with respect to
*                    each reaction coordinate
*  z                 unit gradient vector
*  CK                equilibrium constants calculated from
*                    approximate equilibrium mole fractions
*  RelErr            relative error of calculated
*                    equilibrium constants
*  PrevErr           relative error of calculated
*                    equilibrium constants from previous
*                    iteration
*  ErrImp            improvement in relative errors of
*                    equilibrium constants
*  flag              boolean variable indicating gradient
*                    descent convergence
*  seed              integer seed for random number
*                    generation
*  MaxIter           maximum allowable gradient descent
*                    iterations
*  ImpFlag           boolean variable indicating whether
*                    the gradient descent algortihm is
*                    required to demonstrate improvement

      program equilibrium

*  variable declaration statements for reaction conditions
      double precision notot,no(6)
      double precision Ppsi,Pbar
      double precision TFahr,TCels,TKelv
      double precision K(3)
      double precision HORatio

*  variable declaration statements for reaction system
      double precision nuspec(6,3)
      double precision nureact(3)

*  variable declaration statements defining gas compositions
      double precision Eps(3),InitEps(3)
      double precision y(6),yi(6)
      double precision nf(6)
      double precision deltot

*  variable declaration statements for nonlinear system
*  approximation
      double precision toler
      double precision J(3,3),Jt(3,3),F(3),g
      double precision dYdE(5,3)
      double precision dFdE(3,3)
      double precision z(3)
      double precision CK(3),RelErr(3),PrevErr(3),ErrImp
      integer flag,seed
```

```
*  statements to open output file
      open(unit=11,file='equilibrium.out',status='new')

*  assignment statement for random number generator seed
      seed=605290

*  assignment statement for gradient descent tolerance
      toler=0.001

*  assignment statement for maximum gradient descent
*  iterations
      MaxIter=250000

*  assignment statements defining reaction stoichiometry
      InitEps(1)=0.
      InitEps(2)=0.
      InitEps(3)=0.
      nuspec(1,1)=1.
      nuspec(1,2)=-1.
      nuspec(1,3)=-1.
      nuspec(2,1)=0.
      nuspec(2,2)=1.
      nuspec(2,3)=0.
      nuspec(3,1)=0.
      nuspec(3,2)=0.
      nuspec(3,3)=1.
      nuspec(4,1)=1.
      nuspec(4,2)=1.
      nuspec(4,3)=-3.
      nuspec(5,1)=-1.
      nuspec(5,2)=-1.
      nuspec(5,3)=1.
      nuspec(6,1)=0.
      nuspec(6,2)=0.
      nuspec(6,3)=0.
      nureact(1)=1.
      nureact(2)=0.
      nureact(3)=-2.

*  statements to read input of reaction conditions
      write(*,*)
      write(*,*)'          Steam Gasification Equilibrium ',
     &          'Calculation'
      write(*,*)
      write(*,*)'Enter the reaction temperature in degrees',
     &' Fahrenheit.'
      read(*,*)TFahr
      write(*,*)
      write(*,*)'Enter the reaction pressure in psia.'
      read(*,*)Ppsi
      write(*,*)
```

```
      write(*,*)'Enter the moles of carbon monoxide ',
     &'initially present.'
      read(*,*)no(1)
      write(*,*)
      write(*,*)'Enter the moles of carbon dioxide ',
     &'initially present.'
      read(*,*)no(2)
      write(*,*)
      write(*,*)'Enter the moles of methane initially ',
     &'present.'
      read(*,*)no(3)
      write(*,*)
      write(*,*)'Enter the moles of hydrogen initially ',
     &'present.'
      read(*,*)no(4)
      write(*,*)
      write(*,*)'Enter the moles of water vapor initially ',
     &'present.'
      read(*,*)no(5)
      write(*,*)
      write(*,*)'Enter the moles of inert gases initially ',
     &'present.'
      read(*,*)no(6)
      write(*,*)

*     statements to convert temperature to degrees Celsius and
*     Kelvin
      TKelv=(TFahr+459.67)/1.8
      TCels=TKelv-273.15

*     statement to convert pressure to bar
      Pbar=Ppsi/14.5038

*     statement to calculate total number of moles initially
*     present
      notot=no(1)+no(2)+no(3)+no(4)+no(5)+no(6)

*     statements to calculate hydrogen-to-oxygen molar ratio
      HORatio=(4.*no(3)+2.*no(4)+2.*no(5))/
     &(no(1)+2.*no(2)+no(5))

*     statements to calculate equilibrium constants
      K(1)=exp(-15702./TKelv+1.384*log(TKelv)-0.621e-03
     &     *TKelv+39900./TKelv**2.+7.6416)
      K(2)=exp(5872.4/TKelv+1.860*log(TKelv)-0.27e-03*TKelv
     &     -58200./TKelv**2.-18.013)
      K(3)=exp(22785./TKelv-7.951*log(TKelv)+4.354e-03*TKelv
     &     -3.6067e-07*TKelv**2.-4850./TKelv**2.+24.899)
```

```
*  statements to generate initial reaction coordinates
*  approximation
 500  call epsinit(Eps,seed)

*  statement initializing gradient descent algorithm
 502  iter=0
 501  flag=0
 20   if (flag.eq.0) then
         iter=iter+1
         count=count+1
         if (iter.gt.MaxIter) then
            goto 500
         endif

*  statements to calculate mole fractions
         call molfrac(y,notot,no,nuspec,nureact,Eps)

*  statements to calculate value of nonlinear system
*  functions
         call Fvector(F,y,Pbar,K)

*  statements to calculate the value of multivariable
*  function g
         call gcalc(g,F)

*  statements to calculate appropriate partial derivatives
         call pderiv(dYdE,dFdE,y,no,notot,Eps,Pbar,K)

*  statements to construct Jacobian matrix and the transpose
*  of the Jacobian matrix
         call Jacobi(J,Jt,dFdE)

*  statements to calculate the gradient unit vector
         call gradient(z,Jt,F,flag)

*  statements to adjust reaction coordinates
         call refine(Eps,g,z,notot,no,nuspec,nureact,Pbar,K,
     &               toler,flag)

*  statement to check for negative mole fractions
         if (flag.eq.1) then
            do 510 i=1,6
               if (y(i).lt.0.) then
                  goto 500
               endif
 510        continue
         endif
         goto 20

*  end statement for gradient descent iterations
      endif
```

```
*  statements to calculate initial and final compositions
      deltot=0.
      do 591 n=1,3
         deltot=deltot+nureact(n)*Eps(n)
 591  continue
      call molfrac(y,notot,no,nuspec,nureact,Eps)
      call molfrac(yi,notot,no,nuspec,nureact,InitEps)
      do 592 i=1,6
         nf(i)=y(i)*(notot+deltot)
 592  continue

*  statements to validate solution
      CK(1)=y(1)*y(4)*Pbar/y(5)
      CK(2)=y(2)*y(4)/(y(1)*y(5))
      CK(3)=y(3)*y(5)/(y(1)*y(4)**3.*Pbar**2.)
      do 593 i=1,3
         PrevErr(i)=RelErr(i)
         RelErr(i)=abs(K(i)-CK(i))/K(i)*100.
 593  continue
      ErrImp=0.
      do 650 i=1,3
         ErrImp=ErrImp+(PrevErr(i)-RelErr(i))
 650  continue
      if (ErrImp.lt.0.001.and.ImpFlag.eq.1.and.(RelErr(1)
     &    +RelErr(2)+RelErr(3)).gt.300.) then
         ImpFlag=0
         goto 500
      endif
      if (ImpFlag.eq.0) then
         ImpFlag=1
      endif
      do 594 i=1,3
         if (RelErr(i).gt.0.01) then
            toler=toler/2.
            goto 502
         endif
 594  continue

*  statements to output header
      write(11,*)'Equilibrium conditions for steam ',
     &           'gasification reactions'
      write(11,*)

*  statements to output reaction conditions
      write(11,*)'I.  Reaction Conditions Summary'
      write(11,*)
      write(11,600)TFahr,TCels,TKelv
 600  format(5x,'Temperature = ',1x,f6.1,' degrees F = ',
     &       f6.1,' degrees C = ',f6.1,' K')
```

```
      write(11,601)Ppsi,Pbar
 601  format(5x,'Pressure = ',f6.1,' psia = ',f6.2,' bar')
      write(11,599)HORatio
 599  format(5x,'Hydrogen-to-oxygen ratio = ',f7.3,' mol H',
     &' / mol O')
      write(11,*)

*  statements to output initial and final compositions
      write(11,*)'II.  Composition Summary'
      write(11,*)
      write(11,602)
 602  format(15x,'Initial',9x,'Final',9x,'Initial',9x,
     &'Final')
      write(11,603)
 603  format(16x,'Moles',10x,'Moles',6x,'Mole Fraction',2x,
     &'Mole Fraction')
      write(11,*)
      write(11,604)no(1),nf(1),yi(1),y(1)
 604  format(5x,'CO',8x,f7.4,8x,f7.4,8x,f7.5,8x,f7.5)
      write(11,605)no(2),nf(2),yi(2),y(2)
 605  format(5x,'CO2',7x,f7.4,8x,f7.4,8x,f7.5,8x,f7.5)
      write(11,606)no(3),nf(3),yi(3),y(3)
 606  format(5x,'CH4',7x,f7.4,8x,f7.4,8x,f7.5,8x,f7.5)
      write(11,607)no(4),nf(4),yi(4),y(4)
 607  format(5x,'H2',8x,f7.4,8x,f7.4,8x,f7.5,8x,f7.5)
      write(11,608)no(5),nf(5),yi(5),y(5)
 608  format(5x,'H2O',7x,f7.4,8x,f7.4,8x,f7.5,8x,f7.5)
      write(11,609)no(6),nf(6),yi(6),y(6)
 609  format(5x,'Inert',5x,f7.4,8x,f7.4,8x,f7.5,8x,f7.5)
      write(11,*)

*  statements to output validation results
      write(11,*)'III.  Calculation Summary'
      write(11,*)
      write(11,610)
 610  format(18x,'Actual',12x,'Calculated',6x,'Relative ',
     &'Error (%)')
      write(11,611)K(1),CK(1),RelErr(1)
 611  format(5x,'K1',8x,f12.5,8x,f12.5,10x,f8.4)
      write(11,612)K(2),CK(2),RelErr(2)
 612  format(5x,'K2',8x,f12.5,8x,f12.5,10x,f8.4)
      write(11,613)K(3),CK(3),RelErr(3)
 613  format(5x,'K3',8x,f12.5,8x,f12.5,10x,f8.4)
      write(11,*)

*  stop/end statements
      stop
      end
```

```
*  subroutine name:  epsinit
*
*  purpose:  The purpose of this subroutine is to generate
*  an initial approximation to the equilibrium reaction
*  coordinates.  The random number algorithm generates a
*  sequence of random numbers from a positive integer seed
*  value.  The algorithm is based on the Sandia National
*  Laboratories Technical Report "A Portable Random Number
*  Generator for Use in Signal Processing" by S. D. Stearns.
*
*  variable name      description
*  ----------------   ------------------------------------
*  seed               positive integer seed
*  rand               random number between 0.0 and 1.0
*  epsilon            reaction coordinate for each reaction
*

      subroutine epsinit(epsilon,seed)

*  variable declaration statements
      integer seed
      real rand
      double precision epsilon(3)

*  generation of random reaction coordinates
      do 10 i=1,3
         seed=2045*seed+1
         seed=seed-(seed/1048576)*1048576
         rand=real(seed+1)/1048577.0
         epsilon(i)=rand
 10   continue

*  return/end statements
      return
      end

*  subroutine name:  molfrac
*
*  purpose:  The purpose of this subroutine is to calculate
*  the mole fraction of each species in the vapor phase.
*  The equations for each mole fraction are based on the
*  individual reaction and overall system stoichiometry.
*
*  variable name      description
*  ----------------   ------------------------------------
*  y                  mole fraction of each species
*  notot              total number of moles initially
*                     present
*  no                 initial number of moles of each
*                     species
```

```
*  nuspec              stoichiometric coefficient of each
*                      species for each reaction
*  nureact             overall stoichiometric coefficent for
*                      each reaction
*  Eps                 reaction coordinate for each reaction
*  delspec             change in moles of each species
*  deltot              change in total number of moles

      subroutine molfrac(y,notot,no,nuspec,nureact,Eps)

*  variable declaration statements
      double precision y(6)
      double precision notot,no(6)
      double precision nuspec(6,3),nureact(3)
      double precision Eps(3)
      double precision delspec,deltot

*  calculation of mole fractions
      do 30 i=1,6
         delspec=0.
         deltot=0.
         do 40 j=1,3
            delspec=delspec+nuspec(i,j)*Eps(j)
            deltot=deltot+nureact(j)*Eps(j)
 40      continue
         y(i)=(no(i)+delspec)/(notot+deltot)
 30   continue

*  return/end statements
      return
      end

*  subroutine name:  Fvector
*
*  purpose:  The purpose of this subroutine is to calculate
*  the value of the column vector F.  The elements of the
*  vector are f1, f2, and f3.  These functions approach zero
*  as the reaction coordinates approach equilibrium.
*
*  variable name       description
*  ----------------    ---------------------------------------
*  F                   column vector containing elements f1,
*                      f2, and f3 of the nonlinear system
*  y                   mole fraction of each species
*  Pbar                system pressure in bar
*  K                   equilibrium constant for each reaction

      subroutine Fvector(F,y,Pbar,K)

*  variable declaration statements
      double precision F(3),y(6),Pbar,K(3)
```

```
*  calculation of column vector elements
      F(1)=(y(1)*y(4)*Pbar/y(5)-K(1))/K(1)
      F(2)=(y(2)*y(4)/(y(1)*y(5))-K(2))/K(2)
      F(3)=(y(3)*y(5)/(y(1)*y(4)**3.*Pbar**2.)-K(3))/K(3)

*  return/end statements
      return
      end

*  subroutine name:  gcalc
*
*  purpose:  The purpose of this subroutine is to calculate
*  the multivariable function g.  The function maps the
*  three dimensional space of F into a single real value.
*  This function is minimized to find the equilibrium state.
*
*  variable name      description
*  ----------------   ------------------------------------
*  g                  value of multivariable function g
*  F                  column vector of nonlinear function
*                     values

      subroutine gcalc(g,F)

*  variable declaration statements
      double precision g,F(3)

*  statements to evaluate the multivariable function g
      g=0.
      do 50 i=1,3
         g=g+F(i)**2.
 50   continue

*  return/end statements
      return
      end

*  subroutine name:  pderiv
*
*  purpose:  The purpose of this subroutine is to calculate
*  the partial derivatives of each nonlinear function with
*  respect to each reaction coordinate.  This requires the
*  partial derivative of each mole fraction with respect to
*  each reaction coordinate.  The partial derivatives of
*  mole fractions for inert species are not necessary for
*  determining the equilibrium state and, therefore, are
*  not calculated.
*
*  variable name      description
*  ----------------   ------------------------------------
*  dYdE               partial derivatives of mole fractions
```

```
*   dFdE                partial derivatives of nonlinear
*                       functions
*   y                   mole fraction for each species
*   no                  initial moles of each species
*   notot               total number of moles initially
*                       present
*   Eps                 reaction coordinate of each reaction
*   Pbar                system pressure in bar
*   denom               denominator for mole fraction partial
*                       derivatives

      subroutine pderiv(dYdE,dFdE,y,no,notot,Eps,Pbar,K)

*   variable declaration statements
      double precision dYdE(5,3),dFdE(3,3),y(6)
      double precision no(6),notot,Eps(3),Pbar,K(3)
      double precision denom

*   calculation of denominator common to several partial
*   derivatives
      denom=(notot+Eps(1)-2.*Eps(3))**2.

*   calculation of partial derivative values for mole
*   fractions
      dYdE(1,1)=(notot-no(1)+Eps(2)-Eps(3))/denom
      dYdE(1,2)=-1./(notot+Eps(1)-2.*Eps(3))
      dYdE(1,3)=(-notot+2.*no(1)+Eps(1)-2.*Eps(2))/denom
      dYdE(2,1)=(-no(2)-Eps(2))/denom
      dYdE(2,2)=1./(notot+Eps(1)-2.*Eps(3))
      dYdE(2,3)=(2.*no(2)+2.*Eps(2))/denom
      dYdE(3,1)=(-no(3)-Eps(3))/denom
      dYdE(3,2)=0.
      dYdE(3,3)=(notot+2.*no(3)+Eps(1))/denom
      dYdE(4,1)=(notot-no(4)-Eps(2)+Eps(3))/denom
      dYdE(4,2)=1./(notot+Eps(1)-2.*Eps(3))
      dYdE(4,3)=(-3.*notot+2.*no(4)-Eps(1)+2.*Eps(2))/denom
      dYdE(5,1)=(-notot-no(5)+Eps(2)+Eps(3))/denom
      dYdE(5,2)=-1./(notot+Eps(1)-2.*Eps(3))
      dYdE(5,3)=(notot+2.*no(5)-Eps(1)-2.*Eps(2))/denom

*   calculation of partial derivative values for nonlinear
*   functions
      do 60 i=1,3
         dFdE(1,i)=(Pbar*(y(5)*(y(1)*dYdE(4,i)+y(4)*dYdE
     &             (1,i))-y(1)*y(4)*dYdE(5,i))
     &             /y(5)**2.)/K(1)
         dFdE(2,i)=(y(1)*y(5)*(y(2)*dYdE(4,i)+y(4)*dYdE
     &             (2,i))-y(2)*y(4)*(y(1)*dYdE
     &             (5,i)+y(5)*dYdE(1,i)))
     &             /(y(1)**2.*y(5)**2.)/K(2)
```

```
          dFdE(3,i)=(1./Pbar**2.)*(y(1)*y(4)**3.*
     &              (y(3)*dYdE(5,i)+y(5)*dYdE(3,i))
     &              -y(3)*y(5)*(3.*y(1)*y(4)**2.*
     &              dYdE(4,i)+y(4)**3.*dYdE(1,i)))/(y(1)
     &              **2.*y(4)**6.)/K(3)
 60    continue

*   return/end statements
      return
      end

*   subroutine name:  Jacobi
*
*   purpose:  The purpose of this subroutine is to construct
*   the Jacobian matrix.  The transpose of the Jacobian
*   matrix is then developed.  The transpose is used in the
*   calculation of the gradient vector.
*
*   variable name       description
*   ----------------    -----------------------------------
*   J                   Jacobian matrix
*   Jt                  transpose of the Jacobian matrix
*   dFdE                partial derivative of each nonlinear
*                       function with respect to each reaction
*                       coordinate

      subroutine Jacobi(J,Jt,dFdE)

*   variable declaration statements
      double precision J(3,3),Jt(3,3),dFdE(3,3)

*   construction of Jacobian matrix and respective transpose
      do 70 m=1,3
         do 80 n=1,3
            J(m,n)=dFdE(m,n)
            Jt(n,m)=J(m,n)
 80      continue
 70   continue

*   return/end statements
      return
      end

*   subroutine name:  gradient
*
*   purpose:  The purpose of this subroutine is to determine
*   the gradient vector for specified reaction coordinates.
*   gradient vector indicates the direction of steepest
*   descent on the multivariable g surface.  The magnitude of
*   the gradient is calculated using the Euclidean norm.  The
*   magnitude is then used to convert the gradient vector to
```

```
*  the unit gradient vector.
*
*  variable name      description
*  ----------------   ------------------------------------
*  z                  gradient vector on g surface
*  Jt                 transpose of the Jacobian matrix
*  F                  column vector of nonlinear function
*                     values
*  flag               boolean variable indicating solution
*  length             magnitude of unnormalized gradient
*                     vector

      subroutine gradient(z,Jt,F,flag)

*  variable declaration statements
      double precision z(3),Jt(3,3),F(3),length,temp
      integer flag

*  statements to calculate the gradient vector
      do 90 i=1,3
         z(i)=0.
         do 100 j=1,3
            z(i)=z(i)+2.*Jt(i,j)*F(j)
 100     continue
 90   continue

*  statements to calculate the magnitude of the gradient
*  vector
      temp=0.
      do 110 i=1,3
         temp=temp+z(i)**2.
 110  continue
      length=temp**0.5

*  statements to test for minimization
      if (length.eq.0.) then
         flag=1
      else

*  statements to normalize the gradient vector
         do 120 i=1,3
            z(i)=z(i)/length
 120     continue
      endif


*  return/end statements
      return
      end
```

```
*  subroutine name:  refine
*
*  purpose:  The purpose of this subroutine is to refine the
*  reaction coordinates.  The coordinates are refined by
*  fitting a quadratic polynomial through three points
*  collinear with the gradient unit vector.  The minimum of
*  the polynomial over this range is used as the new
*  approximation for the reaction coordinates.
*
*  variable name      description
*  ----------------   ------------------------------------
*  Eps                reaction coordinate of each reaction
*  g                  value of the multivariable function g
*  F                  column vector of nonlinear function
*                     values
*  alpha              factors used to place points used in
*                     quadratic polynomial curve fitting
*  z                  unit gradient vector
*  P                  value of polynomial at three points
*  minalp             polynomial minimum
*  a                  coefficient of degree two term in
*                     polynomial
*  b                  coefficient of degree one term in
*                     polynomial
*  c                  coefficient of degree zero term in
*                     polynomial
*  critical           critical point of polynomial
*  Pcrit              value of polynomial at critical point
*  notot              total number of moles initially
*                     present
*  no                 initial number of moles of each
*                     species
*  nuspec             stoichiometric coefficient of each
*                     species for each reaction
*  nureact            overall stoichiometric coefficient for
*                     each reaction
*  Pbar               system pressure in bar
*  K                  equilibrium constant for each reaction
*  y                  mole fraction of each species
*  epsilon            reaction coordinates at each point on
*                     polynomial
*  toler              tolerance for gradient descent
*  flag               boolean variable indicating solution

      subroutine refine(Eps,g,z,notot,no,nuspec,nureact,
     &                  Pbar,K,toler,flag)

*  variable declaration statements
      double precision Eps(3),g,F(3),alpha(3),P(3)
      double precision notot,no(6),nuspec(6,3),nureact(3)
      double precision epsilon(3,3),temp(3),z(3),toler,Pcrit
```

```
      double precision minalp,a,b,c,critical,Pbar,K(3),y(6)
      integer flag,check

*  statement to locate first point on polynomial
      alpha(1)=0.
      P(1)=g
      do 130 j=1,3
         epsilon(1,j)=Eps(j)
 130  continue

*  statement to locate second point on polynomial
      check=0
      alpha(3)=1.
 140  if (check.eq.0.and.alpha(3).gt.toler) then
         do 150 i=1,3
            epsilon(3,i)=Eps(i)-alpha(3)*z(i)
            temp(i)=epsilon(3,i)
 150     continue
         call molfrac(y,notot,no,nuspec,nureact,temp)
         call Fvector(F,y,Pbar,K)
         call gcalc(P(3),F)
         if (P(3).lt.P(1)) then
            check=1
         else
            alpha(3)=alpha(3)/2.
         endif
         goto 140
      endif

*  statements to check for solution
      if (alpha(3).lt.toler) then
         flag=1
         goto 210
      endif

*  statements to locate third point on polynomial
      alpha(2)=alpha(3)/2.
      do 160 m=1,3
         epsilon(2,m)=Eps(m)-alpha(2)*z(m)
         temp(m)=epsilon(2,m)
 160  continue
      call molfrac(y,notot,no,nuspec,nureact,temp)
      call Fvector(F,y,Pbar,K)
      call gcalc(P(2),F)

*  statements to calculate coefficients of polynomial
      a=(2.*P(1)-4.*P(2)+2.*P(3))/alpha(3)**2.
      b=(-3.*P(1)+4.*P(2)-P(3))/alpha(3)
      c=P(1)
```

```
*  statement to calculate critical point of polynomial
      critical=-b/(2.*a)

*  statement to find minimum of polynomial
      if (critical.ge.0..and.critical.le.1.) then
         do 170 i=1,3
            temp(i)=Eps(i)-critical*z(i)
 170     continue
         call molfrac(y,notot,no,nuspec,nureact,temp)
         call Fvector(F,y,Pbar,K)
         call gcalc(Pcrit,F)
         if (Pcrit.le.P(3)) then
            minalp=critical
         else
            minalp=alpha(3)
         endif
      else
         minalp=alpha(3)
      endif

*  statements to calculate refined reaction coordinates
      do 200 i=1,3
         Eps(i)=Eps(i)-minalp*z(i)
 200  continue

*  return/end statements
 210  return
      end
```

Appendix II

Sample Output from Equilibrium Analysis Program

Equilibrium conditions for steam gasification reactions

I. Reaction Conditions Summary

Temperature = 1300.0 degrees F = 704.4 degrees C = 977.6 K
Pressure = 50.0 psia = 3.45 bar
Hydrogen-to-oxygen ratio = 2.000 mol H / mol O

II. Composition Summary

	Initial Moles	Final Moles	Initial Mole Fraction	Final Mole Fraction
CO	0.0000	0.3136	0.00000	0.21792
CO2	0.0000	0.2201	0.00000	0.15294
CH4	0.0000	0.0947	0.00000	0.06579
H2	0.0000	0.5644	0.00000	0.39223
H2O	1.0000	0.2462	1.00000	0.17112
Inert	0.0000	0.0000	0.00000	0.00000

III. Calculation Summary

	Actual	Calculated	Relative Error (%)
K1	1.72178	1.72189	0.0062
K2	1.60869	1.60869	0.0001
K3	0.07204	0.07204	0.0018

Appendix III

Operating Procedures for Broiler Litter Pyrolysis Apparatus

1. Clean any remaining tars and oils from the 1.25-inch outer diameter (OD), Schedule 40 stainless steel pipe.

2. Insert a circular screen of 200-mesh stainless steel approximately one-third of the reactor length from either end of the reactor. Cut a small slit in the center of the screen to allow insertion of the thermocouple.

3. Place up to one kilogram of fresh broiler litter into the reactor. Fill the reactor from the end opposite of the original stainless steel screen. It is easiest to fill the reactor in the vertical position. The stainless steel screen is easily disrupted, however. Take particular care to make sure the screen does not collapse or move under the weight of the litter.

4. After the litter has been placed in the reactor, insert another circular section of 200-mesh stainless steel from the end opposite of the first screen. Again, be careful not to disrupt the original stainless steel screen.

5. Verify that the bed of fresh broiler litter does not exceed the heated zones of the Mellen Model TS-2200-231-3 split-tube furnace. If the bed is too lengthy, less litter must be used to ensure that sufficient pyrolysis temperatures will be reached.

6. Now, attach the steel caps to each end of the reactor body. Use Teflon tape to prevent the entry of oxygen into the reactor.

7. Place the assembled reactor in the Mellen furnace. Secure the latches on the furnace.

8. Attach the nitrogen inlet line and volatiles outlet line to the tubing fitting on each cap. Insert the Type K thermocouple through the nitrogen inlet line and into the litter bed.

9. Establish the nitrogen flow. A flow rate of 10 cubic centimeters per second should be sufficient. Allow the nitrogen to purge the reactor of any oxygen. A purge time of ten minutes should be adequate. While the reactor is being purged, check the system for any possible leaks.

10. Once the pyrolysis apparatus has been purged, increase the furnace temperature to 1300°F. Monitor the temperature with the Omega Model 650 thermocouple meter.

11. Hold the reactor temperature at 1300°F for six hours. This will ensure that all moisture and volatile species are removed from the litter.

12. After the six hours are complete, allow the furnace to cool to room temperature. Maintain nitrogen flow during the cooling. This will ensure that no oxygen enters the system and oxidizes the hot char.

13. Remove the pyrolyzed char from the apparatus by removing the caps and screens. Store the char in an air-tight container in an inert glovebox.

14. Empty the condensed water and volatiles from the condenser. Clean any tars and oils generated by the pyrolysis process from the reactor.

Appendix IV

Operating Procedures for
High Pressure Fixed Bed Gasifier

Reactor Preparation

1. Clean internal surfaces of the reactor body including the ¾-inch Type 304 stainless steel tubing and stainless steel caps.

2. Attach a cap to the bottom of the reactor. Place a circular screen of 200-mesh stainless steel at the bottom of the reactor body. It should lie flush on the internal side of the bottom cap. This prevents ceramic packing from leaving the reactor.

3. Fill the reactor to approximately 40 percent of the reactor length with ceramic packing. This packing will support the char bed.

4. Place a circular screen of 200-mesh stainless steel above the ceramic packing. Using a screen constructed of two layers of the mesh ensures that the screen will not deteriorate at the reactor conditions. This screen will support the char bed.

5. Load up to five grams of char and catalyst into the reactor. Be sure to measure the mass of char and catalyst added to the reactor.

6. Place a circular screen of construction identical to that of Step 4 above the char. This screen will separate the char from the packing above the char bed.

7. Fill the remainder of the reactor with ceramic packing. This ceramic packing will provide adequate mixing and distribution of the inlet gases.

8. Attach the cap and inlet gas assembly to the top of the reactor body.

9. Connect the complete reactor assembly to the inlet and outlet lines. Verify that the apparatus has no leaks by opening all valves and bringing the system to the operating pressure.

Startup Mode

1. Fill the burette with distilled water.

2. Close valves 2, 4, and 8. This will configure the apparatus so that there are two independent flow paths through the apparatus. Figure A4.1 shows the apparatus with valve numbers and configurations.

3. Verify that valves 1, 3, 5, 6, and 7 are open. These valves are located on the flow paths and should be open at this time.

4. Establish water flow through the metering pump. Set the flow selection gauge so that the flow rate is approximately 3.00 milliliters per minute.

5. Establish the nitrogen flow. A flow rate of approximately 1.5 cubic feet per hour is sufficient. This will prevent oxidation of the char during startup.

6. Increase the temperature of the gas preheater/steam generator and reactor furnaces to the target temperature for the experimental trial.

7. As the steam generator temperature increases, the backpressure regulator should be operated to bring the steam bypass line to the target operating pressure.

8. When the steam bypass line and reactor stabilize at the target temperature, steady state operations have been established. At this point, the apparatus is ready to be converted to the gasification mode.

Gasification Mode

1. Immediately before switching to gasification mode, record the current reading from the cumulative gas flowmeter and refill the burette to the zero millimeter graduation. Reduce the water flow rate through the pump to approximately 0.40 milliliters per minute.

2. Adjust the backpressure regulator such that the pressure on the steam bypass line is reduced to atmospheric pressure.

3. Close valve 1. Immediately thereafter, open valve 2. The nitrogen flow has now been switched to the steam bypass line.

4. Close valves 3 and 7. This will complete the isolation of the nitrogen flow path.

5. Close valves 5 and 6 simultaneously. This will terminate flow through the steam bypass line.

6. Open valves 4 and 8 simultaneously. This will allow flow of the nitrogen, steam, and any additional reactants to the differential fixed bed reactor. Adjust the backpressure regulator so that the apparatus reaches the target operating pressure.

7. Start the stopwatch or other timing device.

8. Sample reactor effluent gases either manually or automatically at predetermined times. For each gas sample collected, also record the reactor temperature,

condenser temperature, cumulative gas flowmeter reading, and burette reading.

9. After the concentration of carbonaceous compounds in the gas reaches an undetectable level or stabilizea at a very low level, the trial can be ended.

Post-gasification Operations

1. Adjust the backpressure regulator so that the apparatus returns to atmospheric pressure.

2. Close valves 4 and 8. Open valves 5 and 6. These valve adjustments will move the flow of steam and other gases back to the steam bypass line.

3. Close valve 2 to isolate the nitrogen flow path from the steam bypass line. Terminate the flow of water from the pump to the system. Stop the flow of any other reactant gases to the system.

4. Open valves 1, 3, and 7 to allow nitrogen to flow through the reactor. This inert flow will prevent any oxidation of char during reactor cooling.

5. Cool the reactor and steam generator to room temperature.

6. When the apparatus has reached room temperature, stop the flow of nitrogen through the reactor.

7. Return all valves on the apparatus to the open position.

8. Remove the partially reacted char sample from the furnace. Weigh the sample and perform any additional analyses.

9. If gases were collected manually, analyze the composition of each sample on the gas chromatograph.

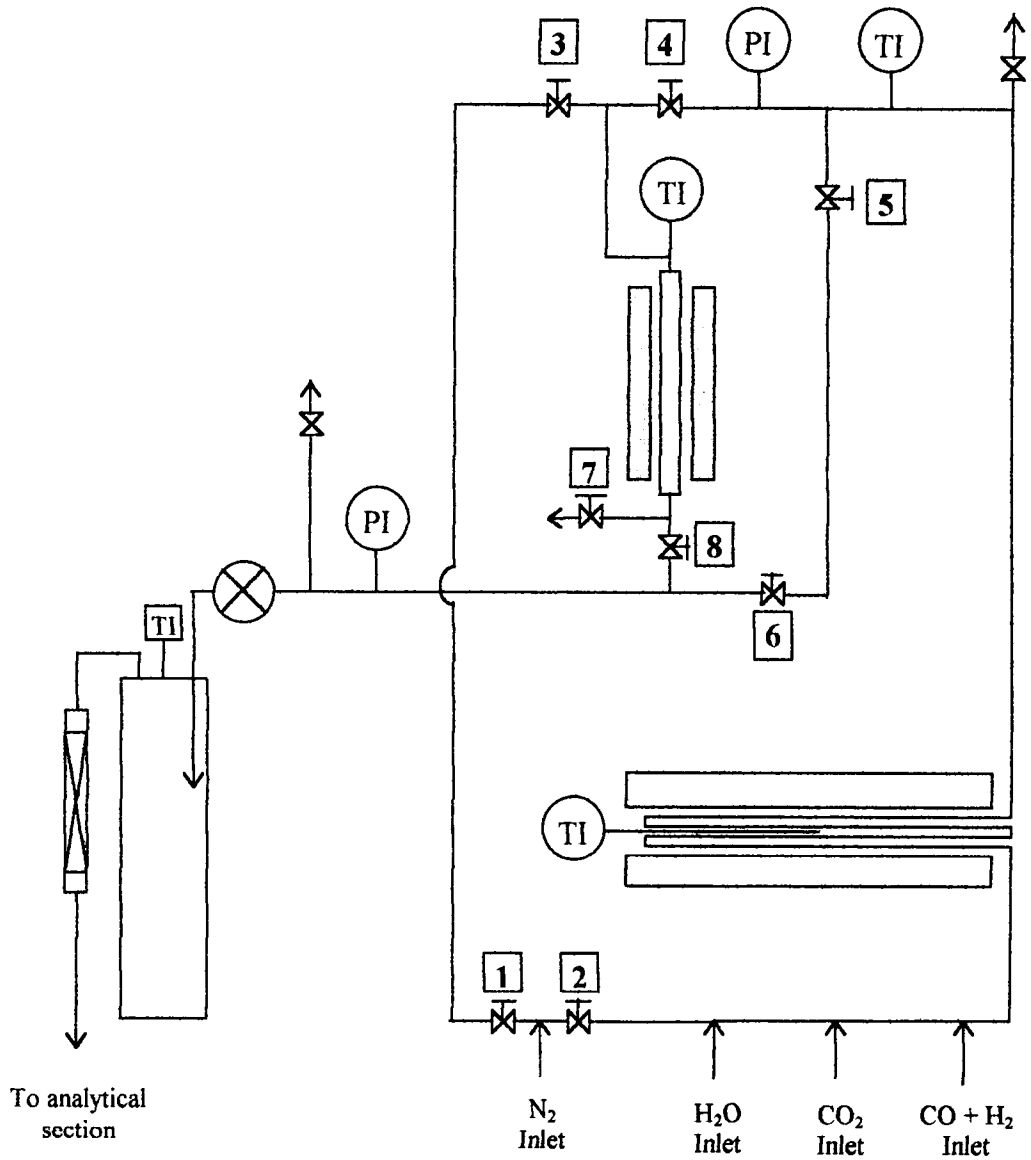

Figure A4.1 High Pressure Fixed Bed Gasifier – Valve Configurations

Appendix V

Experimental Data

Experimental Data for Trial 1

Target Temperature: 1300°F

Target Pressure: 150 psia

Catalyst: none

Catalyst Loading (weight percent on char basis): 0 %

Atmospheric Pressure: 735.0 mm Hg

Initial Cumulative Flowmeter Reading: 101.080 cubic feet

Initial Sample Weight: 3.00 grams

Initial Catalyst-Free Sample Weight: 3.00 grams

Initial Ash-to-Carbon Ratio: 0.7986 grams ash / grams carbon

Final Sample Weight: 1.72 grams

Final Catalyst-Free Sample Weight: 1.72 grams

Final Ash-to-Carbon Ratio: 4.0000 grams ash / grams carbon

Char Carbon Conversion: 0.7938

Average Specific Reaction Rate: $0.0006218 \frac{mol\ Carbon}{g\ Carbon \bullet \min}$

Table A5.1 Reactor Conditions for Trial 1

Time (minutes)	Reactor Temperature (°F)	Condenser Temperature (°F)	Gas Flowmeter Reading (cubic feet)	Burette Reading (milliliters)
5	1176	76	101.175	1.60
10	1307	76	101.238	3.20
15	1302	76	101.350	5.40
20	1249	77	101.473	6.80
25	1284	77	101.565	8.70
30	1290	76	101.665	10.60
40	1265	76	101.763	13.00
50	1320	76	101.850	15.75
60	1305	76	102.050	19.35
70	1320	76	102.175	22.70
80	1270	76	102.540	25.80
90	1369	76	102.975	29.20
120	1300	76	104.160	38.30
150	1301	73	105.260	47.50
180	1323	74	106.350	56.75
210	1351	73	107.200	61.50
240	1304	73	107.900	61.50
270	1324	73	108.555	71.70

Table A5.2 Gas Chromatograph Results for Trial 1

Time (minutes)	Oxygen Peak Area	Nitrogen Peak Area	Carbon Monoxide Peak Area	Methane Peak Area	Carbon Dioxide Peak Area
5	25.450	12929.317	3.670	0	32.157
10	16.374	13017.578	4.216	0	39.602
15	9.768	13102.002	13.820	0	98.186
20	6.496	12750.371	30.910	0	256.718
25	7.337	12896.052	25.308	0	244.392
30	18.516	12680.898	35.520	0	293.771
40	5.840	12627.332	49.276	0	349.234
50	6.457	13482.855	52.176	0	390.493
60	8.792	12425.978	50.808	0	375.906
70	6.121	13382.793	50.566	0	372.861
80	33.570	12924.002	13.202	0	98.826
90	4.806	13245.096	11.589	0	78.098
120	13.848	13189.682	7.055	0	48.308
150	4.800	13525.862	8.568	0	61.476
180	5.305	13273.471	8.079	0	49.007
210	6.031	13557.886	8.226	0	42.701
240	4.400	13272.214	3.525	0	14.695
270	4.576	13185.632	1.012	0	10.476

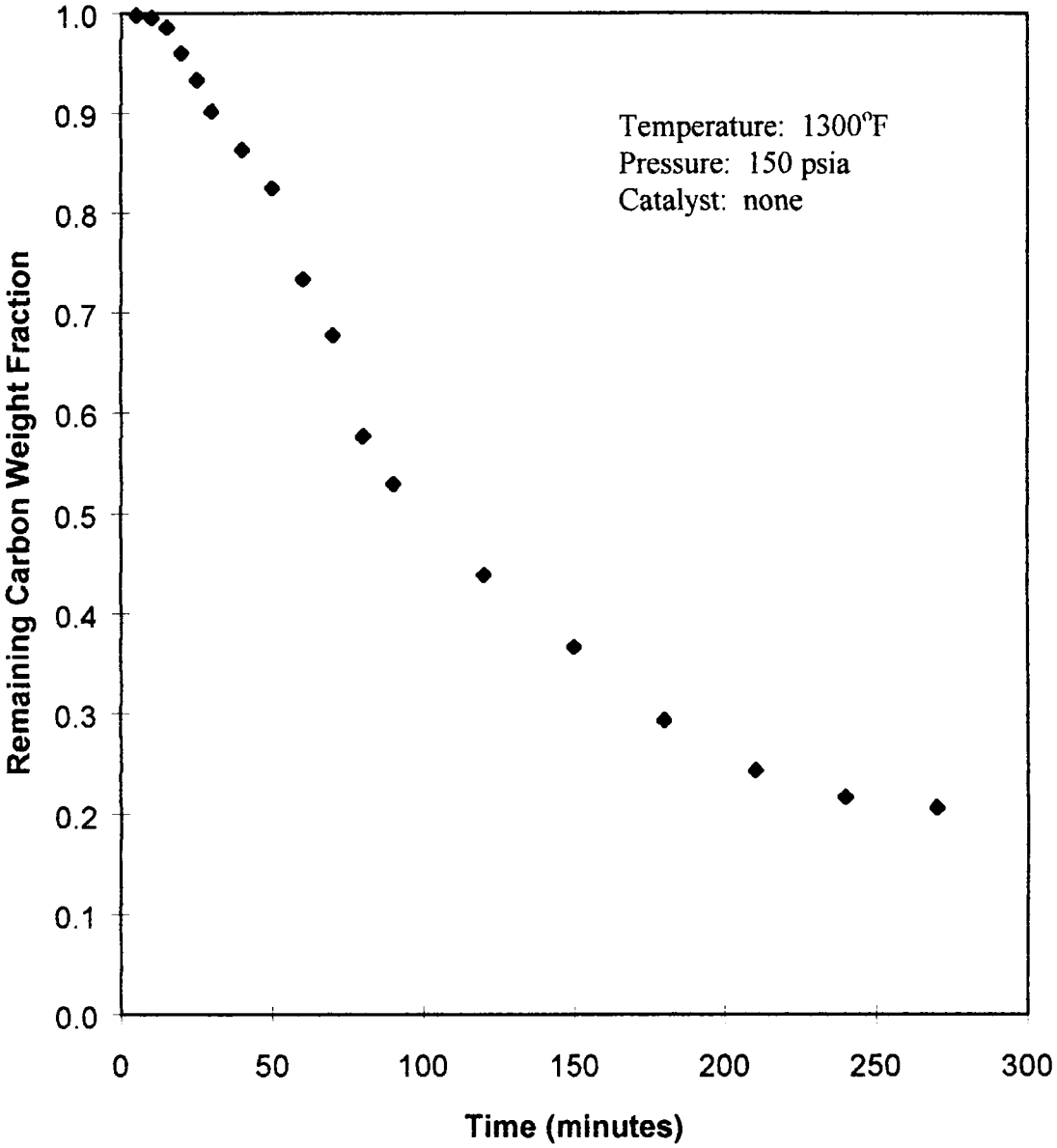

Figure A5.1. Remaining Carbon Weight Fraction – Trial 1

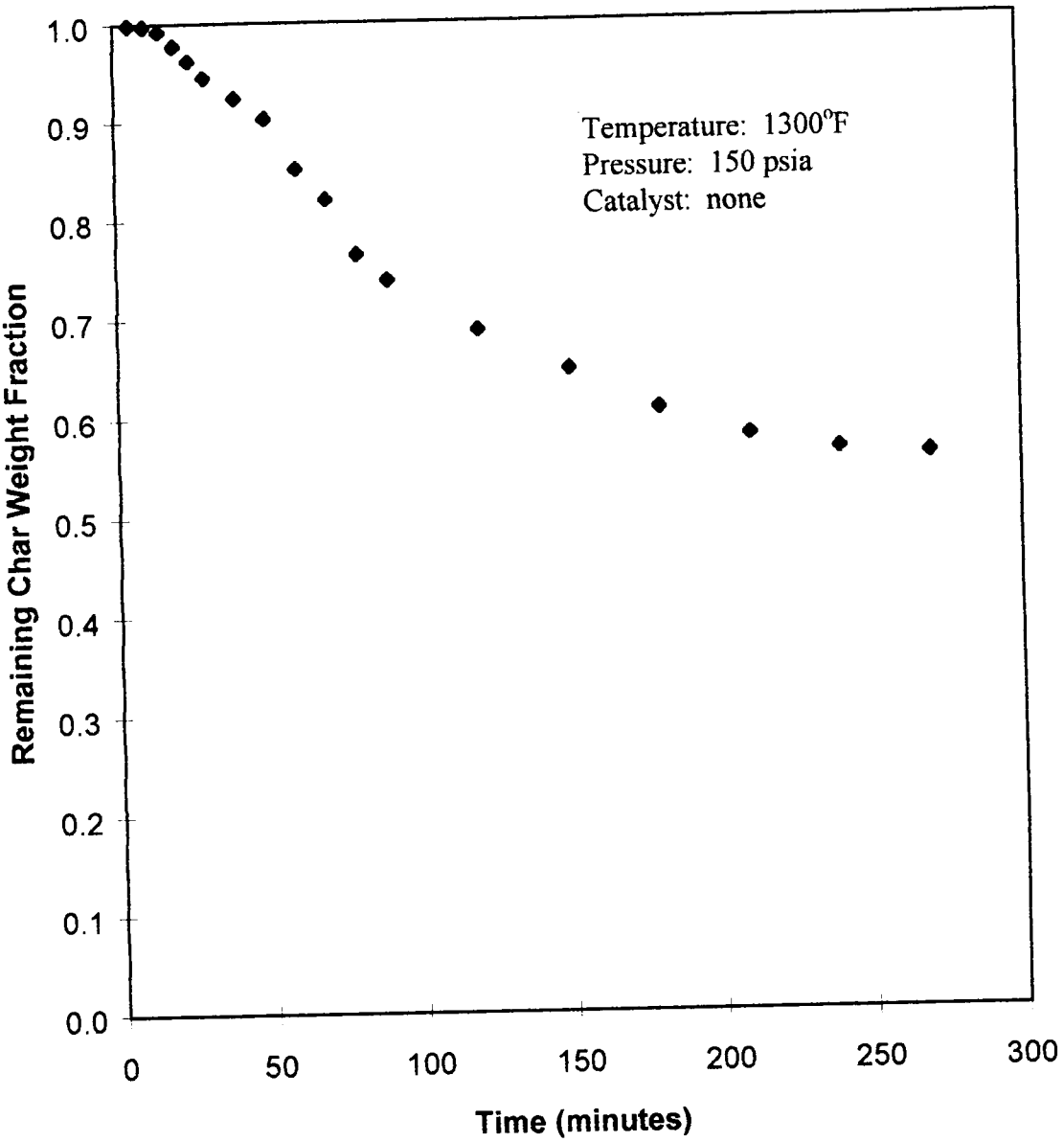

Figure A5.2 Remaining Char Weight Fraction – Trial 1

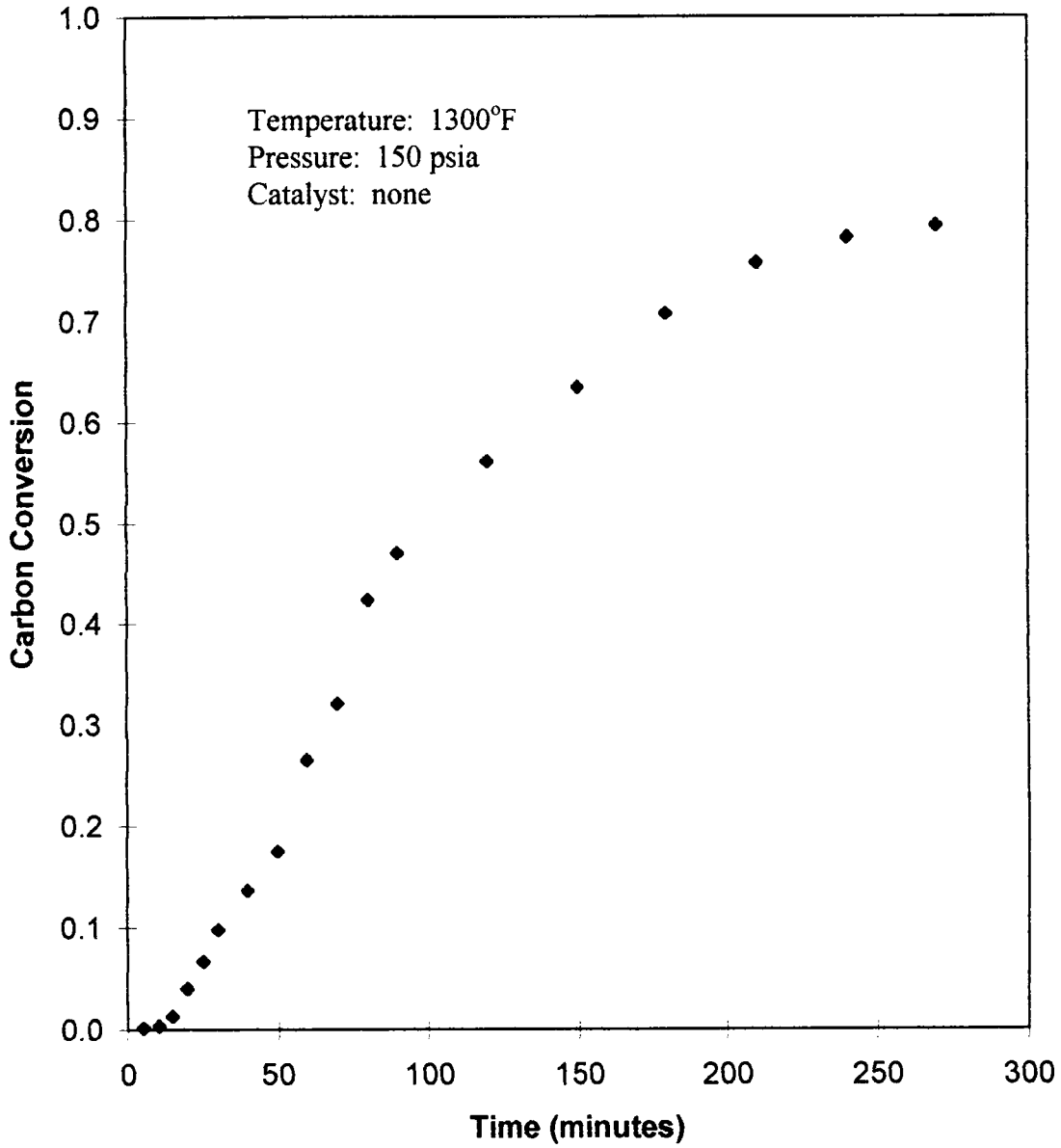

Figure A5.3 Carbon Conversion in Char – Trial 1

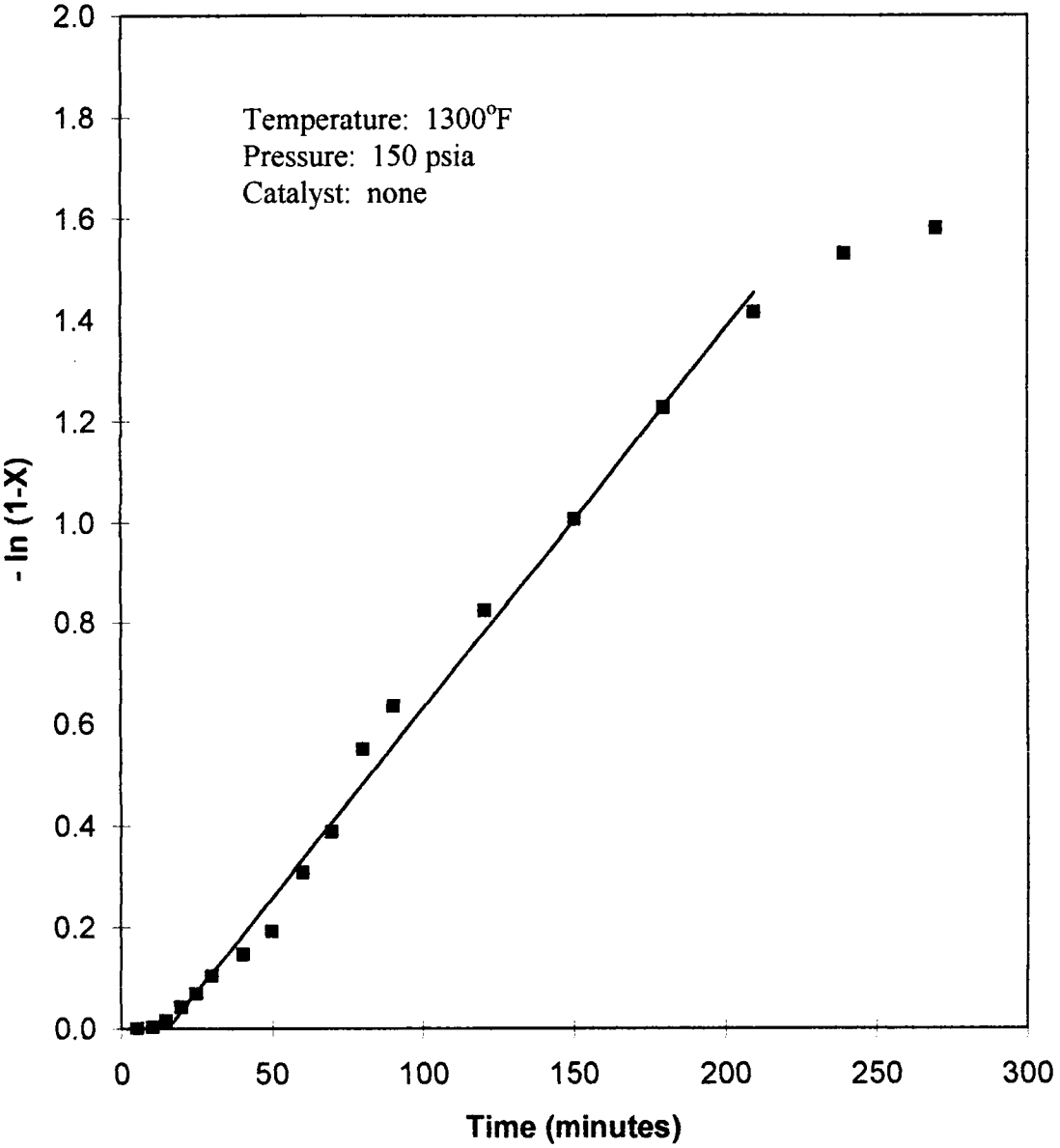

Figure A5.4 Determination of Specific Reaction Rate – Trial 1

Experimental Data for Trial 2

Target Temperature: 1300°F

Target Pressure: 50 psia

Catalyst: none

Catalyst Loading (weight percent on char basis): 0 %

Atmospheric Pressure: 735.0 mm Hg

Initial Cumulative Flowmeter Reading: 122.892 cubic feet

Initial Sample Weight: 3.00 grams

Initial Catalyst-Free Sample Weight: 3.00 grams

Initial Ash-to-Carbon Ratio: 0.7986 grams ash / grams carbon

Final Sample Weight: 1.50 grams

Final Catalyst-Free Sample Weight: 1.50 grams

Final Ash-to-Carbon Ratio: 7.9286 grams ash / grams carbon

Char Carbon Conversion: 0.8993

Average Specific Reaction Rate: 0.0008494 $\frac{mol\ Carbon}{g\ Carbon \bullet \min}$

Table A5.3 Reactor Conditions for Trial 2

Time (minutes)	Reactor Temperature (°F)	Condenser Temperature (°F)	Gas Flowmeter Reading (cubic feet)	Burette Reading (milliliters)
5	1288	75	123.108	1.8
10	1282	75	123.350	3.6
15	1268	75	123.710	5.35
20	1241	75	123.930	7.00
25	1289	74	124.200	8.70
30	1335	74	124.428	10.45
40	1280	74	124.950	13.85
50	1284	74	125.435	17.90
60	1333	75	125.880	20.80
70	1341	74	126.393	24.20
80	1285	75	126.875	27.60
90	1240	74	127.360	31.10
100	1309	75	127.860	35.10
110	1340	75	128.330	37.75
120	1310	75	128.800	41.30
130	1282	74	129.275	44.90
140	1329	74	129.725	48.65
150	1286	74	130.150	51.90
170	1315	74	130.990	58.20
190	1282	75	131.840	65.10
210	1359	74	132.665	72.20
230	1275	74	133.480	79.30
250	1323	74	134.280	86.05
270	1240	74	135.065	93.05
300	1273	74	136.210	102.70

Table A5.4 Gas Chromatograph Results for Trial 2

Time (minutes)	Oxygen Peak Area	Nitrogen Peak Area	Carbon Monoxide Peak Area	Methane Peak Area	Carbon Dioxide Peak Area
5	5.462	13360.392	14.939	0	146.815
10	4.422	12905.080	14.278	0	112.843
15	4.501	12698.673	13.153	0	129.642
20	4.623	13143.487	14.024	0	135.240
25	235.886	12864.174	13.642	0	125.146
30	4.862	12901.056	33.945	0	230.971
40	5.355	12966.508	19.833	0	148.750
50	6.302	12979.281	19.344	0	153.761
60	6.522	12970.755	25.354	0	177.223
70	5.998	13006.615	24.633	0	168.140
80	4.693	12896.256	14.427	0	106.727
90	5.157	13246.566	9.500	0	79.063
100	5.024	12819.223	9.363	0	77.865
110	8.460	13123.737	17.905	0	127.661
120	58.730	13522.443	16.441	0	118.250
130	17.197	13231.392	6.923	0	121.926
140	4.350	12519.690	10.007	0	80.681
150	4.877	13403.587	8.041	0	68.826
170	4.784	13527.443	5.826	0	49.947
190	4.296	13041.652	3.247	0	33.791
210	7.650	13445.795	4.972	0	40.052
230	22.542	13186.276	1.242	0	17.087
250	4.713	13177.380	2.308	0	19.656
270	3.740	13185.632	-----	0	3.542
300	5.680	13537.470	-----	0	4.115

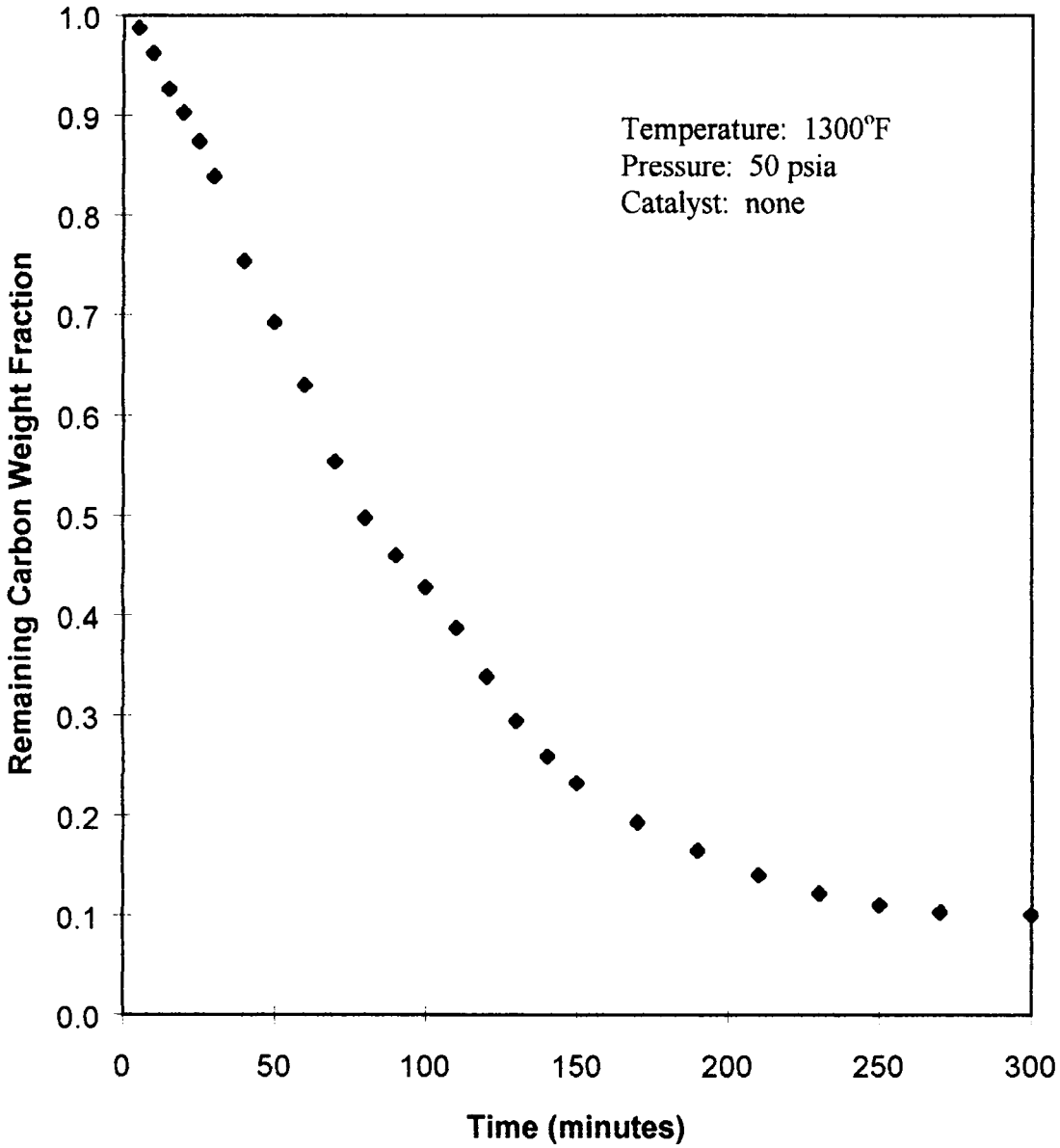

Figure A5.5 Remaining Carbon Weight Fraction – Trial 2

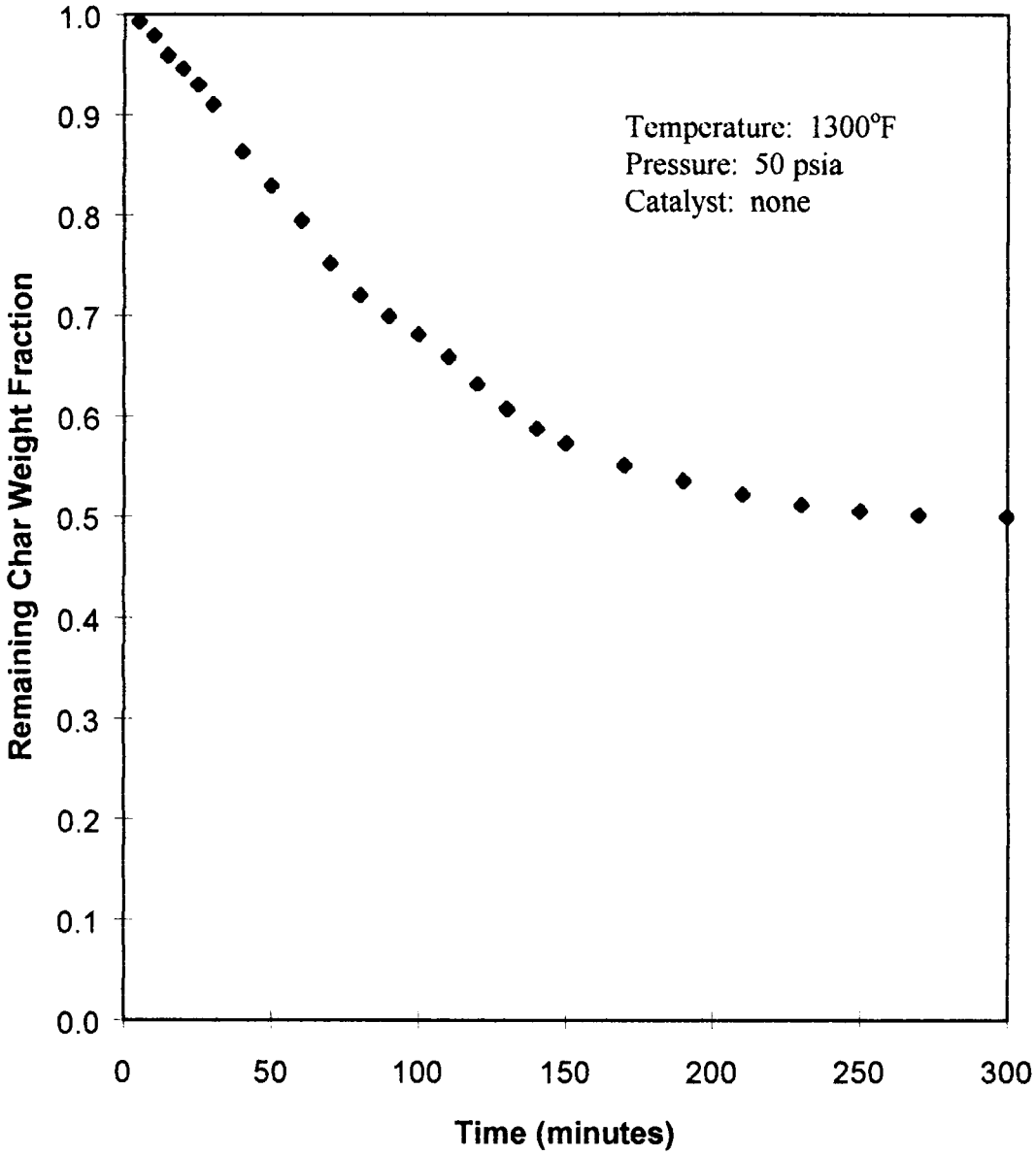

Figure A5.6 Remaining Char Weight Fraction – Trial 2

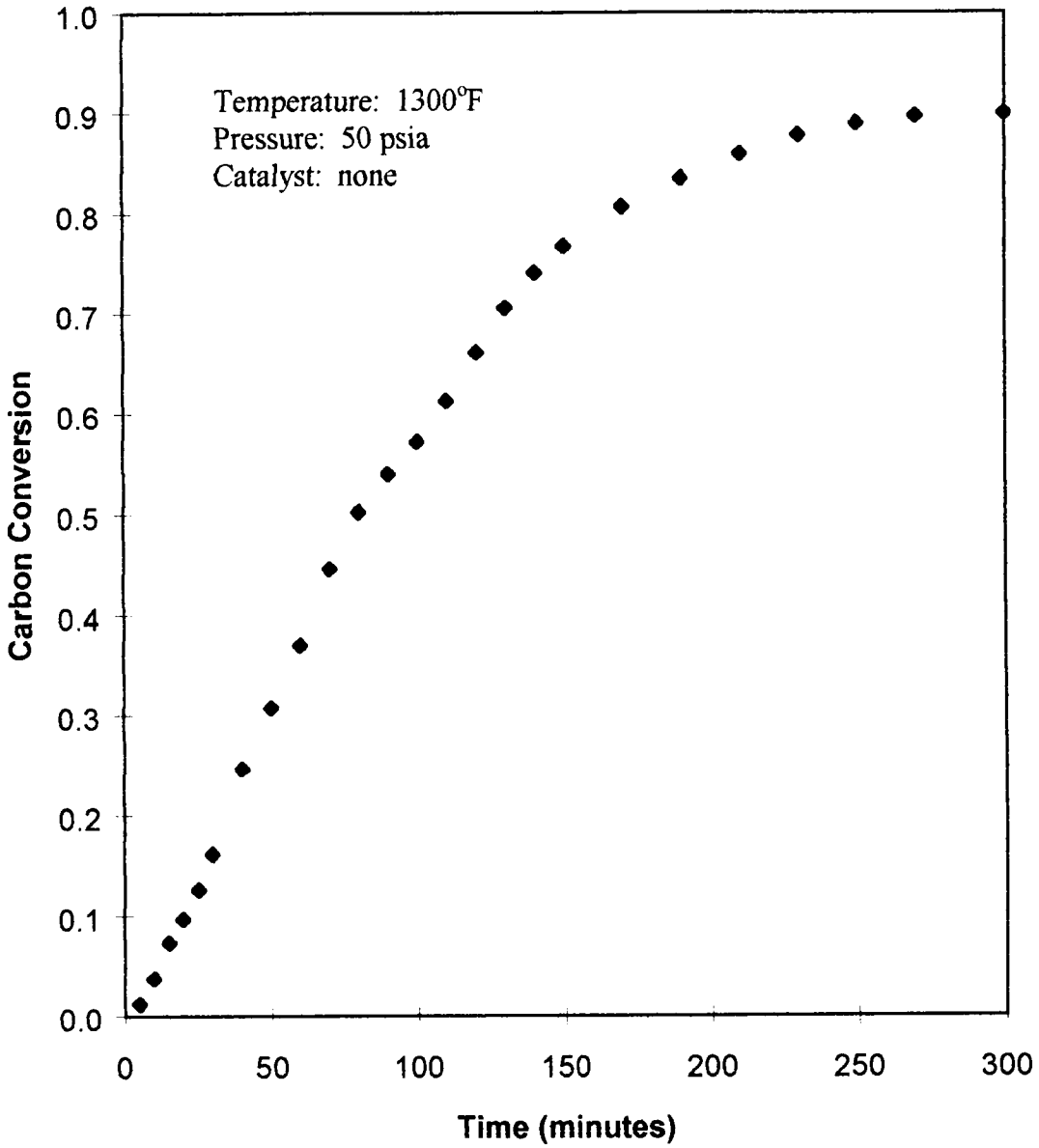

Figure A5.7 Carbon Conversion in Char – Trial 2

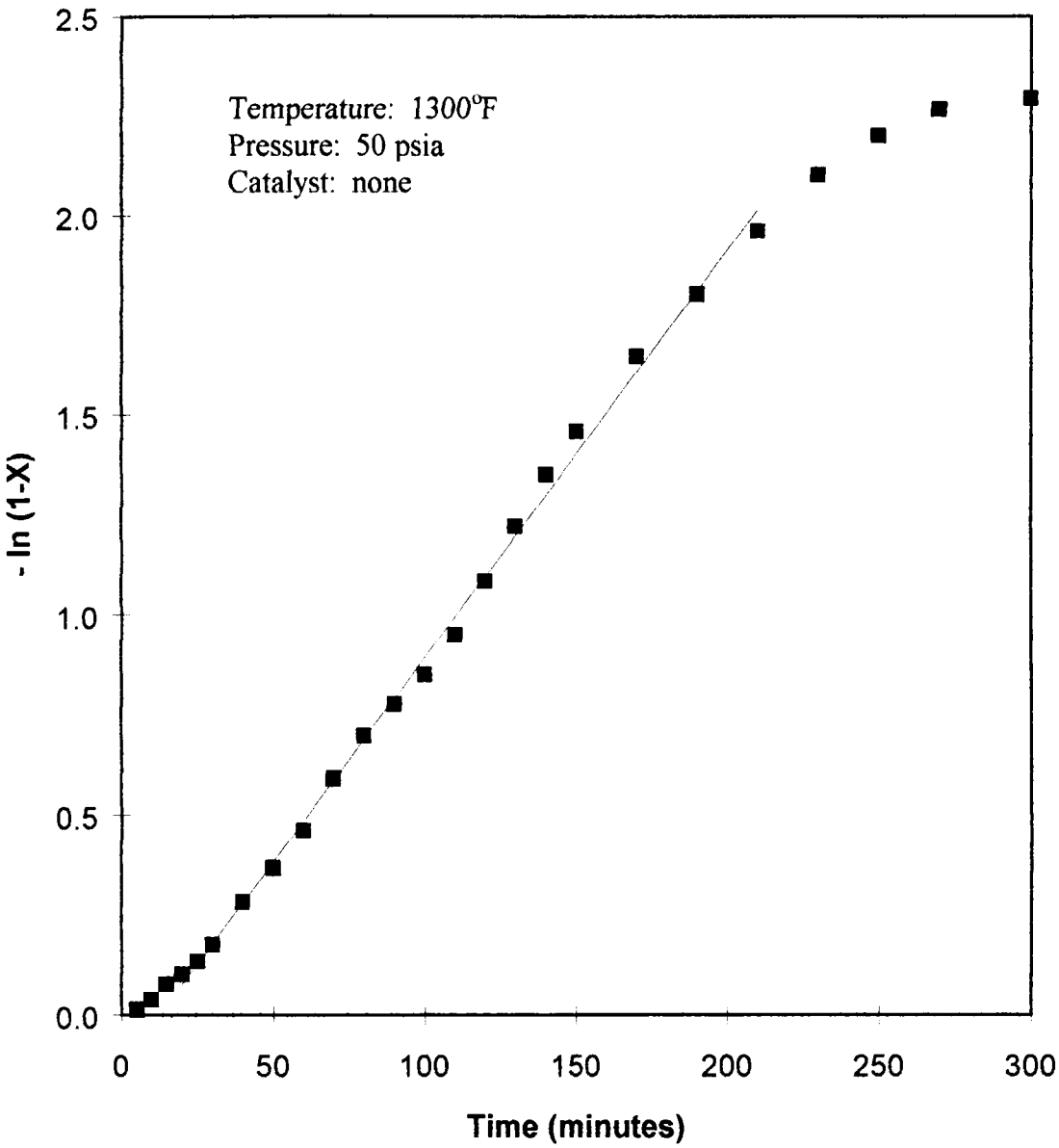

Figure A5.8 Determination of Specific Reaction Rate – Trial 2

Experimental Data for Trial 3

Target Temperature: 1000°F

Target Pressure: 150 psia

Catalyst: none

Catalyst Loading (weight percent on char basis): 0 %

Atmospheric Pressure: 735.0 mm Hg

Initial Cumulative Flowmeter Reading: 136.758 cubic feet

Initial Sample Weight: 3.00 grams

Initial Catalyst-Free Sample Weight: 3.00 grams

Initial Ash-to-Carbon Ratio: 0.7986 grams ash / grams carbon

Final Sample Weight: 2.60 grams

Final Catalyst-Free Sample Weight: 2.60 grams

Final Ash-to-Carbon Ratio: 1.085 grams ash / grams carbon

Char Carbon Conversion: 0.2398

Average Specific Reaction Rate: 0.00008584 $\frac{mol\ Carbon}{g\ Carbon \bullet \text{min}}$

Table A5.5 Reactor Conditions for Trial 3

Time (minutes)	Reactor Temperature (°F)	Condenser Temperature (°F)	Gas Flowmeter Reading (cubic feet)	Burette Reading (milliliters)
5	979	75	136.790	2.65
10	1001	75	136.865	3.60
15	982	75	136.970	5.10
20	1009	75	137.050	6.80
25	997	75	137.185	8.80
30	1019	75	137.310	10.80
50	955	75	137.817	16.10
60	955	75	138.105	19.50
70	968	74	138.477	22.80
80	1013	74	138.825	26.00
90	1012	74	139.165	29.20
100	1029	75	139.485	32.35
110	1029	75	139.810	35.40
120	1000	75	140.150	38.60
130	1035	75	140.495	41.75
140	1022	75	140.835	45.00
150	1022	75	141.150	48.10
170	1022	75	141.935	54.20
190	1030	75	142.700	61.50
210	1010	74	143.320	67.50
240	982	74	144.260	86.85
270	897	74	145.222	88.40
300	989	74	146.175	96.00

Table A5.6 Gas Chromatograph Results for Trial 3

Time (minutes)	Oxygen Peak Area	Nitrogen Peak Area	Carbon Monoxide Peak Area	Methane Peak Area	Carbon Dioxide Peak Area
5	591.209	12495.212	-----	0	4.346
10	279.774	12773.022	-----	0	18.166
15	222.562	12759.335	-----	0	18.000
20	20.042	12686.895	-----	0	19.115
25	11.798	12754.156	0.670	0	22.712
30	13.698	12764.226	0.707	0	23.198
50	6.116	12922.050	0.206	0	14.080
60	10.856	12907.614	0.190	0	12.302
70	4.631	13061.288	0.284	0	12.524
80	4.241	13798.168	0.425	0	11.374
90	4.369	13076.322	0.180	0	12.347
100	15.448	12304.623	-----	0	14.525
110	11.034	12607.746	-----	0	10.476
120	8.110	12606.954	-----	0	12.634
130	6.398	12753.728	-----	0	11.160
140	6.602	12569.106	-----	0	13.967
150	9.628	12546.066	-----	0	13.119
170	6.272	12685.338	-----	0	10.876
190	6.926	12761.975	-----	0	8.858
210	10.517	12762.578	-----	0	9.108
240	13.870	12711.127	-----	0	8.876
270	6.380	12842.222	-----	0	7.909
300	5.194	12878.246	-----	0	9.332

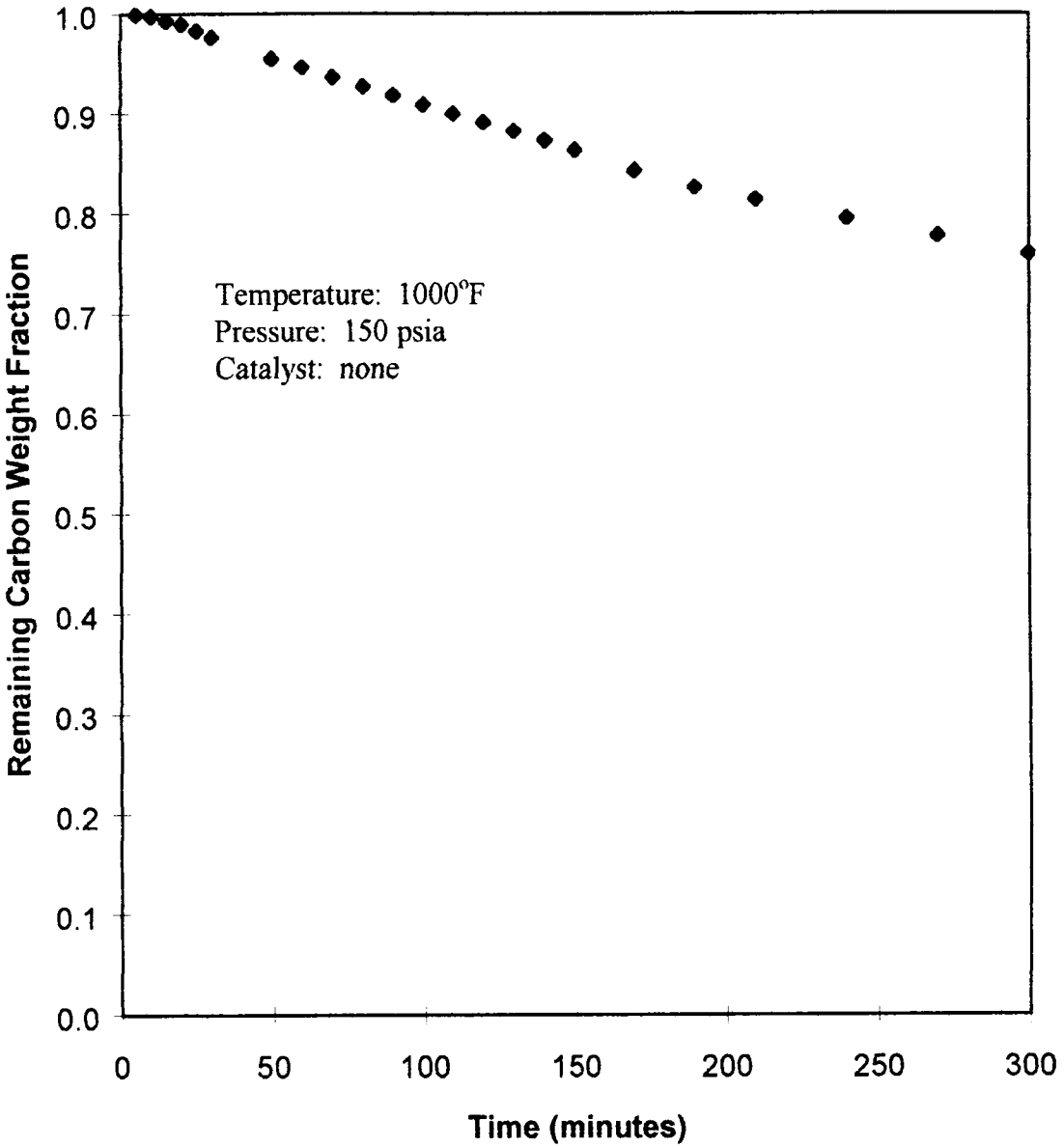

Figure A5.9 Remaining Carbon Weight Fraction – Trial 3

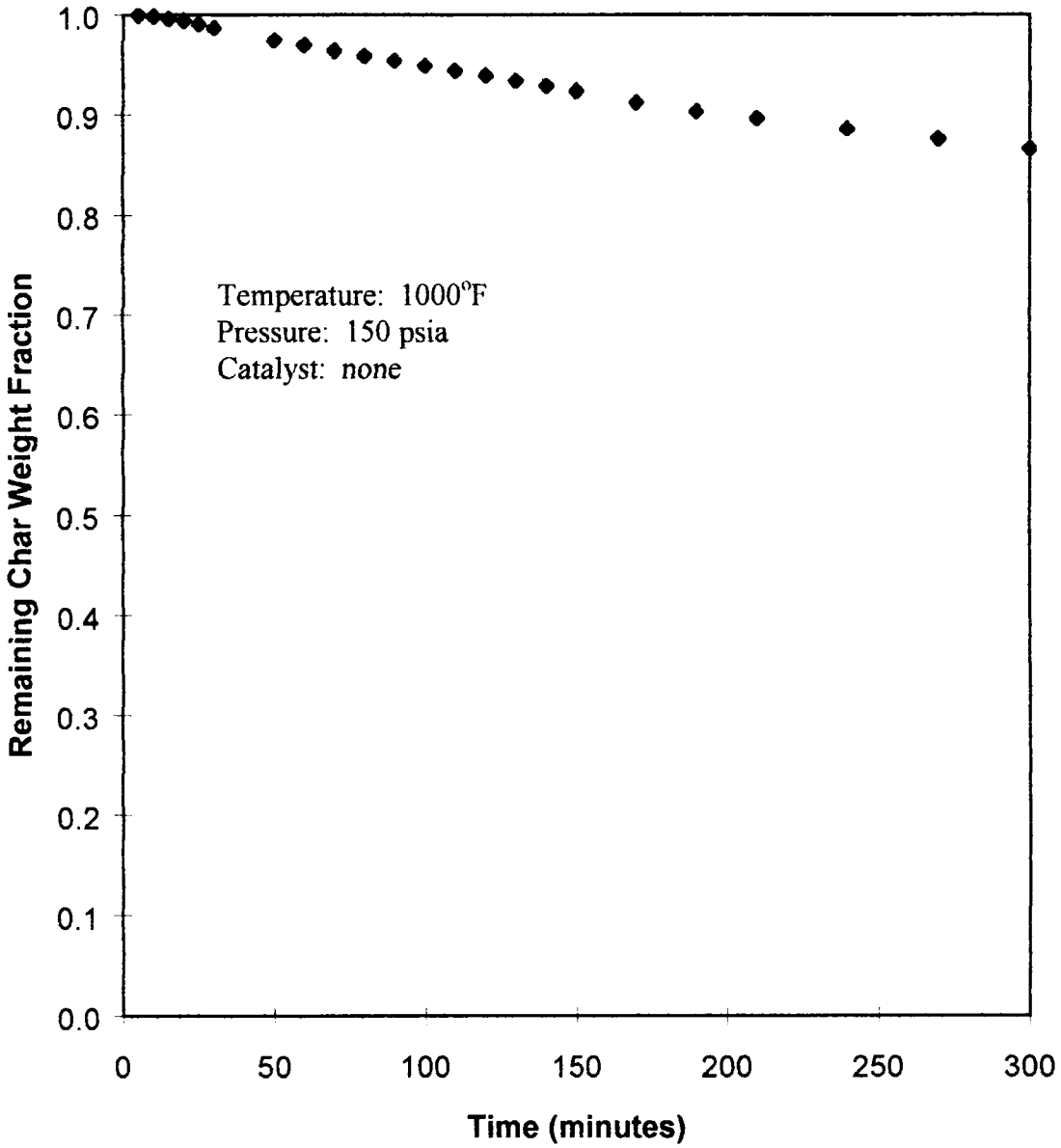

Figure A5.10 Remaining Char Weight Fraction – Trial 3

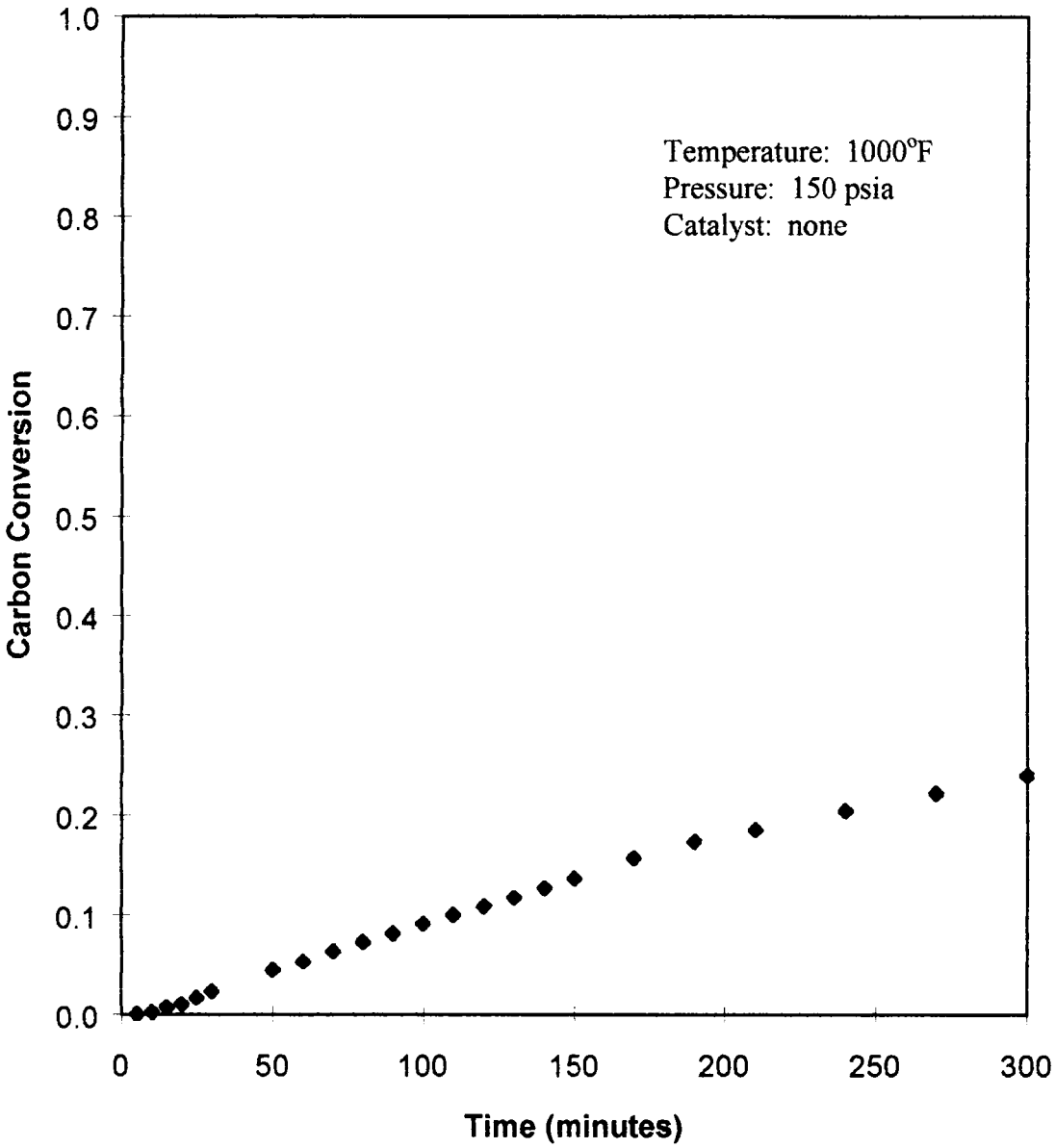

Figure A5.11 Carbon Conversion in Char – Trial 3

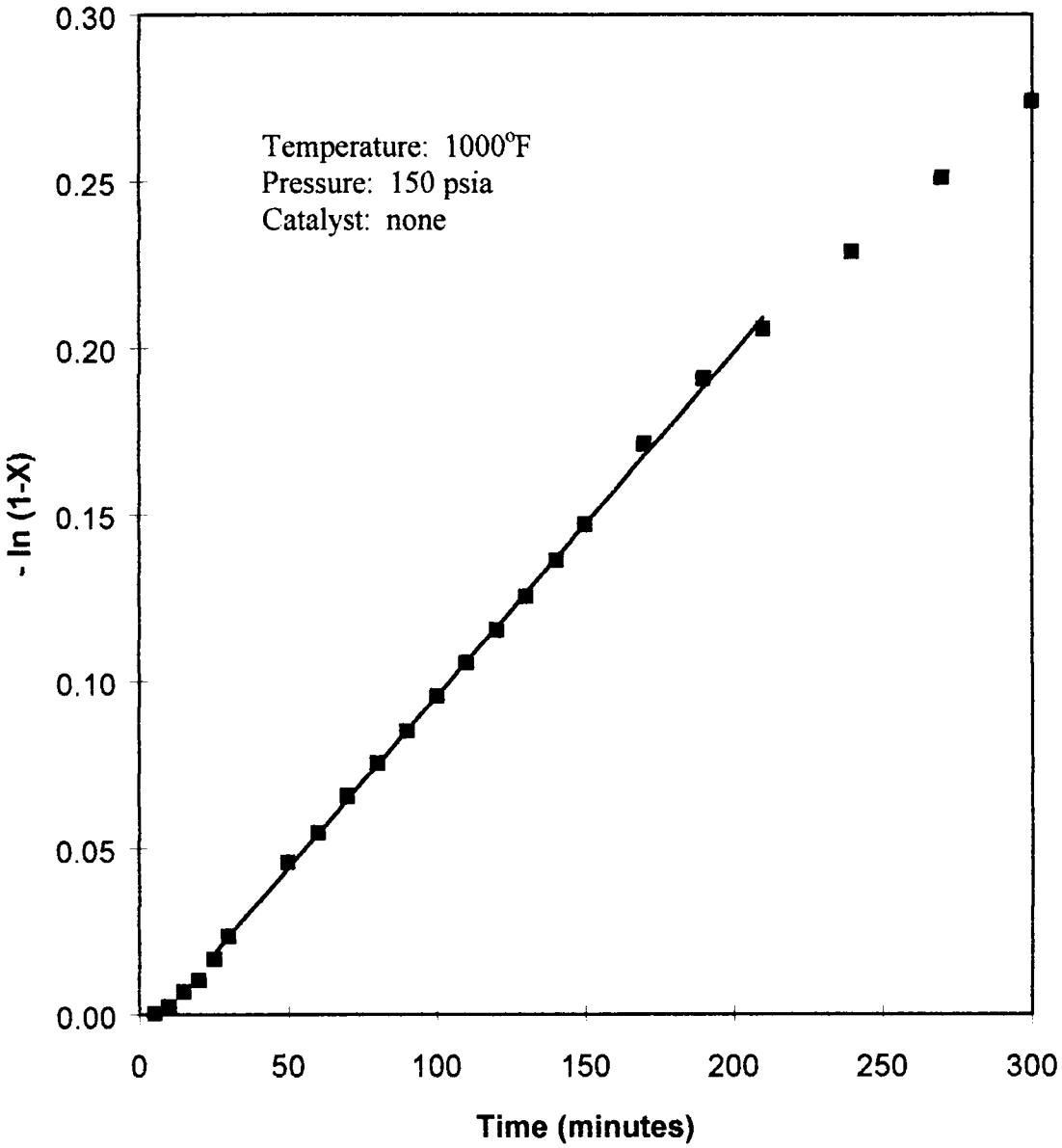

Figure A5.12 Determination of Specific Reaction Rate – Trial 3

Experimental Data for Trial 4

Target Temperature: 1300°F

Target Pressure: 150 psia

Catalyst: Langbeinite

Catalyst Loading (weight percent on char basis): 10.0 %

Atmospheric Pressure: 735.0 mm Hg

Initial Cumulative Flowmeter Reading: 161.266 cubic feet

Initial Sample Weight: 3.31 grams

Initial Catalyst-Free Sample Weight: 3.01 grams

Initial Ash-to-Carbon Ratio: 0.7986 grams ash / grams carbon

Final Sample Weight: 1.82 grams

Final Catalyst-Free Sample Weight: 1.52 grams

Final Ash-to-Carbon Ratio: 8.6712 grams ash / grams carbon

Char Carbon Conversion: 0.8875

Average Specific Reaction Rate: $0.0008354 \frac{mol\ Carbon}{g\ Carbon \bullet \text{min}}$

Table A5.7 Reactor Conditions for Trial 4

Time (minutes)	Reactor Temperature (°F)	Condenser Temperature (°F)	Gas Flowmeter Reading (cubic feet)	Burette Reading (milliliters)
2	1229	75	161.315	1.00
4	1289	75	161.406	1.45
6	1329	75	161.500	2.20
8	1320	75	161.600	2.80
10	1327	75	161.695	3.40
12	1293	75	161.788	4.00
14	1208	75	161.870	4.60
16	1268	75	161.980	5.15
18	1339	75	162.062	5.70
20	1272	75	162.163	6.30
22	1354	75	162.265	7.00
24	1299	75	162.368	7.70
26	1291	75	162.460	8.40
28	1242	75	162.562	8.85
30	1267	75	162.650	9.45
35	1316	75	162.900	10.98
40	1295	75	163.151	12.50
45	1289	75	163.370	14.00
50	1264	75	163.568	15.50
55	1279	75	163.776	17.00
60	1327	75	163.977	18.40
70	1303	75	164.417	21.30
80	1271	75	164.910	24.50
90	1266	75	165.352	27.50
100	1275	75	165.805	30.45
115	1330	75	166.502	35.20
145	1352	75	167.825	44.22
160	1290	75	168.465	48.70
180	1311	75	169.355	54.15
200	1192	75	170.265	60.85
220	1315	75	171.058	67.05
240	1316	75	171.840	73.20

Table A5.8 Gas Chromatograph Results for Trial 4

Time (minutes)	Oxygen Peak Area	Nitrogen Peak Area	Carbon Monoxide Peak Area	Methane Peak Area	Carbon Dioxide Peak Area
2	5.786	14451.986	2.135	0	35.971
4	9.892	14367.224	2.004	0	42.869
6	4.367	14842.241	7.213	0	92.157
8	6.592	13148.526	12.817	0	143.116
10	9.616	12749.283	22.360	0	207.324
12	7.236	13004.971	20.298	0	207.324
14	4.994	13395.228	18.954	0	221.409
16	4.630	13447.020	15.461	0	199.394
18	4.892	13428.717	15.984	0	206.548
20	4.449	12838.492	21.969	0	235.950
22	5.553	14140.301	29.962	0	293.228
24	6.773	13196.466	30.961	0	287.559
26	3.053	13221.794	28.665	0	273.170
28	4.800	13304.352	20.915	0	242.017
30	4.804	12983.507	14.138	0	177.946
35	4.862	13426.814	12.984	0	186.630
40	4.289	13410.891	13.655	0	190.842
45	4.467	13440.997	10.031	0	167.446
50	4.964	13537.694	6.874	0	131.298
55	5.207	13438.721	9.764	0	158.369
60	4.429	13334.457	13.496	0	193.987
70	9.602	13097.317	8.479	0	119.373
80	4.482	12829.348	4.349	0	84.649
90	7.863	13485.535	4.196	0	77.594
100	192.552	13186.934	3.566	0	63.085
115	19.542	13321.761	6.132	0	92.834
145	4.344	13348.380	5.822	0	82.160
160	7.298	13436.881	1.760	0	31.221
180	4.232	13633.399	1.664	0	32.127
200	4.086	13586.941	0.904	0	20.913
220	8.127	13393.025	1.891	0	32.557
240	2.134	13185.632	1.107	0	23.310

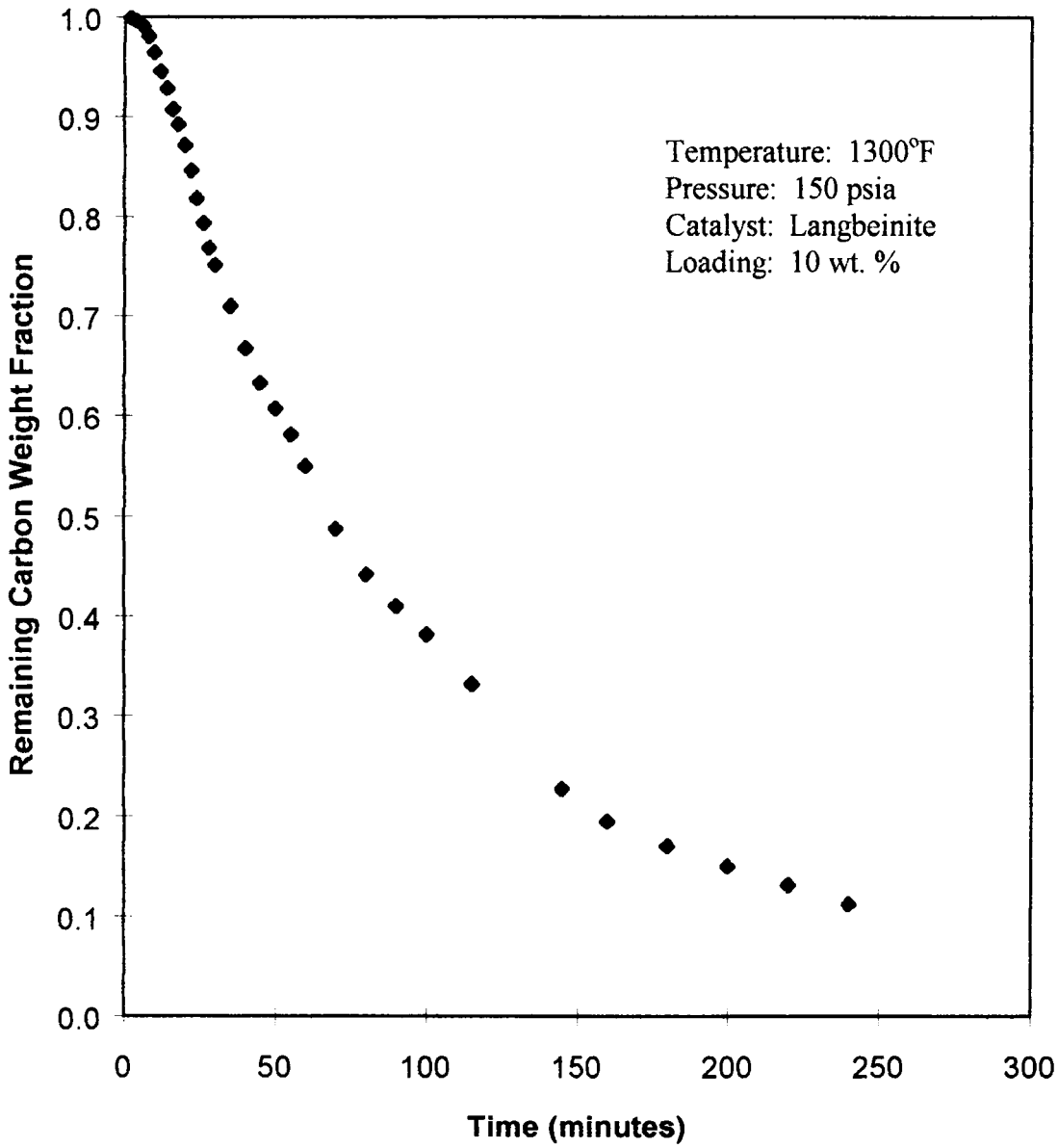

Figure A5.13 Remaining Carbon Weight Fraction – Trial 4

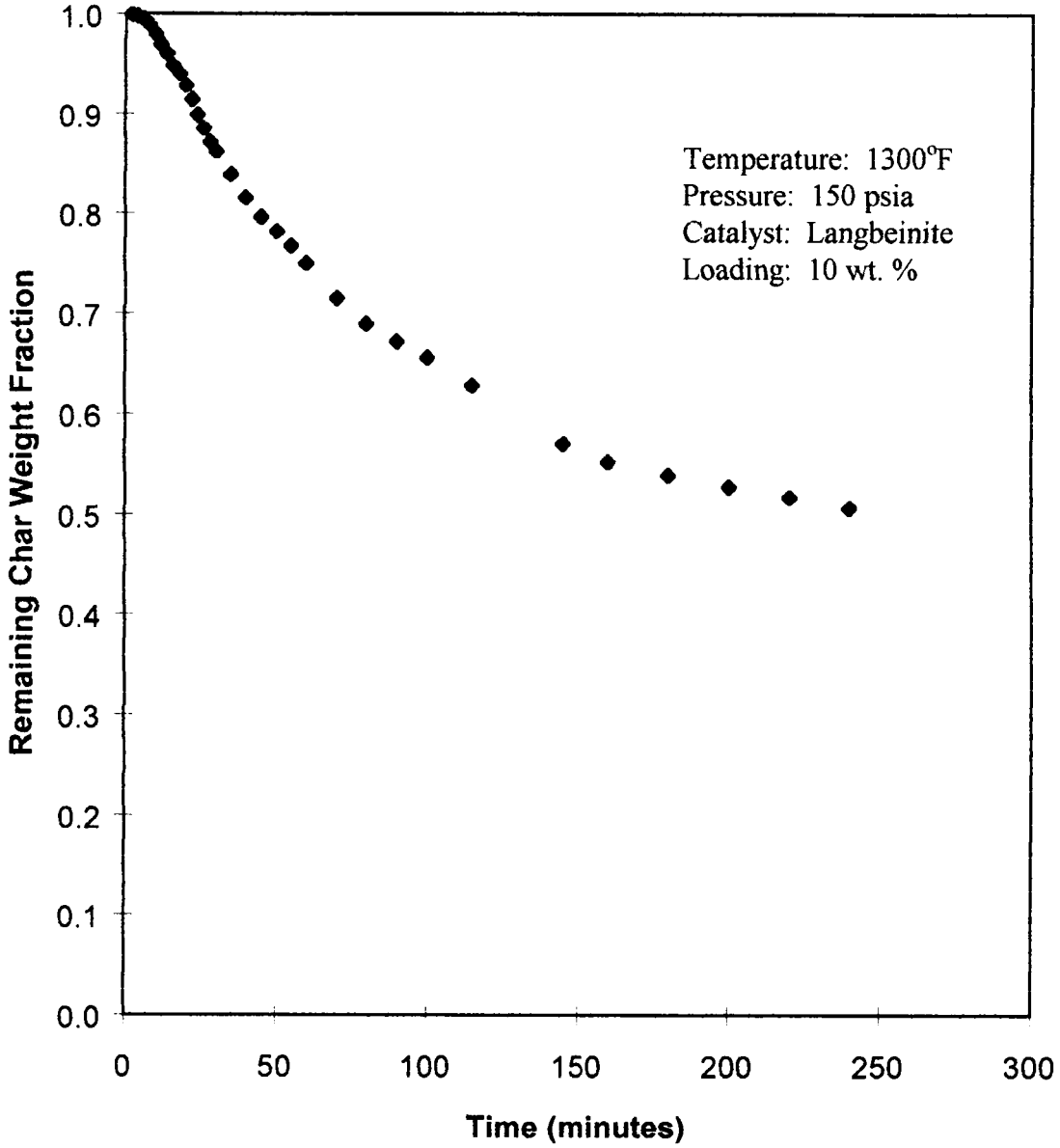

Figure A5.14 Remaining Char Weight Fraction – Trial 4

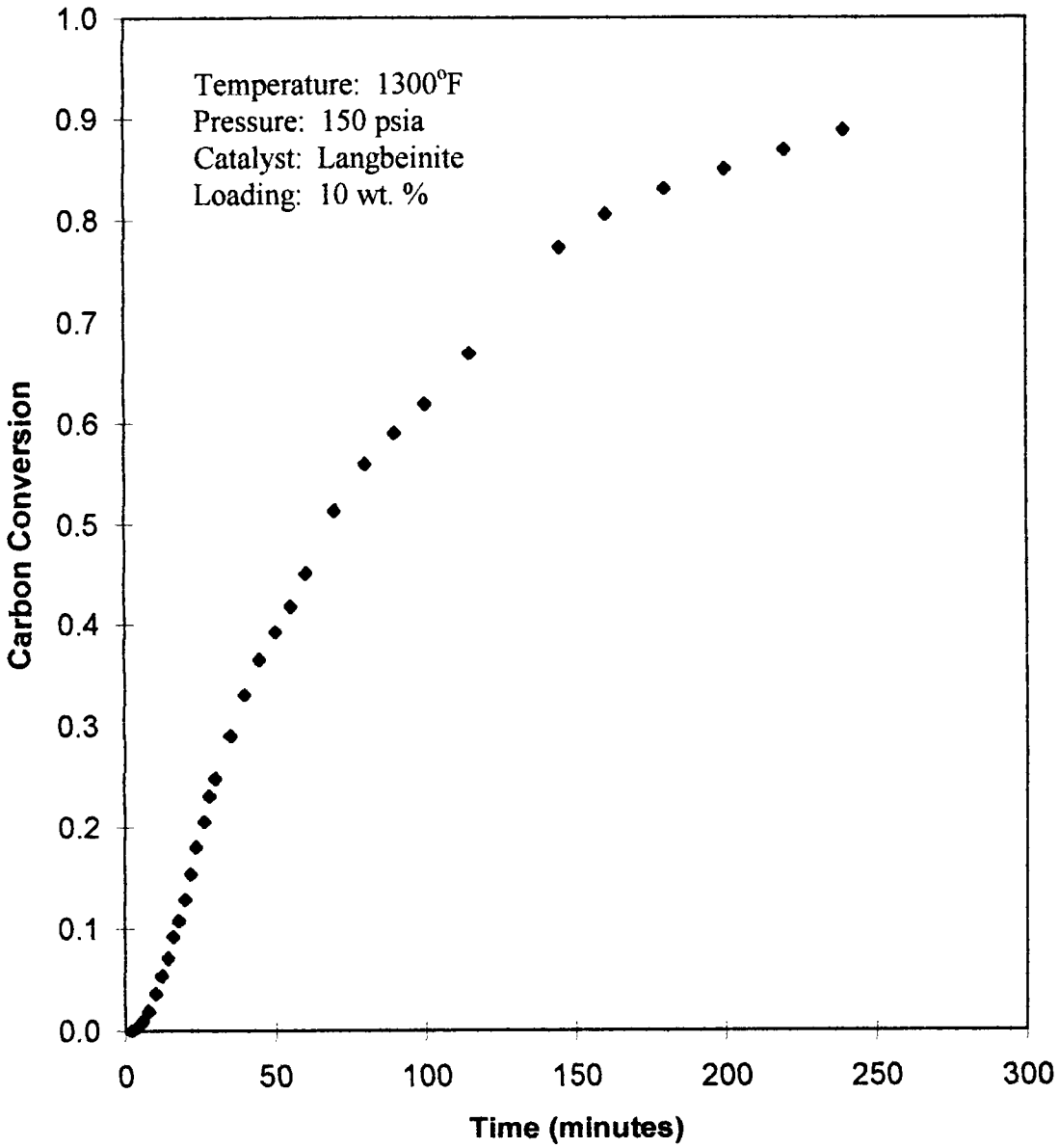

Figure A5.15 Carbon Conversion in Char – Trial 4

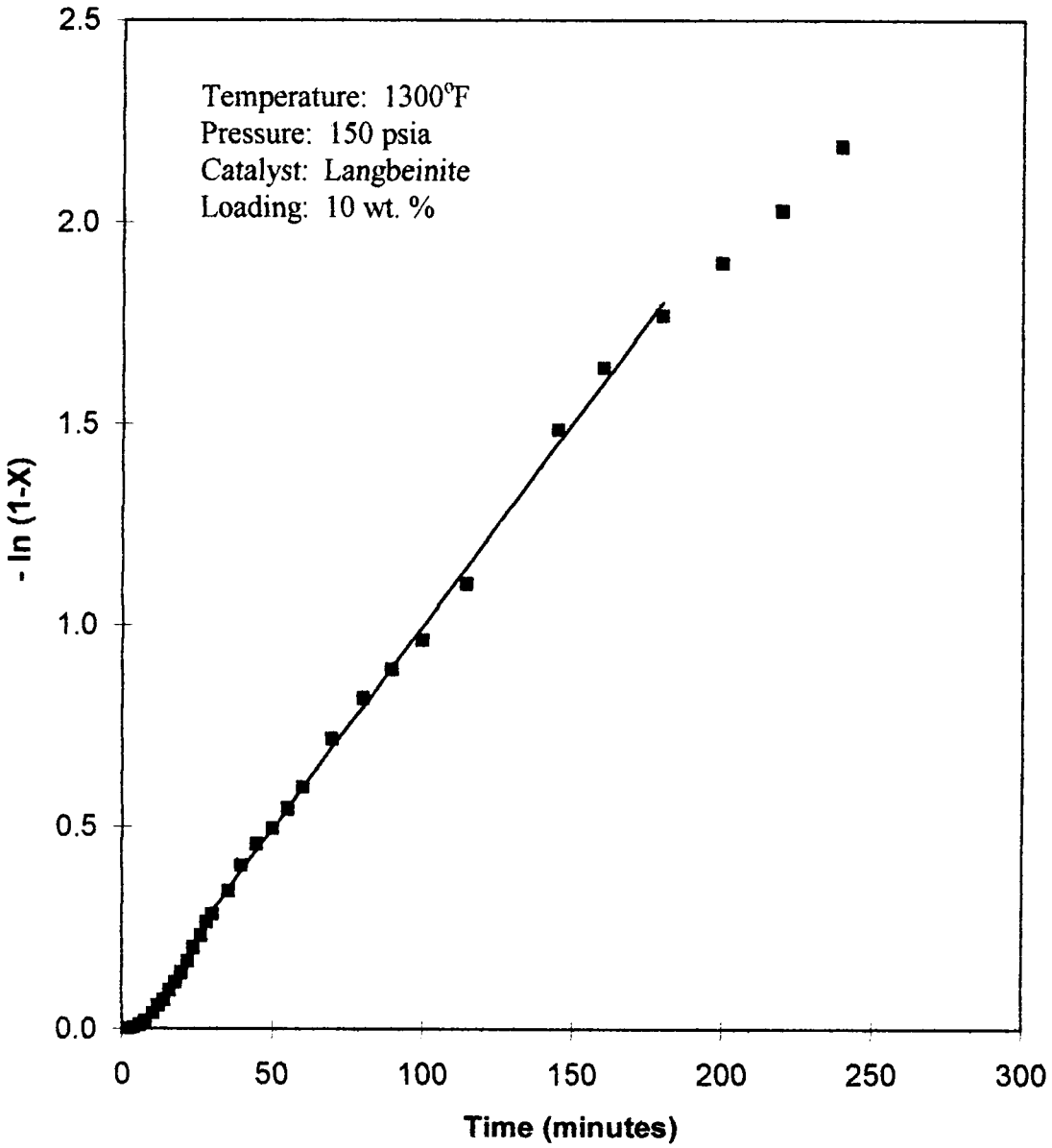

Figure A5.16 Determination of Specific Reaction Rate – Trial 4

Experimental Data for Trial 5

Target Temperature: 1300°F

Target Pressure: 150 psia

Catalyst: Potassium Carbonate

Catalyst Loading (weight percent on char basis): 10.0 %

Atmospheric Pressure: 735.0 mm Hg

Initial Cumulative Flowmeter Reading: 172.397 cubic feet

Initial Sample Weight: 3.30 grams

Initial Catalyst-Free Sample Weight: 3.00 grams

Initial Ash-to-Carbon Ratio: 0.7986 grams ash / grams carbon

Final Sample Weight: 1.74 grams

Final Catalyst-Free Sample Weight: 1.44 grams

Final Ash-to-Carbon Ratio: 12.3333 grams ash / grams carbon

Char Carbon Conversion: 0.9218

Average Specific Reaction Rate: $0.0014085 \frac{mol\ Carbon}{g\ Carbon \bullet \min}$

Table A5.9 Reactor Conditions for Trial 5

Time (minutes)	Reactor Temperature (°F)	Condenser Temperature (°F)	Gas Flowmeter Reading (cubic feet)	Burette Reading (milliliters)
2	1192	78	172.445	0.65
4	1332	78	172.575	1.30
6	1330	78	172.715	1.90
8	1314	78	172.832	2.45
10	1278	78	172.960	3.15
12	1256	78	173.090	3.70
14	1255	78	173.210	4.50
16	1249	78	173.315	4.98
18	1265	78	173.425	5.60
20	1310	78	173.540	6.25
22	1312	78	173.645	6.80
24	1320	78	173.750	7.45
26	1321	78	173.852	8.15
28	1277	78	173.958	8.70
30	1279	78	174.058	9.30
35	1281	79	174.295	10.80
40	1281	79	174.532	12.40
45	1283	79	174.745	13.90
50	1270	79	174.950	15.50
55	1267	79	175.145	17.00
60	1259	79	175.333	18.35
70	1321	80	175.692	21.60
80	1281	80	176.022	24.70
90	1318	80	176.315	27.85
100	1274	80	176.595	30.90
110	1230	80	176.846	33.90
120	1306	81	177.075	37.00
140	1243	81	177.520	43.20
160	1272	81	177.880	49.40
180	1281	81	178.155	55.20
200	1334	81	178.410	61.65
220	1286	81	179.375	67.50
240	1295	81	180.714	73.55
260	1285	81	182.035	79.60

Table A5.10 Gas Chromatograph Results for Trial 5

Time (minutes)	Oxygen Peak Area	Nitrogen Peak Area	Carbon Monoxide Peak Area	Methane Peak Area	Carbon Dioxide Peak Area
2	34.241	12177.022	4.969	0	58.015
4	15.518	13107.416	4.440	0	77.049
6	7.244	12961.534	27.655	0	190.475
8	7.108	12781.382	42.715	0	270.965
10	4.600	12497.289	35.196	0	235.861
12	6.982	12904.878	24.796	0	231.364
14	9.928	12980.691	17.339	0	195.753
16	5.660	13018.389	15.720	0	222.300
18	14.760	12886.301	16.014	0	203.461
20	16.898	12792.749	21.293	0	240.063
22	5.414	12779.528	33.836	0	296.192
24	6.141	12774.628	29.866	0	286.473
26	130.027	12511.285	30.049	0	278.099
28	5.838	12667.500	38.732	0	322.993
30	4.813	12211.206	33.986	0	300.401
35	5.220	12814.072	28.888	0	287.380
40	5.236	12818.774	20.067	0	259.129
45	3.844	12946.162	12.858	0	227.286
50	5.358	12941.116	11.021	0	209.743
55	3.979	13041.349	7.108	0	182.662
60	5.314	12728.027	6.740	0	160.932
70	4.326	12553.346	14.832	0	237.522
80	5.739	12696.834	8.207	0	187.335
90	6.143	13044.419	3.718	0	131.080
100	5.303	12857.260	5.224	0	148.842
110	4.853	12890.373	2.472	0	100.879
120	6.010	12850.026	3.927	0	101.900
140	5.429	12978.209	0.424	0	41.519
160	6.430	12962.007	1.268	0	74.002
180	4.560	13043.226	-----	0	41.569
200	5.228	13045.064	0.645	0	37.657
220	4.324	12715.266	-----	0	6.816
240	0	12981.135	0.272	0	6.399
260	3.317	13185.632	-----	0	2.525

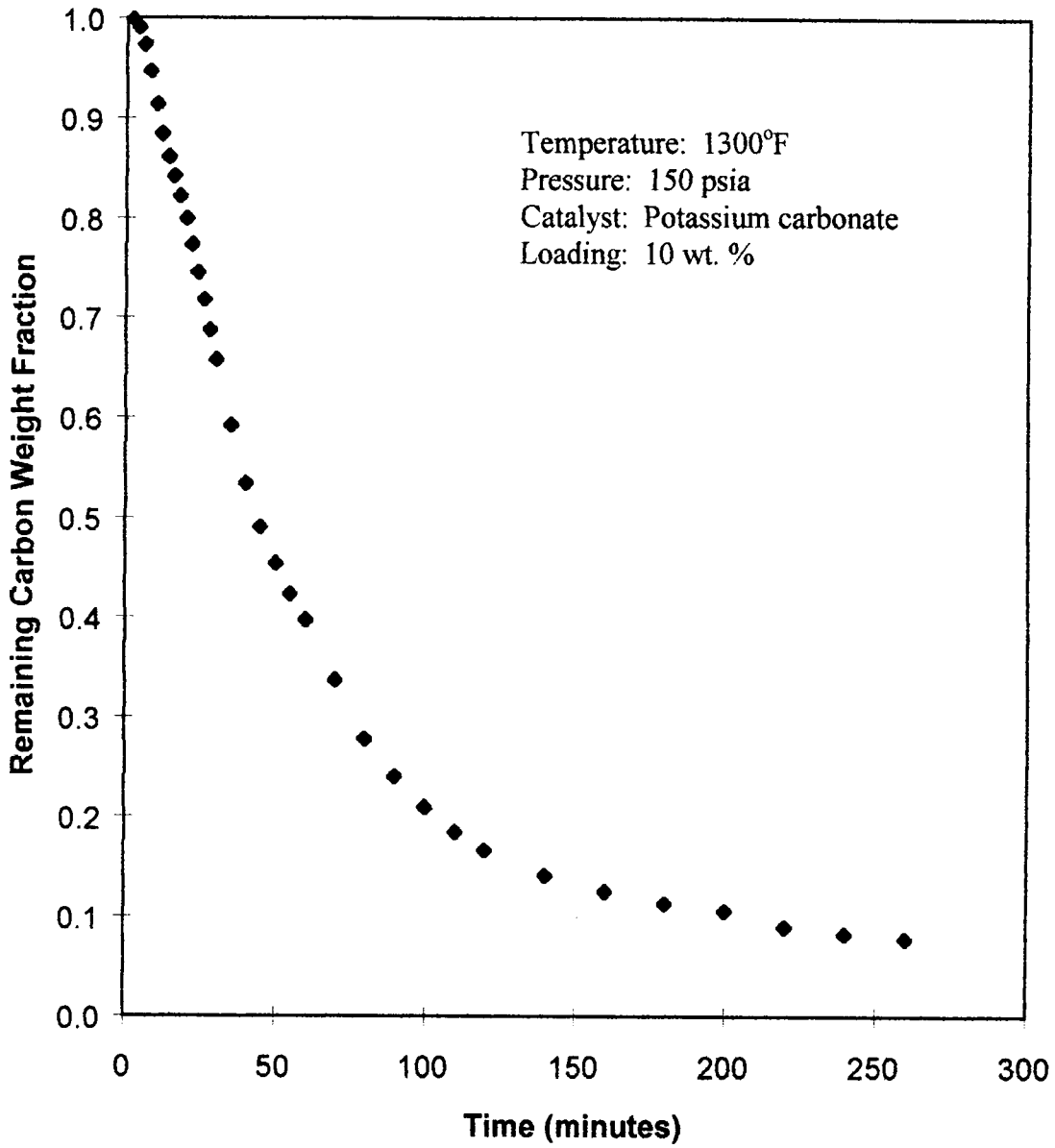

Figure A5.17 Remaining Carbon Weight Fraction – Trial 5

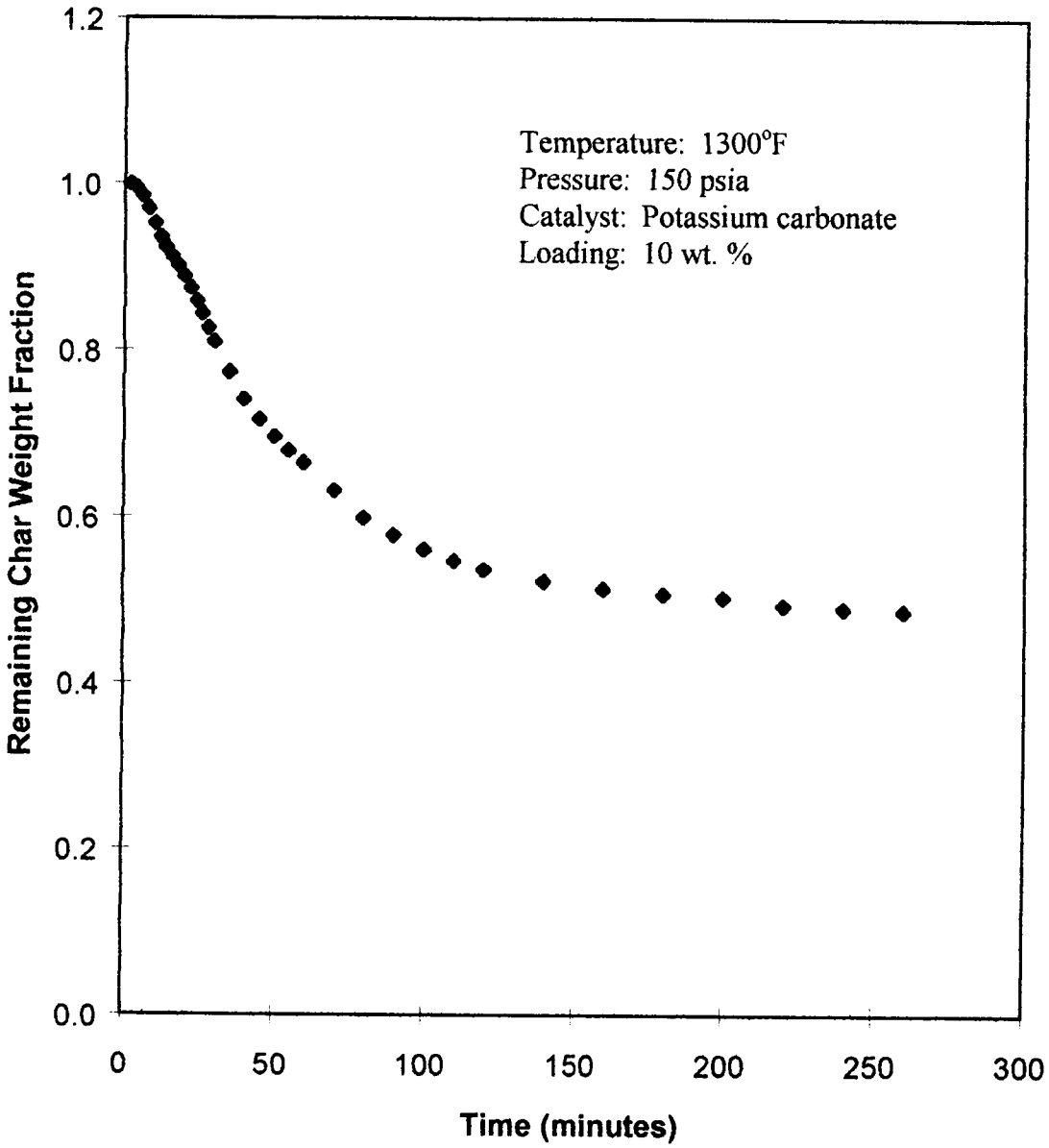

Figure A5.18 Remaining Char Weight Fraction – Trial 5

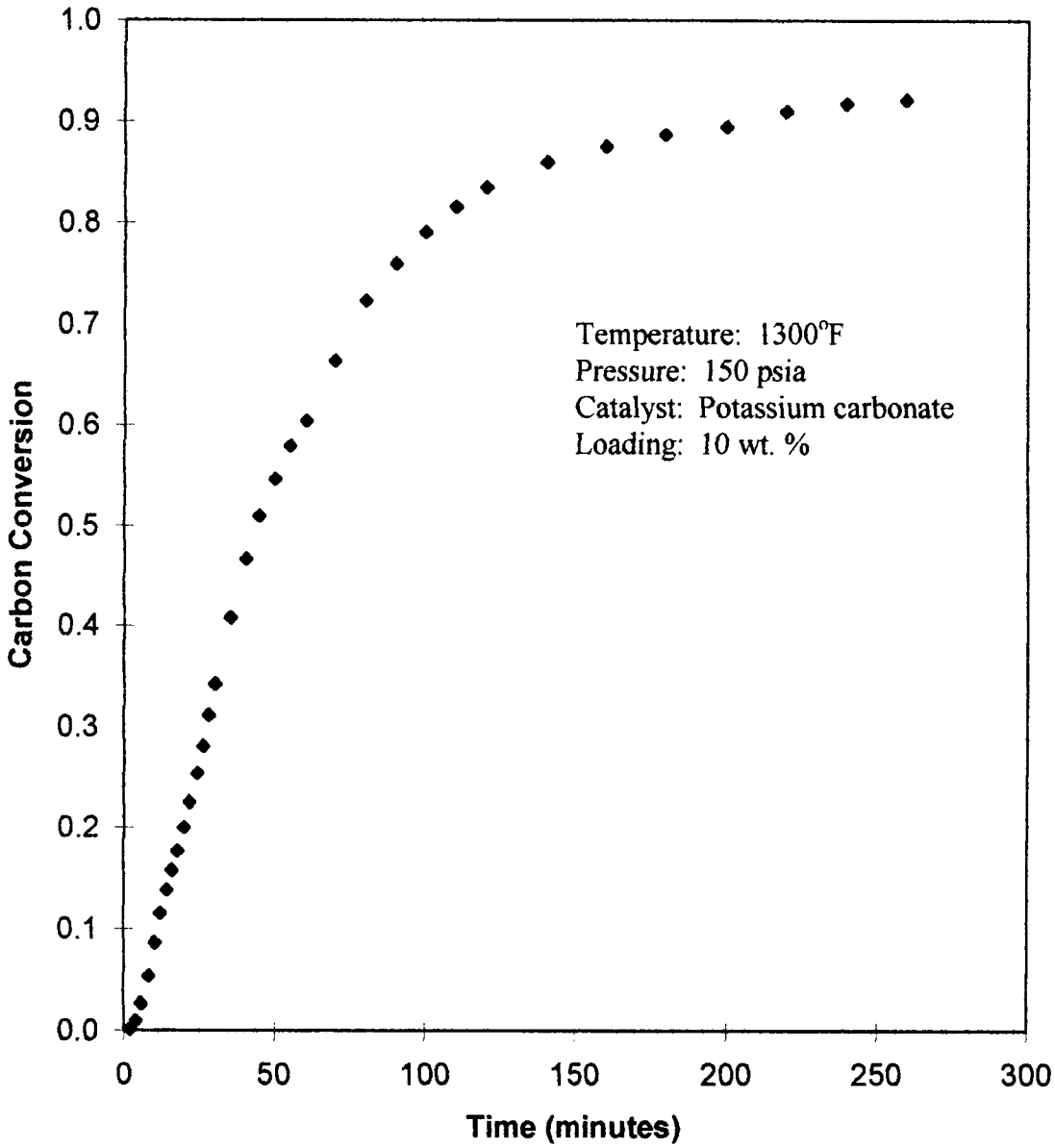

Figure A5.19 Carbon Conversion in Char – Trial 5

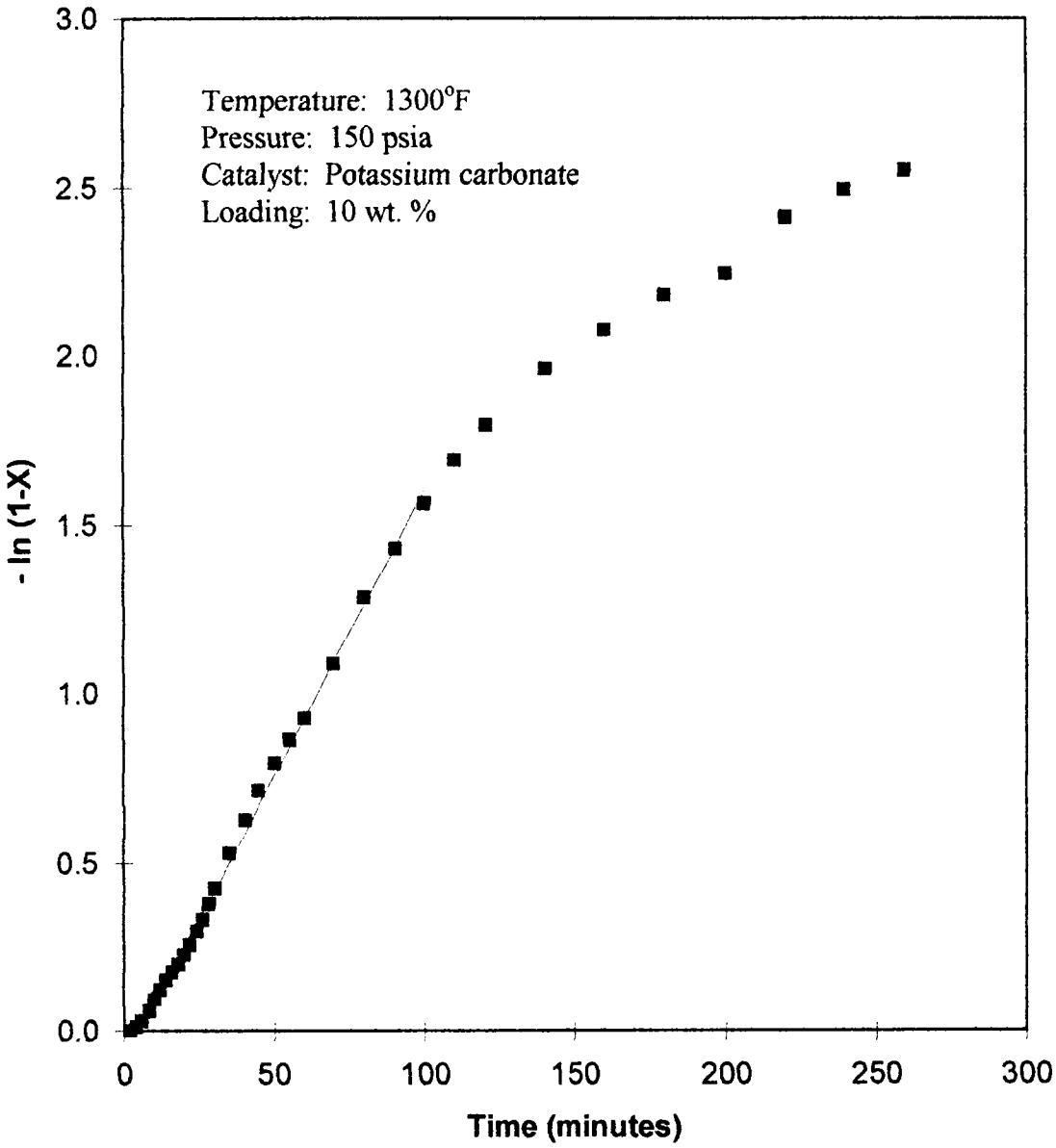

Figure A5.20 Determination of Specific Reaction Rate – Trial 5

VITA

Jerald Andrew Jones was born in Kingsport, Tennessee on April 6, 1974. He attended schools in the Sullivan County Public School System, where he graduated from Sullivan South High School in May 1992. He entered Tennessee Technological University during August of 1992. In May 1996, he received the Bachelor of Science degree in Chemical Engineering. He entered the Master of Science program in Chemical Engineering at the University of Tennessee, Knoxville in August of 1996. He was employed as a Graduate Research Assistant at the University of Tennessee Space Institute while a graduate student. He officially received the Master of Science degree in August 1998.

Jerald Andrew Jones is presently working as a Process Technology Engineer with Albemarle Corporation. He is currently located at the Magnolia, Arkansas facility.